

SOLVENT RECOVERY FROM PHOTOLITHOGRAPHY WASTE USING
CELLULOSE ULTRAFILTRATION MEMBRANES

A THESIS SUBMITTED TO
THE GRADUATE SCHOOL OF NATURAL AND APPLIED SCIENCES
OF
MIDDLE EAST TECHNICAL UNIVERSITY

BY

AYGEN SAVAŞ ALKAN

IN PARTIAL FULFILLMENT OF THE REQUIREMENTS
FOR
THE DEGREE OF MASTER OF SCIENCE
IN
CHEMICAL ENGINEERING

AUGUST 2021

Approval of the thesis:

**SOLVENT RECOVERY FROM PHOTOLITHOGRAPHY WASTE USING
CELLULOSE ULTRAFILTRATION MEMBRANES**

submitted by **AYGEN SAVAŞ ALKAN** in partial fulfillment of the requirements
for the degree of **Master of Science in Chemical Engineering, Middle East
Technical University** by,

Prof. Dr. Halil Kalıpçılar
Dean, Graduate School of **Natural and Applied Sciences**

Prof. Dr. Pınar Çalık
Head of the Department, **Chemical Engineering**

Assoc. Prof. Dr. Zeynep Çulfaz Emecen
Supervisor, **Chemical Engineering, METU**

Examining Committee Members:

Prof. Dr. Levent Yılmaz
Chemical Engineering, METU

Assoc. Prof. Dr. Zeynep Çulfaz Emecen
Chemical Engineering, METU

Prof. Dr. Birgül Tantekin Ersolmaz
Chemical Engineering, İTÜ

Assoc. Prof. Dr. Erhan Bat
Chemical Engineering, METU

Asst. Prof. Dr. Emre Büküşoğlu
Chemical Engineering, METU

Date: 12.08.2021

I hereby declare that all information in this document has been obtained and presented in accordance with academic rules and ethical conduct. I also declare that, as required by these rules and conduct, I have fully cited and referenced all material and results that are not original to this work.

Name Last name : Aygen Savaş Alkan

Signature :

ABSTRACT

SOLVENT RECOVERY FROM PHOTOLITHOGRAPHY WASTE USING CELLULOSE ULTRAFILTRATION MEMBRANES

Savaş Alkan, Aygen
Master of Science, Chemical Engineering
Supervisor : Assoc. Prof. Dr. Pınar Zeynep Çulfaz Emecen

August 2021, 129 pages

Cellulose flat sheet ultrafiltration membranes were fabricated for the investigation of their separation performance in Organic Solvent Ultrafiltration (OSU) applications and for the solvent recovery from photolithography wastes. Firstly, cellulose acetate membranes were produced and then, these were converted into cellulose membranes via alkaline hydrolysis.

The membranes were cast from polymer solutions containing cellulose acetate as polymer with 20-30% concentration range, dimethyl sulfoxide (DMSO) as solvent, acetone as co-solvent and polyethylene glycol (PEG) as pore former agent. Before use in photolithography waste purification, performance tuning was carried out by changing the polymer, co-solvent, pore former composition; coagulation bath temperature and applying the process of annealing for the main aim of obtaining membranes having high rejection performance accompanying a reasonable permeance. The separation performance of the membranes was tested with the molecular weight cut-off tests and the MWCO tests were firstly done in water. Then, the change in MWCO performance in different solvents was investigated in DMSO and methanol. In MWCO tests, PEG probes with different molecular weights were

used for the filtration and Gel Permeation Chromatography (GPC) was used for the analysis. In MWCO tests performed in water, the obtained MWCO range with different membranes was 3-10 kDa. On the other hand, the MWCO tests performed in DMSO, water and methanol for the comparison resulted in 1.3, 3 and 5 kDa.

Photolithography is a process widely used in the fabrication of microelectronic devices and it requires high purity metal-free solvents for the process steps to prevent short-circuit failures. In the study, the mimic of developer bath solution with propylene glycol monomethyl ether acetate (PGMEA) consisting of 0.5-2.5 g/L SU-8 photoresist were firstly prepared and filtered via two-stage filtration by the cellulose ultrafiltration membranes. At the end, 91% and 80% SU-8 rejection values were obtained for the first and second filtration stages, respectively. Then, the permeate mixture of two-stage filtrations were tested in photolithography and the pattern results of recycled PGMEA were compared with the pattern of the photolithography applied with fresh PGMEA. As a result, the obtained pattern imprinted via recycled solvent was promising and so, a critical outcome was obtained from cost-efficiency, sustainability and circular economy aspects for the large-scale applications in the microelectronics industry.

Keywords: Membranes, cellulose, ultrafiltration, photolithography, molecular weight cut-off

ÖZ

SELÜLOZ ULTRAFİLTRASYON MEMBRANLARI İLE FOTOLİTOGRAFI ATIKLARINDAN ÇÖZÜCÜ GERİ KAZANIMI UYGULAMASI

Savaş Alkan, Aygen
Yüksek Lisans, Kimya Mühendisliği
Tez Yöneticisi: Doç. Dr. Pınar Zeynep Çulfaz Emecen

Ağustos 2021, 129 sayfa

Bu çalışmada, organik çözücüde ultrafiltrasyon uygulamalarında ve fotolitografi atıklarından çözücü geri kazanımında selüloz membranların ayırma performanslarının incelenmesi için selüloz ultrafiltrasyon membranları üretilmiştir. Selüloz membranların üretimi için, ilk olarak selüloz asetat membranlar üretilmiş ve ardından alkali hidroliz yöntemi ile selüloz membranlar elde edilmiştir.

Membranlar; %20-30 derişim aralığında selüloz asetat, çözücü olarak dimetil sülfoksit (DMSO), ortak çözücü olarak aseton ve gözenek oluşturucu olarak polyethylen glycol (PEG) içeren polimer çözeltilerinin dökülmesi ile üretilmiştir. Fotolitografi atıklarının saflaştırılması uygulamalarının öncesinde yüksek tutulum ve makul bir geçirgenlik performansına sahip membranların elde edilmesi amacıyla; polimer, ortak çözücü, gözenek oluşturucu kompozisyonları ve koagülasyon banyosu sıcaklığı değiştirilerek ve tavlama işlemi uygulanarak performans optimizasyonu gerçekleştirilmiştir. Membranların ayırma performansı molekül ağırlığı ayırma sınırı analizleri ile test edilmiş ve bu testler ilk olarak sulu ortamda gerçekleştirilmiştir. Daha sonra, DMSO ve metanol ortamında membranların farklı çözücülerde molekül ağırlığı ayırma sınırı performansındaki deęişim incelenmiştir.

Molekül ağırlığı ayırma sınırı testlerinde, farklı molekül ağırlığına sahip PEG molekülleri filtrasyon testlerinde kullanılmış ve analizler için, Jel Geçirgenlik Kromatografisi yöntemi uygulanmıştır. Suda gerçekleştirilen molekül ağırlığı ayırma sınırı testlerinde, farklı membranlara ait molekül ağırlığı ayırma sınırı aralığı 3-10 kDa olarak belirlenmiştir. Öte yandan; DMSO, su ve metanol ortamında karşılaştırma amacıyla yapılan molekül ağırlığı ayırma sınırı testleri sırasıyla 1.3, 3 ve 5 kDa değerleriyle sonuçlanmıştır.

Fotolitografi, mikroelektronik aletlerin fabrikasyonunda yaygın olarak kullanılan bir yöntem olup işlem aşamalarında kısa devre arızalarının engellenmesi için metal içermeyen yüksek saflık düzeyine sahip çözücülerin kullanımını gerektirmektedir. Bu çalışmada, tab banyosunun sentetik olarak elde edilmesinde 0.5-2.5 g/L konsantrasyonunda SU-8 fotorezisti içeren propilen glikol monometil eter asetat (PGMEA) çözeltileri hazırlanmış ve selüloz ultrafiltrasyon membranları ile iki aşamalı filtrasyonda filtrelenmiştir. 1. ve 2. filtrasyon aşamalarının sonunda sırasıyla %91 ve %80 SU-8 tutulum değerleri ölçülmüştür. Ardından, iki aşamalı filtrasyonda elde edilen süzüntülerin karışımı fotolitografide test edilmiş ve geri kazanılmış PGMEA'de elde edilen desen sonuçları, saf PGMEA ile uygulanan fotolitografinin desen sonuçlarıyla karşılaştırılmıştır. Sonuç olarak, geri kazanılmış çözücü ile elde edilen desen umut vaat eden nitelikte olup; mikroelektronik endüstrisindeki büyük ölçekli uygulamalar için maliyet etkinliği, sürdürülebilirlik ve döngüsel ekonomi çerçevesinde kritik bir çıktı elde edilmiştir.

Anahtar Kelimeler: Membranlar, Selüloz, Ultrafiltrasyon, Fotolitografi, Moleküler Ağırlık Ayırma Sınırı

To my precious Mother & Father

and

My better half

ACKNOWLEDGMENTS

First of all, I would like to mention my special thanks to my advisor Assoc. Prof. Dr. Zeynep Çulfaz-Emecen for her support, vision, effort and mentorship. I am truly impressed and inspired by her innovative approach to issues. Thanks to her, my approach to science, research and engineering improved day by day.

I would like to remark and emphasize my gratefulness to my mother and father Nurcan & Adnan Savaş for all their endless and termless love, support, guidance and patience for all my career journey and everything. They raised me from every aspect to the point where I am, so I owe all my achievements to them. As the child of two engineers, I always wanted to be a chemical engineer and desired to study in Middle East Technical University (METU) because my mother also was alumni of METU Electrical – Electronics Engineering department. Hence, I am so happy that I realized my dream. Besides, I am thankful to my better half Fırat Alkan for all his lovely, supportive and appreciative approach to me and my effort during this challenging journey. I am so lucky to have my family for all their endless love and support, they always believed in me and my dreams.

To my colleagues, I would like to thank my labmates for all their support. Especially, I have learnt lots of things from Zeynep İmir and she always guided me in a lovely and patient way when I needed her. I would like to mention Toprak with all her energy and sympathy, she made me smile and supported me in any case. Besides, I would like to thank Ecem for her kind guidance and support. In addition, I also thank Begüm, Perihan, Onur, Seden, Ceren, Berk, Feyza, Fatma and Işın.

I would like also to mention my special thanks to Asst. Prof. Dr. Emre Büküşoğlu for all his support and The Scientific and Technological Council of Turkey (TÜBİTAK) for the grant of the project coded 218M509 related to my thesis study.

TABLE OF CONTENTS

| | |
|--|-------|
| ABSTRACT..... | v |
| ÖZ..... | vii |
| ACKNOWLEDGMENTS..... | x |
| TABLE OF CONTENTS..... | xi |
| LIST OF TABLES..... | xiv |
| LIST OF FIGURES..... | xv |
| LIST OF ABBREVIATIONS..... | xviii |
| 1 INTRODUCTION..... | 1 |
| 1.1 Membrane Classification and Transport Mechanism..... | 3 |
| 1.2 Membrane Filtration in Organic Solvent Media..... | 8 |
| 1.3 Cellulose as a Membrane Material for Filtrations in Organic Solvents... | 13 |
| 1.4 Cellulose Membrane Fabrication by the Alkaline Hydrolysis of Cellulose Acetate Membranes..... | 15 |
| 1.5 Morphology Control of the Cellulose Membranes..... | 16 |
| 1.5.1 Polymer Type and Composition of the Casting Solution..... | 16 |
| 1.5.2 Casting Solution Solvent Selection..... | 17 |
| 1.5.3 Pore Former Use in the Casting Solution..... | 18 |
| 1.5.4 Co-solvent Use in the Casting Solution..... | 20 |
| 1.5.5 Coagulation Bath Temperature..... | 24 |
| 1.5.6 Annealing after Coagulation..... | 24 |

| | | |
|-------|---|----|
| 1.6 | Molecular Weight Cut-off Tests for the Membrane Characterization..... | 26 |
| 1.7 | Solvent Waste Management in the Electronics Industry | 27 |
| 1.8 | Solvents in the Electronics Industry | 30 |
| 1.9 | Photolithography Process Steps and Photoresists..... | 35 |
| 1.10 | Aim of Study..... | 38 |
| 2 | EXPERIMENTAL METHODS | 39 |
| 2.1 | Materials | 39 |
| 2.2 | Preparation of the Membrane Casting Solution..... | 39 |
| 2.3 | Membrane Fabrication Procedure..... | 40 |
| 2.4 | Membrane Characterization and Performance Tests | 44 |
| 2.4.1 | Solvent Permeance Tests..... | 45 |
| 2.4.2 | Solute Rejection Tests | 46 |
| 2.4.3 | Molecular Weight Cut-off (MWCO) Tests | 48 |
| 2.5 | Sorption Tests | 50 |
| 2.6 | Swelling Tests..... | 50 |
| 2.7 | Gel Permeation Chromatography (GPC)..... | 51 |
| 2.8 | UV-VIS Spectrophotometry | 52 |
| 2.9 | ATR-FTIR Spectroscopy | 52 |
| 2.10 | Scanning Electron Microscopy (SEM)..... | 53 |
| 2.11 | Elemental Analysis | 53 |
| 2.12 | Photolithography Process Details | 54 |
| 3 | RESULTS AND DISCUSSION..... | 55 |
| 3.1 | Alkaline Hydrolysis of Cellulose Acetate Membranes..... | 55 |
| 3.2 | Membrane Morphology | 59 |

| | | |
|-------|---|-----|
| 3.3 | Membrane Characterization and Performance Tests..... | 62 |
| 3.3.1 | Effect of the Alkaline Hydrolysis of the PWP and Blue Dextran (20 kDa) Rejections..... | 62 |
| 3.3.2 | Effect of the Morphology Tuning Factors on the Pure Water Permeance and MWCO of Cellulose Membranes | 64 |
| 3.3.3 | Pure Solvent Permeance and MWCO Test Performance of Cellulose Membranes in Different Solvents | 70 |
| 3.4 | Photolithography Waste Purification | 78 |
| 3.4.1 | SU-8 Resin Elemental Analysis for Photo Acid Generator Concentration Detection | 79 |
| 3.4.2 | SU-8 and Photo Acid Generator UV-VIS Spectra..... | 80 |
| 3.4.3 | Pure PGMEA Permeance of the Membranes..... | 83 |
| 3.4.4 | PGMEA Permeance and SU-8 Rejection Performance During SU-8 Filtration Tests | 84 |
| 3.4.5 | Photolithography Performance of the Recovered Solvent..... | 90 |
| 4 | CONCLUSION..... | 93 |
| | REFERENCES | 95 |
| A. | Calibration Graphs | 117 |
| B. | Membrane Rejection Sample Calculation..... | 123 |
| C. | Membrane Surface SEM Images..... | 124 |
| D. | Elemental Analysis PAG Concentration Calculation..... | 125 |
| E. | SU-8 Calibration Mixture Concentration Calculation and Mixture Preparation | 126 |
| F. | Blue Dextran Rejection Results | 127 |
| G. | Hansen Solubility Parameters in Different Solvents..... | 129 |

LIST OF TABLES

TABLES

| | |
|--|-----|
| Table 1.1 Membrane filtration ranges based on pore size..... | 6 |
| Table 1.2 OSN membrane materials in the literature | 10 |
| Table 1.3 Casting solution compositions in the literature for CA membranes | 21 |
| Table 1.4 Photolithography Applications ^{150,151} | 35 |
| Table 1.5 Photolithography Steps ^{152,153} | 36 |
| Table 2.1 Membrane fabrication steps | 41 |
| Table 2.2 Membrane codes and casting solution compositions | 42 |
| Table 2.3 Membrane codes and applied processes during fabrication | 42 |
| Table 2.4 Photolithography process steps and details | 54 |
| Table 3.1 ATR-FTIR Spectra O-H /C=O Peak Area Ratios of the Cellulose Membranes Fabricated via Alkaline Hydrolysis at Different NaOH Concentration Solutions | 57 |
| Table 3.2. Solvent chemical structure, viscosity, swelling ratio of dense cellulose film, molecular weight, molar volume and pure solvent permeance data..... | 74 |
| Table 3.3 SU-8 resin elemental analysis percentages | 79 |
| Table B.1 Rejection calculation data..... | 123 |
| Table G.1. Hansen solubility parameters in different solvents..... | 129 |

LIST OF FIGURES

FIGURES

| | |
|--|----|
| Figure 1.1. Costs of waste classification..... | 1 |
| Figure 1.2. Membrane transfer mechanisms: Pore flow model (left side) and solution diffusion model (right side) | 3 |
| Figure 1.3. Membrane taxonomy chart..... | 5 |
| Figure 1.4. Integrally skinned asymmetric membrane structure..... | 6 |
| Figure 1.5. Ternary phase diagram ⁵ | 7 |
| Figure 1.6. Alkaline hydrolysis reaction..... | 15 |
| Figure 1.7. Molecular weight cut-off (MWCO) determination | 26 |
| Figure 1.8. Circular economy | 28 |
| Figure 1.9. Solvents with their functions in the microelectronics industry ¹²⁸⁻¹³⁰ .. | 30 |
| Figure 1.10. Solvent categorization by the solvent market annual size in the..... | 31 |
| Figure 1.11. Crosslinking reaction of SU-8 ¹⁶⁰ | 37 |
| Figure 2.1. Casting solution preparation steps..... | 39 |
| Figure 2.2. Dead-end filtration module..... | 44 |
| Figure 2.3. Crossflow filtration module..... | 44 |
| Figure 2.4. MWCO test in crossflow module | 48 |
| Figure 2.5. MWCO test in crossflow module | 51 |
| Figure 3.1. FTIR Spectrum of the Cellulose Acetate Membrane Sample | 56 |
| Figure 3.2. FTIR Spectrum of the Cellulose Membrane Sample Obtained in Aqueous 0.05 M NaOH Solution | 56 |
| Figure 3.3. ATR-FTIR spectra of CA30P10A10-AH..... | 58 |
| Figure 3.4. Cross-sectional SEM images of membranes | 61 |
| Figure 3.5. Pure water permeance comparison of cellulose acetate and cellulose membranes | 62 |
| Figure 3.6. Pure water permeance and Average MWCO trend of the membranes. | 64 |
| Figure 3.7. MWCO curves of cellulose membranes..... | 65 |
| Figure 3.8. Effect of annealing on permeate flux and salt rejection cellulose acetate reverse osmosis membranes ⁵ | 68 |

| | |
|---|-----|
| Figure 3.9. Pure solvent permeance vs. viscosity ⁻¹ data for CA25P10A10-AN-AH membrane | 70 |
| Figure 3.10. Pure solvent permeance vs. viscosity ⁻¹ data for CA20P10-AH membrane | 72 |
| Figure 3.11. MWCO test results in different solvents..... | 75 |
| Figure 3.12. DLS results of PEG20K in Methanol (left), Water (Middle) and DMSO (right)..... | 76 |
| Figure 3.13. UV-VIS spectra of PAG salt (in PGMEA) proportional to SU-8 concentration, SU-8 feed, 1 st and 2 nd stage permeates of SU-8 filtration, 0.025 wt% PAG salt in PGMEA (a), zoomed version of the main spectra (b) | 80 |
| Figure 3.14. Water and PGMEA permeance comparison of the membranes | 83 |
| Figure 3.15. SU-8 rejections and water MWCO values of the membranes | 84 |
| Figure 3.16. SU-8 rejection and PGMEA permeance of CA25P10A10-AH membrane during filtration..... | 86 |
| Figure 3.17. SU-8 rejection and PGMEA permeance of CA25P10A10-AN-AH membrane during filtration..... | 86 |
| Figure 3.18. SU-8 concentration path during filtration | 88 |
| Figure 3.19. SU-8 rejection and Permeance/PSP data at the end of filtration stages | 89 |
| Figure 3.20. Starry imprinted surface via photolithography before UV exposure .. | 90 |
| Figure 3.21. Microscope images of starry pattern after developer bath step with recycled solvent (upper right and bottom) and fresh PGMEA solvent (upper left) | 91 |
| Figure 3.22. SEM images of starry pattern imprinted by fresh developer solvent (left) and recycled solvent (right) | 91 |
| Figure 3.23. Starry pattern imprinted by fresh developer solvent (left) and recycled solvent (right) at x750 magnification | 92 |
| Figure A.1. MW(Da) vs. RT(mins) relation graph for the GPC calibration..... | 118 |
| Figure A.2. PEG 400 Da calibration graph..... | 118 |
| Figure A.3. PEG 2 kDa calibration graph..... | 119 |
| Figure A.4 PEG 6 kDa calibration graph..... | 119 |

| | |
|--|-----|
| Figure A.5. PEG 10 kDa calibration graph..... | 120 |
| Figure A.6. PEG 20 kDa calibration graph..... | 120 |
| Figure A.7. Blue Dextran 5 kDa calibration at 620 nm..... | 121 |
| Figure A.8. Blue Dextran 20 kDa calibration at 620 nm..... | 121 |
| Figure A.9. SU-8 Calibration at 277.5 nm..... | 122 |
| Figure A.10. SU-8 Solutions UV-VIS Spectra..... | 122 |
| Figure A.11. PAG Salt UV Spectrum (0.025 wt % PAG/PGMEA and 0.2405 g PAG in Liter PGMEA)..... | 122 |
| Figure C.1. SEM surface images of the membranes..... | 124 |
| Figure F.1. Blue dextran and PEG probes' rejection comparison..... | 127 |

LIST OF ABBREVIATIONS

ABBREVIATIONS

| | |
|-----------|---|
| μm | : Micrometers |
| AH | : Alkaline Hydrolysis |
| AN | : Annealed |
| ATR-FTIR | : Attenuated Total Reflectance Fourier Transform Infrared |
| CA | : Cellulose Acetate |
| DMAc | : Dimethyl acetamide |
| DMF | : Dimethyl formamide |
| DMSO | : Dimethyl sulfoxide |
| [EMIM]OAc | : 1-ethyl-3-methylimidazolium acetate |
| ISA | : Integrally Skinned Asymmetric |
| kDa | : Kilo Dalton |
| MWCO | : Molecular Weight Cut Off |
| NF | : Nanofiltration |
| NMP | : N-methyl-2-pyrrolidone |
| OSN | : Organic Solvent Nanofiltration |
| OSU | : Organic Solvent Ultrafiltration |
| PAG | : Photoacid Generator |
| PEG | : Polyethylene glycol |
| PGMEA | : Propylene glycol monomethyl ether acetate |
| PSP | : Pure Solvent Permeance |
| PVP | : Polyvinyl pyrrolidone |
| PWP | : Pure Water Permeance |
| SEM | : Scanning Electron Microscope |
| UF | : Ultrafiltration |
| UV-VIS | : Ultraviolet - Visible |

CHAPTER 1

INTRODUCTION

Separation processes account for 40-70% of the capital and operational costs in chemical processes.¹ The new methods with innovative process designs are developed by the accelerating studies on the separation processes because of the continuously increasing need of the world to recycle materials, treat wastes, and separate complex solutions.²

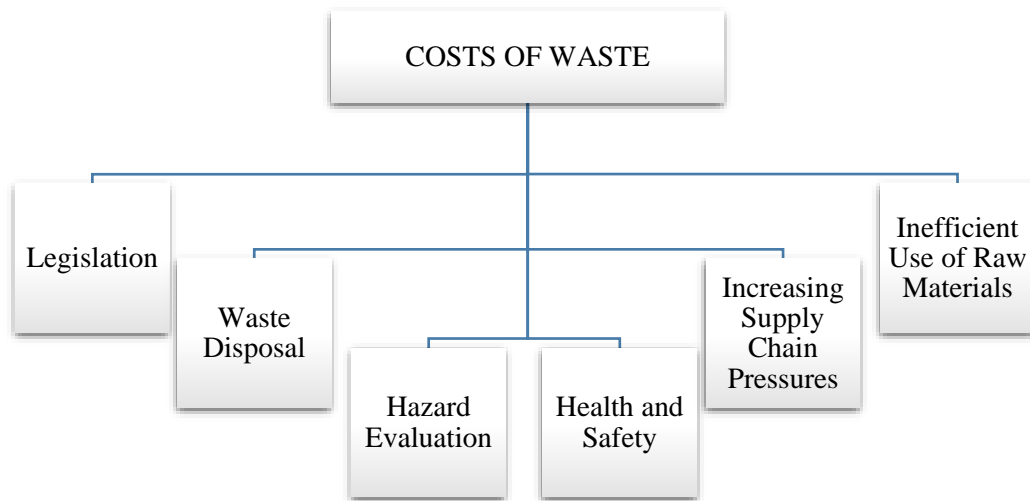


Figure 1.1. Costs of waste classification

As shown in the Figure 1.1., the costs of waste involve different pressurizing aspects like health, safety, environment and legislation in general.³ At this point, the role of the separation processes in different industries should be emphasized. From economical point of view, the separation processes in the industries like

pharmaceuticals and chemical production, have a significant portion of 40-70% of the total operating and capital costs.¹

Separation processes are used in wide range of applications in different industries to purify the chemicals and recover the targeted components. The most conventional separation methods are distillation, extraction and crystallization. However, more energy and material efficient methods are required according to the conventional methods. At this point, membrane applications gain importance as a more energy and material efficient technology. Membranes can be defined as semipermeable barriers which separate components according to distinguishing factors like size, charge, affinity to membrane or diffusivity in the membrane by the aid of a driving force such as pressure, concentration or electrical potential gradient.

The importance of membranes should be evaluated from sustainability aspect in addition to operational efficiency. From global framework, membrane technologies can be related to Sustainable Development Goals of United Nations. Membrane applications have a great potential to increase sustainability in the scope of “SDG 2-Zero Hunger, 3-Good Health, 6-Clean Water and Sanitation, 7-Affordable and Clean Energy, 8-Decent Work and Economic Growth, 9-Industry Innovation and Infrastructure, 12-Responsible Consumption and Production and 13-Climate action”⁴ with the applications in waste water treatment, pharmaceutical production, food production operations and all chemical recovery processes aligned to circular economy. The membrane application areas should be increased with these environmental, health and safety concerns to protect the environment, humanity and the biodiversity. In this study, cellulose UF membrane fabrication for the solvent recovery from photolithography waste, which is a process used in the manufacturing of microelectronics, was studied.

1.1 Membrane Classification and Transport Mechanism

The driving force of the membrane separation processes are mainly pressure, concentration and electrical potential gradient.⁵ Under the existence of driving force, the transport mechanism through the membrane occurs in the form of pore flow and/or solution diffusion models.

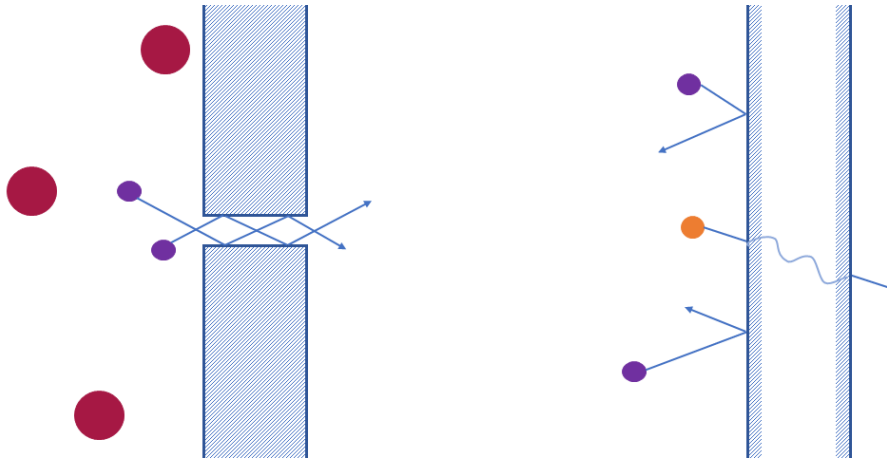


Figure 1.2. Membrane transfer mechanisms: Pore flow model (left side) and solution diffusion model (right side)

The pore flow model (left side) and solution diffusion (right side) transport models are illustrated in Figure 1.2. As can be seen in the figure, pore flow model is a size-based transport mechanism. By applying Hagen Poiseuille's equation shown in equation 1 in the pore flow model, the permeants pass through the cylindrical capillary pores, with diameter d , in the membrane with ε porosity and l thickness by the convective flow with the effect of the pressure gradient.⁵

$$J = \frac{\Delta P \cdot \varepsilon}{32 \cdot \mu \cdot l} \cdot d^2 \quad (1)$$

For the membranes for which pore flow model is applicable, the pore size of the membrane can be calculated via rejection of the membrane for probes with known radius by Ferry-Renkin equation shown in equation 2.

$$\text{Rejection} = \left[1 - 2 \left(1 - \frac{a}{r} \right)^2 + \left(1 - \frac{a}{r} \right)^4 \right] \times 100\% \quad (2)$$

In Ferry-Renkin equation, a and r represent for solute radius and pore radius, respectively.

On the other hand, solution diffusion model takes place with the dissolution and the diffusion of the permeants through the membrane driven by the concentration gradient.⁵ In this model, permeability showing the transmission of the permeants through the membrane material affects separation performance. Permeability of a species can be calculated by multiplying its partition coefficient, or solubility, in the membrane and its diffusion coefficient in the membrane. Permeance showing the transmission rate of the permeants through the membrane can be calculated by the permeability divided by membrane thickness.⁵

Membranes generally can be classified according to their pore size range, structure and material type. The subclasses of this classification are represented in Figure 1.3.^{5,6}

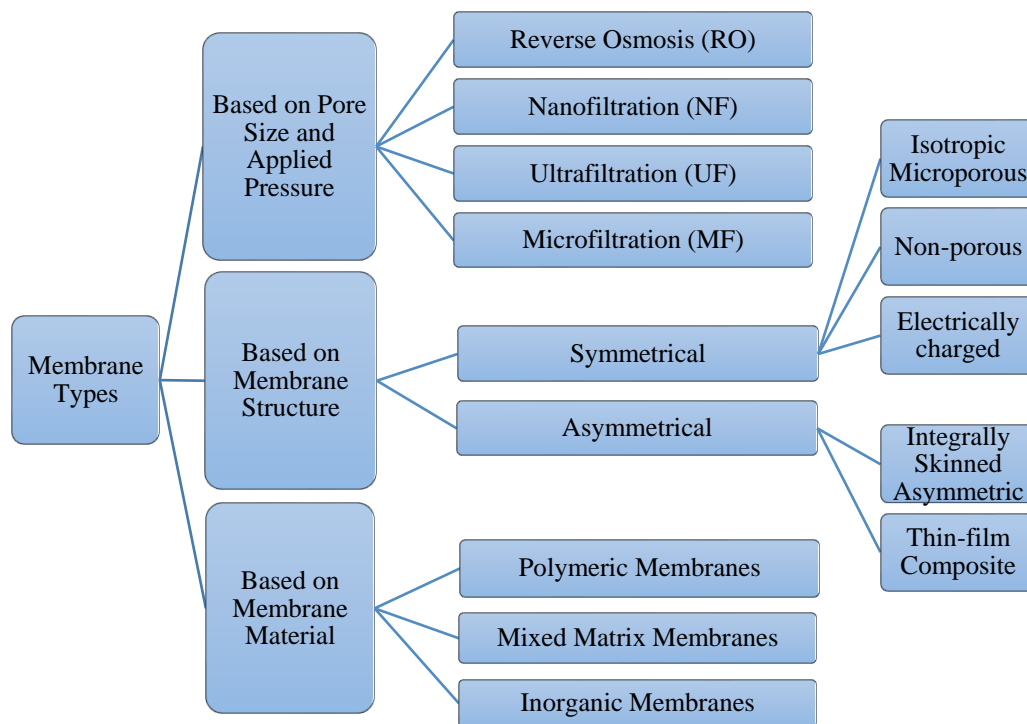


Figure 1.3. Membrane taxonomy chart

According to the pore size-based classification, the membranes can be divided into four major groups for the liquid phase separations as reverse osmosis (RO), nanofiltration (NF), ultrafiltration (UF) and microfiltration (MF) membranes. From transport model aspect, while solution diffusion model transport takes place in the RO membranes, pore flow model works in UF and MF membranes. Combination of pore flow and solution diffusion can be observed in NF membranes which are in the intermediate region. The pore size ranges and the separation applications commonly using these membrane processes are tabulated in Table 1.1.

Table 1.1 Membrane filtration ranges based on pore size

| Membrane Class | Pore Size Range⁷ | Separation Applications¹ |
|-----------------------|------------------------------------|--|
| Reverse Osmosis | < 1 nm (nonporous) | Monovalent ions |
| Nanofiltration | 1-2 nm | Multivalent ions, dyes, drugs |
| Ultrafiltration | 2-100 nm | Proteins, viruses, macromolecules |
| Microfiltration | >100 nm | Bacteria and suspended solids |

Based on membrane structure, membranes are divided into two main classes as symmetrical and asymmetrical membranes. The subclasses of symmetrical membranes are isotropic microporous, non-porous and electrically charged membranes. On the hand, the asymmetrical membranes have two subgroups as integrally skinned asymmetric (ISA) and thin film composite membranes. In this study, ISA type flat sheet cellulose membranes were fabricated. ISA type membrane structure is presented in Figure 1.4. As can be seen in the following figure, ISA type membranes have a selective denser top layer and more porous sublayer in the membrane structure. These membranes were firstly produced by Loeb-Sourirajan so, ISA membranes were also mentioned as Loeb-Sourirajan type membranes which are fabricated via phase inversion method.^{5,8}

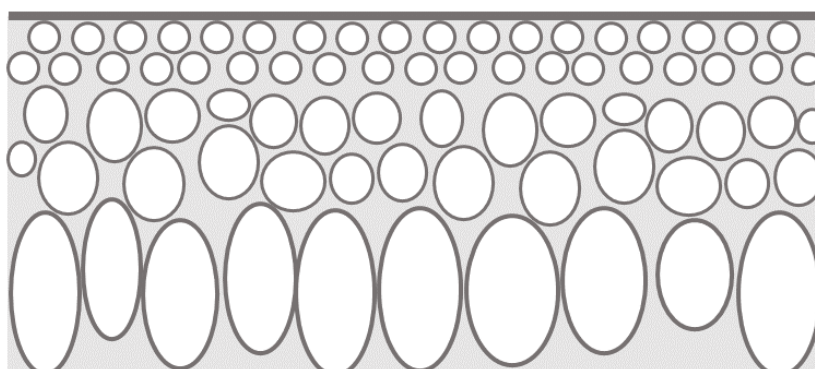


Figure 1.4. Integrally skinned asymmetric membrane structure

The phase inversion method can be applied by two methods as nonsolvent induced phase separation (NIPS) and thermally induced phase separation (TIPS) techniques.⁹ The ternary phase diagram relevant to NIPS type phase inversion method is illustrated in the Figure 1.5 with qualitative points for an exemplified NIPS process. In the scope of this study, NIPS type phase inversion method was applied while fabrication of cellulose acetate precursor membranes. Cellulose acetate, DMSO, water, acetone and polyethylene glycol (PEG) were used as polymer, solvent, nonsolvent, co-solvent and pore former respectively. After the fabrication of the cellulose acetate membranes, the membranes were regenerated into cellulose membranes via alkaline hydrolysis.

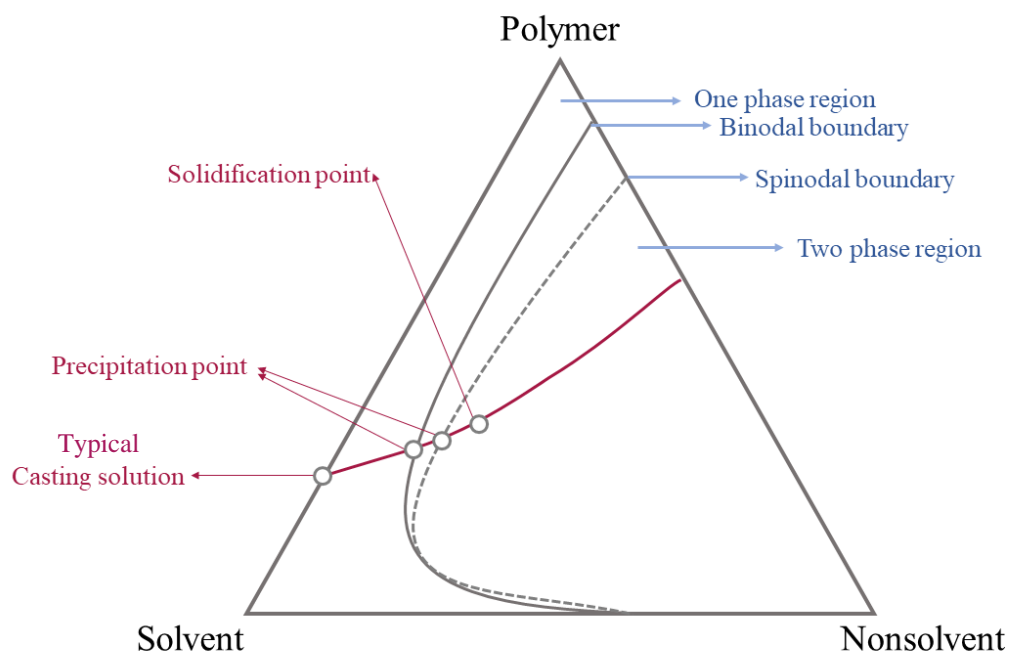


Figure 1.5. Ternary phase diagram⁵

1.2 Membrane Filtration in Organic Solvent Media

Organic solvents are used in wide range of industrial processes for different purposes. The industries mostly using organic solvents can be exemplified as petrochemical, polymer, dye, plastic, textile, pharmaceutical, agricultural product and electronics sectors.¹⁰ However, the separation, purification and recovery processes in organic solvent media are mostly challenging due to harsh operational conditions.

The conventional separation method mostly used in solvent recovery is distillation which is energy intensive. This both increases the cost and the environmental impact.¹¹ Thus, more energy efficient and cost-effective solutions which are easily scalable are necessary and membrane processes offer a promising alternative from these aspects.

Although the membranes are easily and widely used in aqueous media, their use in organic solvents and extreme conditions like highly acidic or basic, high temperature media medium is more challenging than the aqueous processes. The most important challenge is the membrane material.

From this point of view, ceramic and polymeric membranes should be investigated as convenient alternatives for organic solvent filtration processes with pros and cons to achieve the separation in challenging conditions. Ceramic membranes are especially appropriate for the processes consisting of harsh media and requiring high operation temperatures, but they are brittle and expensive.¹² On the other hand, the production of the polymeric membranes cost approximately 20% of the ceramic membranes and furthermore, the polymeric membranes are easily scalable are simpler to fabricate. However, the use of polymeric membranes is more challenging in organic solvent media and operations with high temperatures than ceramic membranes. So, the compatible polymer material selection and/or the additional applications such as crosslinking during the fabrication of polymeric membranes are needed.

As the polymeric type membranes, integrally skinned asymmetric (ISA) and thin film composite (TFC) membranes can be used in the organic solvent filtration processes, but ISA membranes are advantageous according to TFC membranes from cost aspect and ease of fabrication. Therefore, the separation processes with ISA membranes fabricated with phase inversion method should be improved and adapted to different industrial separation applications containing organic solvents.¹

In the literature, the organic solvent filtration processes are mostly in the nanofiltration (NF) range and different polymeric materials are used for organic solvent nanofiltration (OSN) processes. Polyacrylonitrile (PAN), polyimide (PI), polydimethyl siloxane (PDMS), polysiloxane (Psi), polyether ether ketone (PEEK), polyvinylidene difluoride (PVDF), polyaniline (PANI), polybenzimidazole (PBI) and polysulfone (PS) are the polymers commonly used in ISA type OSN membranes.¹ The literature examples of the applications using OSN are listed in Table 1.2 with the type of polymeric material.

Table 1.2 OSN membrane materials in the literature

| Reference | Membrane Material | Application |
|------------------------------|--------------------------|---|
| White et al., 2000 | PI | Lube Oil Solvent Recovery ¹³ |
| De Smet et al., 2001 | PDMS-PAN | Homogeneous and Heterogeneous Catalyst Recovery ¹⁴ |
| Vankelecom, 2002 | PDMS, Nafion | Polymeric Catalytic Membrane Reactor ¹⁵ |
| Scarpello et al., 2002 | PI, PDMS-PSi | Organometallic Catalyst Separation ¹⁶ |
| Sheth et al., 2003 | PDMS | Diafiltration for Solvent Recovery in Pharmaceuticals ¹⁷ |
| Bhosle et al., 2005 | PDMS-PI | Vegetable Oil Deacidification ¹⁸ |
| See Toh et al., 2007 | Crosslinked PI | OSN in Polar Aprotic Solvents ¹⁹ |
| Holda et al., 2013 | PS | Dye Filtration in Isopropanol ²⁰ |
| Valtcheva et al., 2014 | Crosslinked PBI | OSN in Acidic/Basic Environment ²¹ |
| Da Silva Burgal et al., 2015 | PEEK | OSN in DMF and THF ²² |
| Mertens, 2018 | Crosslinked PVDF | Dye Filtration in DMF ²³ |

As can be seen in the table, the OSN membranes were used in a wide range of applications. On the other hand, Organic Solvent Ultrafiltration (OSU) has a very recent history in the use of macromolecule and nanoparticle filtrations etc.^{24–28}

At this point, the difference between the OSN and OSU membranes should be considered. For OSN membranes, both pore flow and solution diffusion models are valid for the membrane transport mechanism. On the other hand, pore flow model is more dominant for OSU. As some of the main problems of the MF and UF membranes operations, concentration polarization and fouling are more severe in UF

and MF membranes compared to NF. So, these problems require intense focus for OSU according to OSN membranes as a research interest.²⁹

As mentioned before, most of the OSU membrane applications are very recently published except few studies. Polotskaya et al. studied on the polyimide UF membranes which were resistant to organic solvents and proved their resistance against harsh organic solvents like amide solvents and swelling in 2009.²⁴ In the study of Pulido et al., thermally crosslinked polytriazole, polybenzimidazole and polyoxindolebiphenylene membranes crosslinked with hot glycerol were tested at 140°C in DMF and it was shown that they kept their stability.³⁰ In another study, Melo et al. used ceramic UF membranes for the filtration of isopropanol-oil miscella in ethanol and higher than 90% rejection was obtained with 5-20 kDa membranes.³¹ Firstly in 2018, Organic Solvent Ultrafiltration (OSU) was mentioned in the literature by Yuan et al, which was on TFC type polyarylene sulfide sulfone (PASS) membranes decorated by nanoparticles .³² In the study, the rejection of PASS membranes was measured as 94%, 85% and 74% for Direct Red 23, Reactive Blue 2 and Reactive Orange 16, respectively.

In 2019, Yang et al. studied on the fabrication and characterization of polyimide UF membranes which were solvent and acid resistant.²⁶ In this study, the resistance of the membrane to HCl as acid and acetone, toluene, methanol and n-hexane as organic solvents was tested and it was reported that the performance of the membrane was not significantly affected and the BSA rejection values were kept above 95% level. In another study published in 2019, Jin et al. produced solvent resistant crosslinkable polyaryletherketone (PAEK) UF membranes via phase inversion method and showed that the membranes were resistant to even polar aprotic solvents.³³ In 2020, Yin et al. published two articles about a study on OSU membranes, which were focused on the fouling behaviour.^{27,28} In the studies, PAN UF membranes were tested with acetonitrile, toluene, n-hexane, acetone, ethanol, ethyl acetate and methanol organic solvents and aluminum, TiO₂, SiO₂ colloidal foulants.

In a study published in 2021, hybrid membranes consisting of fungal chitin nanofibers and cellulose were used in the determination of water and organic solvent permeance showing the ethanol and THF permeance of these membranes.³⁴ As a result, they observed up to 50, 40 and 20 L/h.m².MPa permeance levels for water, THF and ethanol, respectively. In another study, Tohidian et al. fabricated solvent resistant crosslinked polyetherimide (PEI) UF membranes for the two step filtration of water-toluene mixture. The crosslinking was done with diamine reagent and approximately 95% toluene rejection was measured.³⁵ In this study, the membranes fabricated were cellulose OSU membranes tuned for the solvent recovery application from the photolithography wastes, which has previously not been done using membranes.

1.3 Cellulose as a Membrane Material for Filtrations in Organic Solvents

Polysulfone (PS), cellulose acetate (CA), polyacrylonitrile (PAN), polyvinylidene fluoride (PVDF) and cellulose are the main materials commonly used for membrane fabrication.¹² The increasing need to renewable sources and the threat of environmental pollution make the utilization of natural polymers more crucial to create new materials and applications. Furthermore, cellulose with no further modification or treatment has excellent stability in even the harshest polar aprotic solvents.

Cellulose, chitosan and chitin are in the forefront of sustainable biomaterials.³⁶ Cellulose as the most abundant polymer on earth is the most commonly used one among these. In most of the applications, cellulose should be dissolved to be shaped into a new material with different characteristics and properties. By the aid of these cellulose solutions, cellulose and cellulose based composite materials can be used to fabricate materials such as membranes, fibers, films, bioplastics, microspheres, beads, hydrogels and aerogels.³⁷ Ionic liquids like [EMIM]OAc, [EMIM]Cl, LiCl/DMAc, molten inorganic salt hydrates, metal complex solutions, *n*-methylmorpholine-*n*-oxide (NMMO), tetrabutyl ammonium fluoride/DMSO system, aqueous NaOH, NaOH/thiourea and alkali/urea solutions were used to dissolve the cellulose in the literature.³⁷⁻⁴⁰

Solvent resistance of cellulose creates a potential in wide range of industrial applications. Because of the intermolecular and intramolecular hydrogen bonding in the cellulose structure, it does not dissolve in most of the protic and aprotic solvents which dissolves most of the synthetic polymer based membranes.^{36,40-43}

There are no examples of the OSU applications with cellulose membranes in the literature. However, there are studies about OSN applications of cellulose membranes. Anokhina et al. studied on cellulose based OSN membranes and obtained 76% Remazol Brilliant Blue R rejection with 0.40 kg/m².h.bar DMF permeance.⁴⁴ Falca et al. studied on cellulose hollow fiber membrane filtrations for

dye solutions. The highest rejections were obtained with 90% and 100% Congo Red dye rejections in ethanol and water, respectively.⁴⁵ Durmaz et al. produced cellulose membranes cast from cellulose-[EMIM]OAc mixtures and obtained 80% Bromothymol Blue and 90% Blue Dextran (20 kDa) rejections and in ethanol.³⁹ In another study in our research group, Sukma et al. fabricated cellulose membranes from cellulose - [EMIM]OAc mixtures and Bromothymol Blue rejection as 69.8% with accompanying ethanol permeance of 8.4 L/m².h.bar was obtained with the membrane cast from the casting solution having 12% cellulose dissolved in [EMIM]OAc as solvent and acetone as co-solvent with pre-evaporation step.⁴⁶ The highest rejection was obtained as 94% with accompanying ethanol permeance of 0.3 L/m².h.bar with the membrane cast from 20% cellulose, 80% [EMIM]OAc solution and dried after coagulation, in the study of Sukma et al. Konca et al. produced cellulose membranes crosslinked via 1,2,3,4-butanetetracarboxylic acid and cast from 12% cellulose, 25% acetone as co-solvent and 63% [EMIM]OAc casting solutions and 93% Rose Bengal dye rejection in DMSO was obtained with crosslinked cellulose membrane.⁴⁷

In this study, cellulose acetate membranes were firstly produced and then regenerated into cellulose UF membranes. The membranes were tested in the MWCO tests in several solvents with PEG probes and SU-8 photoresist filtration tests in propylene glycol monomethyl ether acetate (PGMEA) solvent. As the first step of the study, the tuning procedure of the cellulose membranes are done, and promising results are obtained in the OSU applications in the concept of study.

1.4 Cellulose Membrane Fabrication by the Alkaline Hydrolysis of Cellulose Acetate Membranes

In most of the studies in the literature, cellulose membranes were fabricated from cellulose-ionic liquid casting solutions via phase inversion. However, this method has some disadvantages like the high viscosity and cost of the ionic liquids. Actually, the use of casting solutions containing cellulose as the polymer is not the only way of the cellulose fabrication. By fabricating cellulose acetate membranes, it is also possible to produce cellulose membranes via deacetylation of the cellulose acetate membranes with alkaline hydrolysis. The alkaline hydrolysis process including the removal of the acetate groups takes place in an alkaline medium and this alkaline medium used for the regeneration process in the literature changes. The alkaline hydrolysis process is shown in the Figure 1.6.

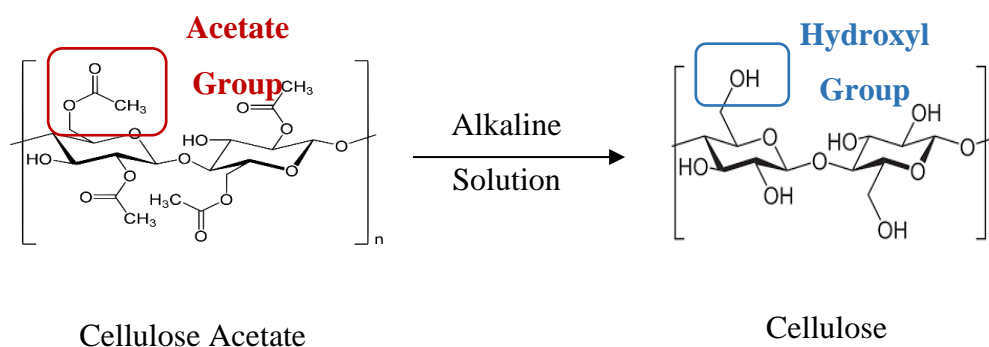


Figure 1.6. Alkaline hydrolysis reaction

In the literature, 0.05 M NaOH-water^{48,49}, 0.05 M NaOH-ethanol^{48,50}, 0.5 M KOH-ethanol⁵¹ solutions were used for the deacetylation of the fibrous membranes and cellulose acetate films. The required time for the complete deacetylation changes according to the concentration of the alkaline solution and it is possible to verify the degree of deacetylation by using FTIR analysis.

1.5 Morphology Control of the Cellulose Membranes

The morphology of the polymeric membranes made via NIPS is mostly affected by the polymer content, solvent type, co-solvent type, pore former agent used in the casting solution, the coagulation bath temperature and the annealing procedure applied after the coagulation process.⁵²⁻⁵⁴

1.5.1 Polymer Type and Composition of the Casting Solution

As one of the main factors affecting membrane morphology, polymer type and the concentration in the casting solution should be considered. In the literature, it was shown that the porosity of the membranes fabricated via Loeb-Sourirajan phase inversion method decreases with the increasing polymer composition in the casting solution.^{5,55-57} This is typically accompanied by a decreasing pore size. In the literature, Madaeni et al. showed that the increase in the polymer content of the casting solution resulted in a change in pore size and a significant permeance decrease with PVDF (polyvinylidene difluoride) membranes.⁵⁸ Sani et al. reported that the solvent permeance decreased and the rejection of dye increased with increasing PPSU (polyphenylsulfone) concentration in the casting solution with the performed solvent resistant nanofiltration applications by using ethanol, isopropanol, methanol as solvents and increasing polymer concentration from 17% to 25%.⁵⁹ Holda et al. stated that the Rose Bengal rejections were doubled and isopropanol permeances were dropped to 10% of the initial permeance with an increase in PS (polysulfone) composition in the casting solution from 13% to 25%.²⁰ İmir et al. observed that the rejection of PES (polyethersulfone) in NMP decreased with the decreasing CA composition in the casting solution.⁶⁰ By the same way, the polymer content of the casting solution was varied to tune the membrane characteristics to improve the rejection performance of the cellulose membranes in this study.

1.5.2 Casting Solution Solvent Selection

The solvent type used in the membrane casting solution affects the morphology and the performance of the membrane. Even if the polymer type used in the membranes are the same, the filtration range can differ according to the solvent because interactions between the casting solution solvent and polymer, co-solvent, pore former, coagulation bath nonsolvent affect the membrane separation performance with the changing pore sizes and interconnections between pores. While analyzing the polymer-solvent interactions, it should be considered whether the selected solvent is good solvent for the polymer or not. If the solvent is good solvent for a polymer, the polymer coils are in more enlarged form.⁶¹

In general, weak solvent use in the casting solution cause slow demixing and symmetrical, microporous structure and good solvent lead to asymmetrical membrane having skin layer and macrovoids. In literature, Tsai et al. studied on the effect of solvent quality on the morphology of membrane fabricated via NIPS method. It was shown that poor solvent use such as 2-pyrrolidone resulted in highly porous polysulfone (PS) membranes having interconnected pores compared to the membranes cast from n-methylpyrrolidone solution as a good solvent.⁶² Yeow et al. showed that use of weak solvents caused a sponge-like porous morphology while dimethyl acetamide (DMAc) as stronger solvent resulted in the formation of macrovoids for PVDF membranes.⁶³ Guillen et al. stated that it is only possible to reduce pore size of polyacrylonitrile (PAN) membranes in strong polar solvents like NMP, DMF and DMAc due to the poor solubility of PAN in most of the solvents.⁶⁴ In another study, PVDF membranes cast from trimethyl phosphate (TMP) solution, which is a poor solvent for PVDF, resulted in sponge-like structure, while the membranes cast from DMAc as a stronger solvent led to asymmetrical membranes.⁶⁵ Therefore, the different casting solution solvents used in the cellulose acetate membrane production in the literature are listed in the Table 1.3. The solvent of the casting solution in the experiments performed for this study was DMSO as a stronger

solvent and more environmentally friendly solvent alternative compared to other solvents like NMP, formamide etc.

1.5.3 Pore Former Use in the Casting Solution

The permeance-rejection trade-off is one of the most significant factors playing role on the selection of the membrane type when the separation application is especially for a known probe. To improve the permeance performance of the membranes, casting solutions additives are used in the literature with specific purposes. Pore former create one of the major groups of the casting solution additives. The purposes of the pore former additive use are to enhance porosity, improve the interconnectivity of the pores, to suppress the formation of macrovoids. Liu et al. stated that PVP, PEG, PEO, LiCl, ZnCl₂ and glycerol were used as the pore former agents in the literature and they used PEG as pore former in PES-NMP casting solutions to increase the water permeances of the membranes.⁵⁵ In another study, Ma et al. used PEG400 as pore former agent in polysulfone/clay-DMAc casting solution with the same purpose.⁶⁶ In the research of Roy et al., the effect of the pore former agent's molecular weight was investigated with PVC-DMAc and PVC-NMP UF membrane systems via PEG400, PEG4000 and PEG20000 Da. As a result, it was reported that the porosity of the membranes increased with increasing molecular weight of PEG pore formers.⁶⁷ In the study of Panda et al., it was searched for the effect of the molecular weight and the concentration of the PEG pore former in the casting solution with the experiments performed with PAN (polyacrylonitrile) membranes. Eventually, it was stated that the increase in the PEG molecular weight make the membrane more porous at the same concentration, BSA rejections were not so affected by the pore former use and still the lowest MWCO was measured with the low molecular weight pore former use by PEG200 and PEG400 additive usage.⁶⁸ Therefore, the use of low molecular weight pore formers can be a better option to obtain high permeance and low MWCO at the same time. Additionally, pore former agents with low molecular weight can be completely removed during coagulation

and it is advantageous because the solvent stability can be kept by this way. The pore former agents commonly used in the cellulose acetate membrane casting solutions were PEG and PVP in the literature.⁶⁹ Arthanareeswaran et al. found that both PVP and PEG additives to CA/PES blend polymer solutions increased the permeance with higher porosity but the PVP use decreased the egg albumin protein rejection more than PEG did.⁷⁰ In the light of such information, PEG400 additive use with 10% casting solution concentration was applied in this study.

1.5.4 Co-solvent Use in the Casting Solution

In membrane processes, an increase in the rejection performance is aimed without lowering the permeance. Co-solvent use followed by a pre-evaporation step before coagulation is one of the methods used for this reason to obtain a membrane having a tighter skin layer with increasing rejection. In the literature, there are different examples of co-solvent use, but cellulose and cellulose acetate membranes are especially searched for by considering the focus of this study. Acetone is one of the mostly used co-solvent additives for cellulose and cellulose acetate membranes because it is very volatile and not toxic. Kim et al. searched for the effect of the acetone addition as co-solvent on the cellulose acetate membranes fabricated from ionic liquid-polymer mixtures and it resulted in improved mechanical properties and better separation performance.⁷¹ In another study, CTA/CA based FO membranes prepared in 1,4-dioxane-acetone solvent mixtures were studied by Nguyen et al.⁷² It was reported that the reduction in the co-solvent ratio resulted in less evaporation of solvent and looser skin layer because of the higher volatility of acetone as co-solvent than the solvent by mentioning the study of Bokhorst et al..^{72,73} Sukma et al. also produced cellulose membranes by using acetone as co-solvent and 1-ethyl-3-methylimidazolium acetate ([EMIM]OAc) as the solvent of casting solution and it was reported that the dye rejection performances became better and ethanol permeances increased with the co-solvent use. So, acetone was added and pre-evaporated also in this study as co-solvent.⁴⁰

Table 1.3 Casting solution compositions in the literature for CA membranes

| Reference | Casting Solution Content | Performance |
|-------------------------------|---|---|
| Nunes et al., 1986 | CA and ternary solvent of acetone, acetic acid, water ⁷⁴ | - |
| Schwarz et al., 1989 | 17.5- 21% CA, Solvent: Acetone:Formamide (3:2 v%) ⁷⁵ | 85-91 % PEG rejection |
| Murphy et al., 1995 | 17% CA, 48-61% Acetone, 22-31% Formamide ⁷⁶ | - |
| Arthanareeswaran et al., 2004 | 10-21% CA 72-82%DMF 2.5-10% PEG 600 ⁷⁷ | BSA, EA and pepsin rejection of 77%, 64% and 49%, respectively |
| Ferjani et al., 2005 | 17-20% CA and Acetone/formamide (2:1) mixture ⁷⁸ | BSA, PEG and sucrose rejection of 80-99%, 77-94% and 51-66%, respectively |
| Duarte et al., 2007 | 45.77% Dioxane, 17.61% Acetone, 8.45% Acetic acid, 14.09% Methanol, 9.86% CDA, 4.22% CTA, 0.5% cellulose fibers in total content of polymer ⁷⁹ | 70-80% salt rejection |
| Arthanareeswaran et al., 2007 | 8.75-17.5%CA, 82.5% DMF and the rest is PVP or PEG 600 ⁸⁰ | 93% BSA rejection |
| Arthanareeswaran et al., 2008 | 17.5% CA 82.5%DMF ⁸¹ | 94% BSA and 80% trypsin rejection |
| Saljoughi et al., 2009 | 15.5% CA, 0-6% PVP, Solvent: NMP ⁸² | - |
| Cano-Odena et al., 2011 | 12-22% CA, 2.4-21%Methanol, 41-56% Dioxane, 20% Acetone ⁸³ | 92-98% Ibuprofen rejection |
| Nolte et al., 2011 | 7% CDA, 7% CTA, 45.7% dioxane, 17.6% acetone, 8.5% acetic acid and 14.2% methanol ⁸⁴ | 80-85% salt rejection |
| Medina-Gonzalez et al., 2011 | 16-20% CA, Solvent: Methyl Lactate ⁸⁵ | MWCO lower than 500 kDa |
| Ghaemi et al., 2012 | 17% CA, 1.5% PVP, Solvent: Acetone:Formamide (2:1 v%) ⁸⁶ | 70-98% DNSA and 50-90% PNP rejection |

| | | |
|-------------------------------|--|---|
| Rana et al., 2012 | 17% CA, 69.2% Acetone, 12.35% Water, 1.45% Magnesium Perchlorate ⁸⁷ | 23.5 L/m ² .h water flux, 87% NaCl Rejection, 60% Carbamazepine Rejection, 59% Ibuprofen Rejection, 85% Sulfamethazine Rejection |
| Krason et al., 2016 | 18% CA, 1-4% PVP, Solvent:DMF ⁸⁸ | 20% rejection for iron or copper solution |
| Afzal et al., 2016 | The weight ratio of CA:PEG:Acetone:Distilled Water; 7.2:2.8:100:3 ⁸⁹ | 30% salt rejection |
| Waheed et al., 2016 | 10.4-10.2 % CA, 69-72.5% Acetic Acid, 6.2% PEG, 4.3-10.2% Glycerol, 4.5-6.8% Distilled water ⁹⁰ | 15.2% sugar selectivity for membrane having 6.2% PEG |
| Zhou et al., 2016 | 15% CA, 2% PVP, 83% DMAc ⁹¹ | 68.5 nm pore diameter |
| Rakhshan et al., 2016 | 20% CA, 45% Acetone, 35% Formamide ⁹² | 75-80% propazine, 80-95% atrazine, 90-100% prometryn, 90-100% MgSO ₄ Rejection |
| Da Silva Pereira et al., 2017 | 10% CA, 17% Acetic Acid, 23% Water, 50% Acetone ⁹³ | 214-1651 L/h m ² water flux range |
| Sprick et al., 2018 | 18% CA, 82% NMP ⁹⁴ | 12% salt rejection |
| Mulijani et al., 2018 | CA:Pluronic Ratio-80:20, Solvent: Acetone ⁹⁵ | Optical sensor membrane having ability to detect 1-30% ethanol concentration |
| Vaulina et al., 2018 | 20-25% CA, Solvent: Acetone, Additive: Formamide ⁹⁶ | 55.34 L/(m ² .h) water flux, 82% dextran rejection |
| Mulyati et al., 2018 | 17.5% CA, 0-10% PEG, Solvent: DMF ⁹⁷ | 50-60 L/m ² .h water flux, 30-35% rejection aqueous Cr(III) solution |

| | | |
|--------------------------|---|--|
| Durmaz et al., 2018 | 8% CA, 30.7-46 % [EMIM]OAc, 46-61.3%DMSO ³⁹ | 90% Blue Dextran (20 kDa) and 80% Bromothymol Blue rejection |
| Nu et al., 2019 | 18% CA, Solvent: DMSO or DMSO/Acetone Mixture (v/v 4:1) ⁹⁸ | 87.3% BSA rejection |
| Marbelia et al., 2020 | 13-22% CA, Solvent: DMSO ⁹⁹ | 95% BSA rejection |

1.5.5 Coagulation Bath Temperature

For the polymeric membranes fabricated via phase inversion method, the coagulation bath temperature is one of the morphology affecting factors. The coagulation bath temperature affects the thermodynamics of the membrane forming system as well as the diffusion rates of the solvent, co-solvent and pore former from the cast membrane during phase inversion process and plays a role in the formation of membrane morphology. As the coagulation bath temperature, the use of the room temperature conditions is common, but the change in the bath temperature is also applied for morphology tuning purposes in the literature.^{100,101} Holda et al. stated that the reduction in the coagulation bath temperature results in the suppression of macrovoid formation due to the decrease in the percolation capability of nonsolvent in the cast film.⁵⁴ Saljoughi reported that the permeance of cellulose acetate membranes decreased by %75 with a temperature reduction from 23°C to 0°C.¹⁰² Arthanareeswaran et al. and Mozia et al. used 10 °C of the coagulation bath medium for denser membranes.^{77,103} Costa et al. also used 0-3°C as the temperature conditions for the coagulation bath of the cellulose acetate membrane fabrication via phase inversion method to obtain denser membranes.¹⁰⁴

1.5.6 Annealing after Coagulation

Annealing is one of membrane morphology tuning factors for the polymeric membranes to improve the performance with the decrease in the free volume between polymer chains. Schwarz et al. and Aburideh et al. stated that annealing resulted in denser skin layer for cellulose acetate and polysulfone-cellulose acetate blend membranes, so it caused an increase in rejection and decrease in permeance.^{105,106} In another study, Mahendran et al. studied on cellulose acetate UF membranes and annealed them at 70, 80 and 90°C. They observed that water permeance decreased and bovine serum albumin (BSA) rejections increased with increasing annealing temperature.¹⁰⁷ Tahun et al. applied annealing to the cellulose

acetate membranes produced for brackish water treatment by NIPS method and observed that higher annealing temperature and greater annealing time caused denser skin layer.¹⁰⁸ Similarly, İmir et al. observed a permeance decrease and rejection increase by Bromothymol Blue filtration tests in ethanol.⁶⁰ In this study, annealing was done for similar purposes to improve the separation performance to obtain membranes with denser skin layer.

1.6 Molecular Weight Cut-off Tests for the Membrane Characterization

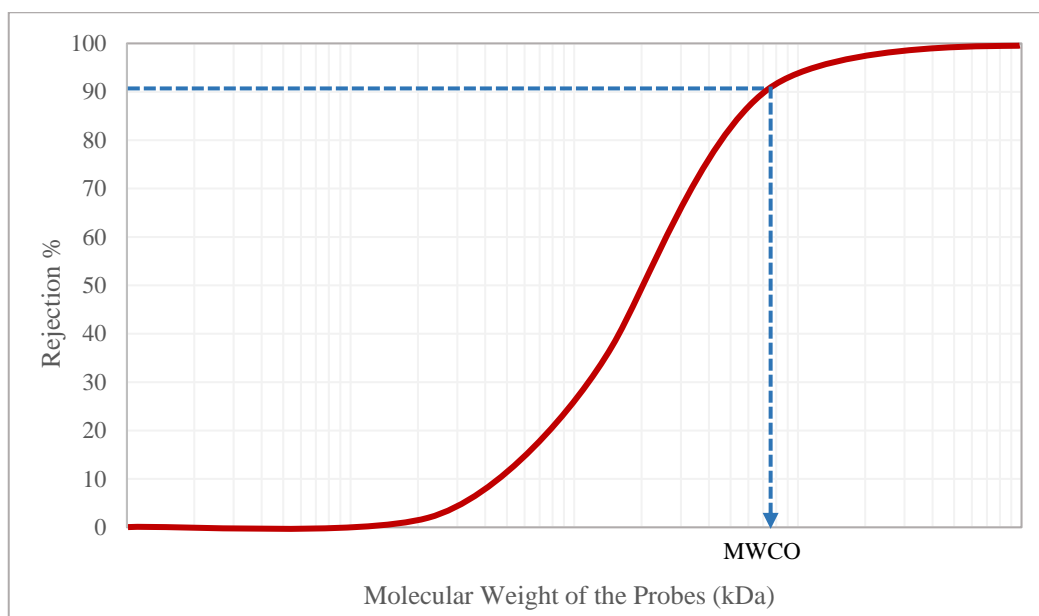


Figure 1.7. Molecular weight cut-off (MWCO) determination

Molecular weight cut-off (MWCO) test is a method which is applied to characterize UF membranes by the pore sizes and the rejection performances for the probes of different molecular weight values. The molecular weight cut-off value of a membrane states the lowest molecular weight value retained by the membrane with 90% rejection performance as shown in Figure 1.7. In the MWCO tests, the probe molecules are selected according to the desired molecular weight range, the solubility of the probes in the solvent in which the MWCO test is performed and the following specific filtration application concerns in the research. Due to the availability in the wide range of molecular weights, polyethylene glycol (PEG) and dextran probes are mostly used in the MWCO detection tests.^{109–112} In this study, PEG probes, in the related molecular weight range for the photoresist removal from the photolithography wastes, were used in the MWCO tests because of the solubility of PEG in water and polar organic solvents. The PEG probe usage in the tests made it possible to measure MWCO in the solvents like methanol and DMSO in addition to the aqueous systems.

1.7 Solvent Waste Management in the Electronics Industry

Solvents have a crucial role in industrial applications such as pharmaceutical, electronics, petrochemical and food industries. The solvent used in the metal cleaning, electronics industry, polymer production, cleaning and personal care products manufacturing follows the paint and coatings industry.¹¹³ The widespread usage and the consumption of industrial solvents require strategic waste management and waste minimization for especially the efficiency, environmental protection and cost-effective, sustainable industrial solutions aligned with the technical process feasibility needs. In today's world, the increasing consumption rates in almost every sector cause a huge amount of waste generation. Therefore, strategic and innovative waste management principles gain a significant role globally for sustainable development.

The framework regulations are also shaped for more sustainable industrial applications. The main aim is to minimize the adverse effects of waste generation from the human health and environmental point of view. According to EU Directive 2008/98/EC The Waste Framework Directive, there is a "Waste Hierarchy" for waste management. In the Waste Hierarchy, the first step contains the reduction and the prevention of the use of resources and raw materials if possible.^{114,115}

Reuse, recycling, recovery and disposal follow the prevention step, in order of priority in the Waste Hierarchy. Based on this hierarchy, fresh solvent use should be minimized via reuse, recycling and recovery. In addition, "Chemicals for the Green Deal" also emphasizes the importance of the recycling of chemicals from circular economy frame.¹¹⁶

To clarify the importance of solvent recycling, the carbon footprint reduction from fresh to recycled solvents were also studied in the report of ETHOS Research for European Solvent Recycler Group (ESRG). In the estimation process of the carbon footprint of the fresh and the recycled solvents, Life Cycle Assessment (LCA) method was used as an approach to analyze emission reductions.¹¹⁷⁻¹²⁰

Therefore, the solvent recycling processes were considered with the transportation of the waste solvents to the plant of recycling and the transportation of the recovered solvents to the new user of it. In the study, the data of the ESG member companies were used; categorized into simple non-chlorinated, chlorinated, mixed solvents groups and 308,750 tons/year recycled solvent was produced totally in 2017. As a result, the carbon footprint of the solvent usage was reduced by 85% from fresh to the recycled solvents in total. ¹²¹

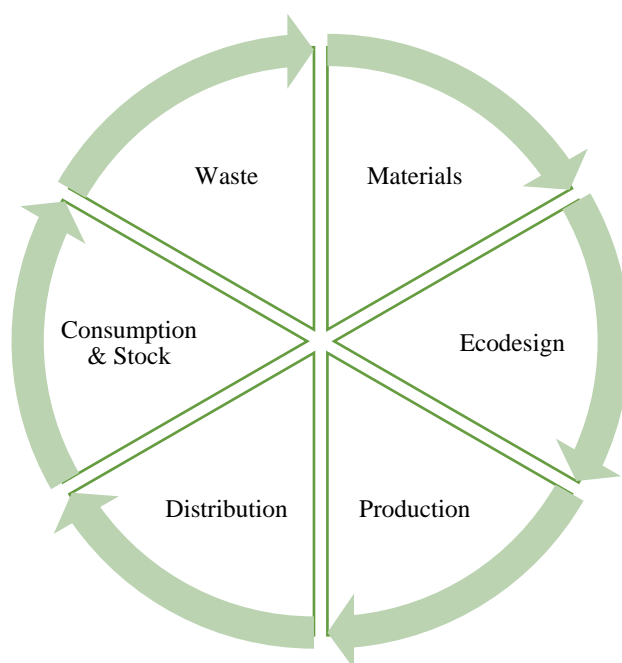


Figure 1.8. Circular economy

From another aspect, solvent recycling is a significant issue for the circular economy. The Circular Economy chart of the European Environment Agency is illustrated in Figure 1.8.¹²² Reduce, reuse, recycle and recover are known as 4R of the circular economy.¹²³ In the circular economy perspective, recycling of the waste materials and recovery of the energy are crucial to close the loop for sustainable consumption.
¹²⁴

Waste disposal should not be the general application if it is not inevitable. In waste management based on circular economy principles, end-of-waste-criteria was

proposed for the waste materials. Accordingly, if the recycled waste is safe for the environment and sufficient for the quality requirements, the best operation techniques for the recycling processes should be discovered and carried out after the environmental, economic and technical feasibility assessments. Additionally, EU Circular Economy Action Plan also states that the focus on the sectors, which are using the resources at most and having high circularity potential; such as electronics, batteries, plastics and buildings is required.¹²⁵ In general, the industrial usage of the solvents and their circularity are critical because they have a widespread application area in the industries using the resources at most. So, if the circular economy in the solvent recovery is considered, the steps can be stated as sourcing of the solvent from raw materials and recovery, manufacturing, distribution, use in the industrial applications and the recovery with the collection, sorting and recycling of the solvents by closing the loop. By this way, a reduction up to 90% of the CO₂ emissions is possible.¹¹⁶ Going further by focusing on the electronics and semiconductor industry emissions, it was determined that the release-to-air-ratio of the VOC solvents, which is the ratio giving the percentage of released solvent into atmosphere as VOC to the solvent input of application, in the industrial and cleaning applications in the electronics and semiconductor manufacturing sector is 70%. According to this data, most of the solvent is lost by the evaporation during the application and if the remaining liquid portion is also left as a waste and not recycled, sustainable consumption cannot be possible¹²⁶. In conventional recycling methods, the contaminated solvents coming from the pharmaceutical, chemical, surface cleaning, textile and paint industries are recycled by the processes based on distillation. The solvent recycling is not only important for the sustainability, but also significant for cost-effectiveness, reduction in the dependency on the availability and the primary production of the raw materials.^{116,127}

1.8 Solvents in the Electronics Industry

In the electronics and semiconductor industry, a wide range of solvents are used with different functions. The mostly used solvent types with their functions and annual market size in the European Economic Area in tons/year are listed in the following Figure 1.9. and 1.10.

| | |
|--|---|
| Etchants | <ul style="list-style-type: none">•1,2-Ethylenediamine 40% |
| Photoresist Developer | <ul style="list-style-type: none">•Propylene Glycol Monomethyl Ether Acetate (PGMEA)•Xylene |
| Photoresist Resin Solvent | <ul style="list-style-type: none">•Cyclohexanone•Cyclopentanone•Gamma-Butyrolactone |
| Semiconductor Rinse Applications | <ul style="list-style-type: none">•Ethylene Glycol |
| Adhesion Promoter of Silicon Wafer and Photoresist | <ul style="list-style-type: none">•Hexamethyldisilazane (HMDS) |
| Cleaning Agent | <ul style="list-style-type: none">•Isopropanol•Methanol |
| Photoresist Remover | <ul style="list-style-type: none">•N-Methylpyrrolidone (NMP)•Acetone•DMSO•Methyl ethyl ketone (MEK)•Photoresist Edge Bead Remover (PBR / EBR) |
| Semiconductor Process Chemical | <ul style="list-style-type: none">•n-Butyl Acetate |

Figure 1.9. Solvents with their functions in the microelectronics industry ¹²⁸⁻¹³⁰

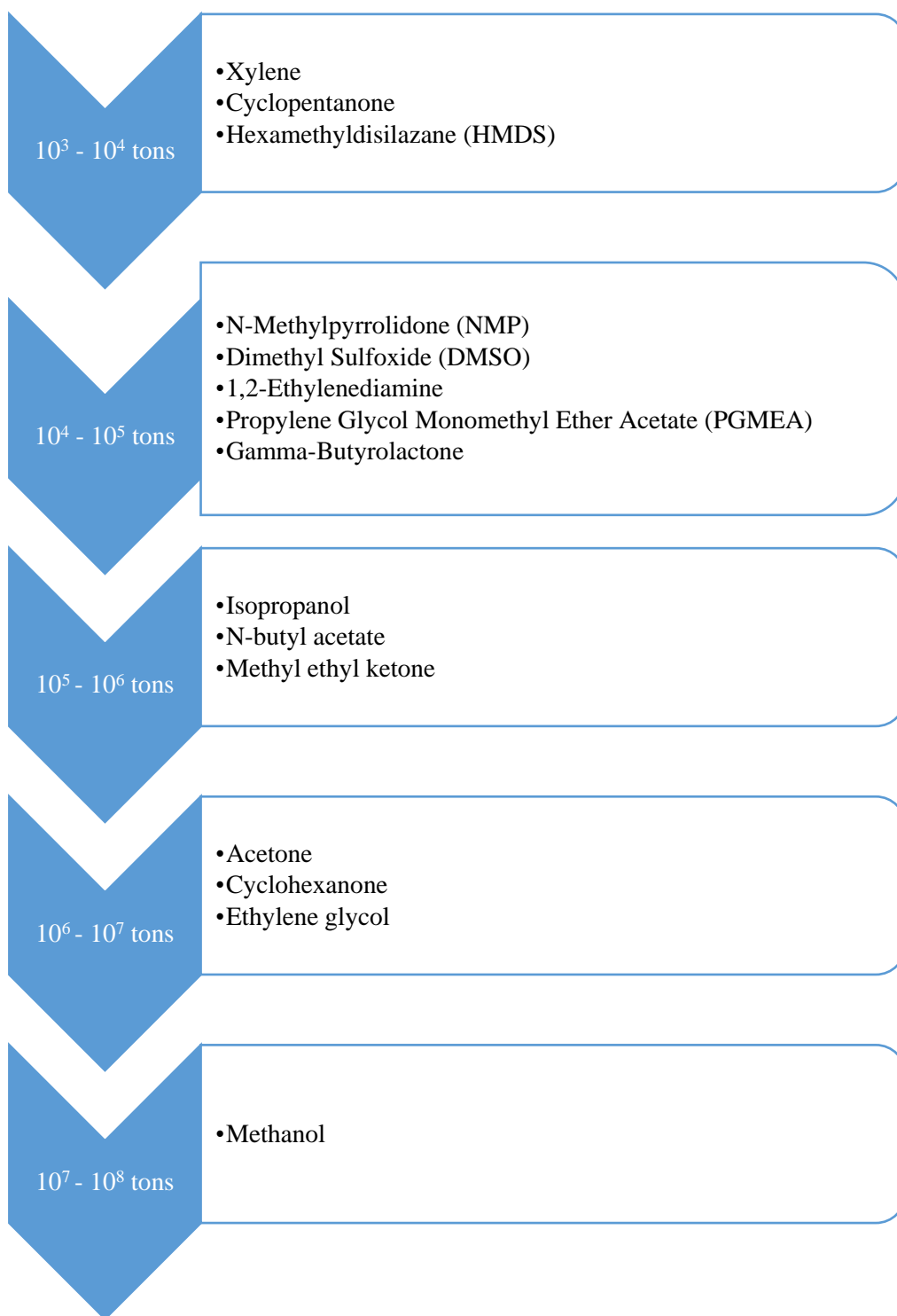


Figure 1.10. Solvent categorization by the solvent market annual size in the

European Economic Area ¹³¹

To apply the circular economy requirements, feasible solvent waste recycling applications and recovery services should be available in the market. These companies and services collect the waste, produce the recycled and recovered solvent with the required quality according to the industrial application needs and transfer the product to the company of the waste source or the new user. In the market, Maratek company works on recycling services with wide range of solvents like acetone, methanol, butanol, isopropanol, methyl ethyl ketone etc.¹³² If the electronics, microelectronics and semiconductor industries are studied with this perspective, there are some available industrial applications of the companies. For example, the recycled photoresist developer solvent propylene glycol monomethyl ether acetate (PGMEA) is produced with minimum of 98% purity from the waste of the various industries in Veolia company for the circular economy.^{133,134} In Industrial Technology Research Institute (ITRI), recycled electronic grade solvents are recovered from the wastes of the optoelectronics and semiconductor industries by dividing-wall column (DWC) distillation method.¹³⁵ In the literature, heterogeneous azeotropic dividing-wall column (HA-DWC) as the recovery technique for the semiconductor industry wastes was also studied and 33.1% reduction in the distillation energy requirement was achieved according to the conventional distillation methods for the more economical and environmentally efficient solutions.¹³⁶ As another example, Vikalp Group also purifies/refines the waste solvents of their clients according to their safety and quality needs with the required product specifications and returns back the recycled solvent to the client. One of the recycling solvents of the Vikalp Group is PGMEA and distillation is stated as the purification method.¹³⁷ In Shinko Organic Chemical Industry company, there are three different models for sustainability as recycling of the used solvent of the client and giving back the refined product, recycling the waste solvent of the user and selling it for other purposes in the market and grading up with refining the general industrial solvent for the new user from metal and impurity management sides. In the recycled solvent products portfolio of the Shinko Organic Chemical Industry company, PGMEA, PGME, acetone, methanol, IPA and NBAC takes

place.¹³⁸ In KMG Chemicals company, the electronics industry solvents like PGME, PGMEA, IPA, NBAC, acetone and methanol are produced in high quality. Besides, it is stated that the reuse of the out-off spec and excess materials is aimed and the materials are re-purposed for sale according to the new market of the downgrade product.^{139–141} Additionally, it was stated that 532912 pounds of waste containing PGMEA was shipped for reclamation in 2013, according to the Hazardous Waste Facility Permit document of IBM. Then, the reclaimed PGMEA was used by the other manufacturing companies being able to utilize the reclaimed solvent at that quality and purity level.¹⁴² As the last example of microelectronics industry solvent recovery, the applications and sustainability targets with their results of Infineon company can be examined. From waste management point of view, one of the sustainability targets of Infineon for 2018 was to keep waste generation under 27.5 gram level per cm² of produced wafer and it was shown that this target was achieved in 2018. The company also aimed to recover 300 tons of PGMEA from the waste containing PGMEA till the end of 2020 and 86.5% of this target was achieved by the recovery of approximately 260 tons of PGMEA solvent in 2018. Furthermore, the recovered solvent by distillation application via the cooperation with external contractors for recycling was reused in production.¹⁴³

To clarify the importance of the recovery of the solvents used in the microelectronics and semiconductor sector, the market volumes of the solvents should also be investigated. Generally, the market size of the electrochemical solvent industry is approximately 1 billion Euros.¹⁴⁴ Besides, the market volume of the aprotic solvents globally was approximately 15 billion dollars in 2015 and the industries mostly using aprotic solvents in the manufacturing processes are electronics, coatings, paints, pharmaceuticals and oil & gas sectors.¹⁴⁵ The market size data of the PGMEA and NMP can be given as examples. The world production capacity of NMP solvent 125000 tons per year.¹⁴⁶ The market volume of PGMEA was approximately 140 million dollars in 2020¹⁴⁷ and the solvent is used in the cleaner, varnish, paint and coating industry with 98-99% purity level and in the electronics industry with at least 99% purity level.

Currently available solvent recycling and purification techniques are mostly based on conventional distillation methods, which is very well established but energy-intensive. In microelectronics, acceptable impurity levels are very low and metal-free solvents are needed for fabrication processes. Solvent recovery with membranes can enable a once metal-free solvent to be recycled free of metal impurities throughout the whole process. As a result, more innovative, cost-effective and energy-efficient methods are needed, so membrane separations of the conditions meeting the purity level and permeance needs for the solvent purification can be used instead of the applications using distillation. Unlike incineration, the solvent waste streams can be recycled and the recovered solvents used in microelectronics manufacturing can be reused in the manufacturing by the successful membrane separation processes. In the case of the achievement of the desired process, it provides critical reductions in the material and energy consumption, financial needs, the generation of waste having hazards and risks. In “Solvent purification and recycling in the process industry using innovation membrane technology” (SOLVER) project studied by Vandezande et al., the recycling of the three different solvents, which are acetone, isopropanol and methanol, used in the semiconductor industry for cleaning purposes were aimed to be recovered from the wastes of the microelectronics industry.¹⁴⁴ Besides all these, there is no study in the literature for the PGMEA recovery from the photolithography wastes via membrane applications.

Additionally, the recovered PGMEA has a potential to be used in other industries even with lower purity than electronics industry limitations. PGMEA is a solvent widely used in surface coatings, ink, agrochemical, cleaner, anti-icing agents and extractant industries.¹⁴⁸ These sectors do not require that high level of purity, so the potential of recovered solvent use is promising even if it is not electronic grade.

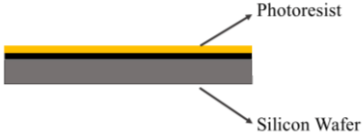

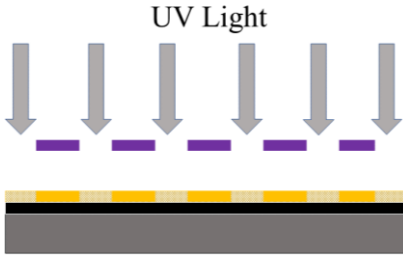

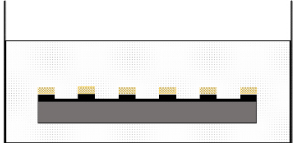

1.9 Photolithography Process Steps and Photoresists

Photolithography is a widely used technique for microfabrication to transfer geometric shapes on semiconductors in the microelectronics industry. The solvents and their quality used in the microelectronics industry have a significant role in the fabrication of microchips and integrated circuits. In order to produce high-quality microelectronic devices, electronic grade solvents are utilized in the processes of the microfabrication to avoid failures and short-circuits.¹⁴⁹ The reason behind the need for this quality level is that the solvents should contain metal ions under a critical level because the existence of metal ions over the threshold may cause short-circuit failures on the microchips. The industrial application areas of the photolithography and the process steps of the photolithography are summarized in the Tables 1.4 and 1.5, respectively.

Table 1.4 Photolithography Applications^{150,151}

| Industrial Applications of Photolithography |
|--|
| Photonics & Optic |
| Microsystems / Sensors |
| BioMEMS, Brain Sciences |
| Microparts / LIGA (a fabrication technology used to form high-aspect ratio microstructures) & Electroforming |
| Microfluidics |
| Semiconductor Manufacturing Fields |
| Micro-Lenses |
| Energy |
| 3D Printing |
| Photovoltaics Manufacturing |
| Flat Panel Display Manufacturing |

Table 1.5 Photolithography Steps^{152,153}

| Process Steps | Scheme | Process Details |
|--------------------------------------|---|--|
| Coating |  <p>The diagram shows a grey rectangular block representing a Silicon Wafer. A thin yellow layer, labeled 'Photoresist', is being applied to the top surface of the wafer.</p> | <p>The surface is coated by the required photoresist resin with a spin-coater.</p> |
| Solvent Evaporation (Soft Baking) |  <p>The diagram shows the silicon wafer with photoresist from the previous step. Above the wafer, several wavy yellow lines represent heat being applied during the soft baking process.</p> | <p>The solvent in the photoresist resin is evaporated by the soft baking application.</p> |
| Exposure |  <p>The diagram shows the silicon wafer with photoresist. Above it, a series of purple rectangular blocks represent a photomask. Grey arrows labeled 'UV Light' point downwards through the transparent regions of the mask onto the photoresist layer.</p> | <p>According to the desired pattern, UV exposure is applied via the transparent regions of the photomask. If a negative photoresist is used as a photoresist material, the regions exposed to UV light are crosslinked and become insoluble in the developer solution. On the contrary, if a positive photoresist is used, the regions become soluble under UV exposure.</p> |
| Developing Bath |  <p>The diagram shows the silicon wafer with photoresist submerged in a liquid bath. Yellow wavy lines represent the developer solution. Some of the photoresist is being dissolved and floating away from the surface.</p> | <p>The dissolved photoresist is removed from the surface by the photoresist developer and the desired pattern for etching is obtained.</p> |
| Etching |  <p>The diagram shows the silicon wafer with photoresist submerged in a liquid bath. The silicon wafer is being etched, creating a recessed area where the photoresist was.</p> | <p>The desired topography is provided by etching the surfaces without photoresist.</p> |
| Removal Bath |  <p>The diagram shows the silicon wafer with photoresist submerged in a liquid bath. The photoresist is being removed from the surface, leaving the final patterned silicon wafer.</p> | <p>In the removal step, the crosslinked photoresist is removed from the surface via the aid of removal solvent and the finalizing required pattern is obtained.</p> |

In this study, SU-8 which is a negative photoresist resin having eight epoxy groups in the chemical structure was used as photoresist resin. Propylene glycol monomethyl ether acetate (PGMEA) was used as the developer bath solvent in the photolithography. As photoacid generator (PAG) for crosslinking reaction, triaryl sulfonium hexafluoroantimonate salts were used.^{154–159}

In SU-8 photoresist crosslinking reaction, triarylsulfonium hexafluoroantimonate salts photoacid generators initiate the reaction under UV exposure and SU-8 crosslinking occurs after bond break of epoxy groups as shown in Figure 1.11.

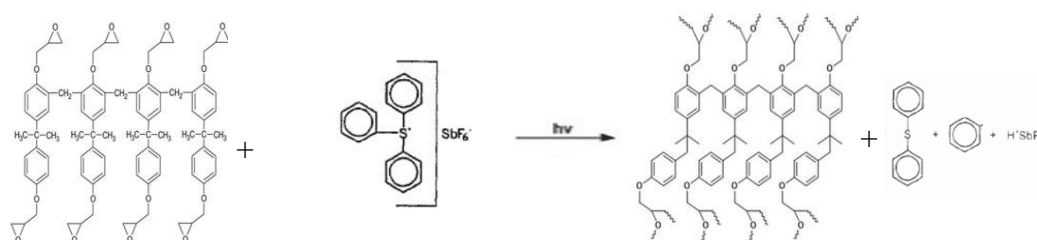


Figure 1.11. Crosslinking reaction of SU-8¹⁶⁰

Photoresists are generally used for the pattern transfer via photolithography, but they are also used as a structural material in nano and micro systems. SU-8 as a negative photoresist is also a structural material used in wide range of microelectronics applications.

As a material, the properties of SU-8 like low Young modulus and strong chemical resistance makes it advantageous for microelectronic and microfluidic systems.¹⁶¹ EPON SU-8 resist belonging to Shell Chemicals and the SU-8 series of MicroChem contain triaryl sulfonium salts as photoacid generator and the initiation of pattern imprinting takes place by this way under UV exposure. Besides, one of the SU-8 types was patented by IBM in 1989 so, it has a long history as a photoresist. In addition to all these features, the strong biocompatibility and chemical compatibility makes SU-8 suitable for labs-on-chips and microelectromechanical system (MEMS) applications.¹⁶²

1.10 Aim of Study

In this study, it was aimed to fabricate cellulose ultrafiltration membranes by phase inversion and alkaline hydrolysis of cellulose acetate membranes, to investigate the performance of the membranes in a variety of polar solvents and; to tune the morphology of the membrane to determine a suitable membrane for PGMEA solvent recovery from SU-8 photolithography wastes. MWCO and solvent permeance of the membranes were investigated. For the control of the membrane performance, the morphology affecting factors were tuned. In the second part of the study, the recovery of PGMEA from SU-8 photolithography waste were examined using these cellulose UF membranes. At the end, the change in the imprinted pattern quality and the success of the recycled solvent from membrane filtration compared to the fresh developer solvent were considered.

CHAPTER 2

EXPERIMENTAL METHODS

2.1 Materials

Cellulose acetate (Mn~ 50000 Da by GPC), acetone (99%), blue dextran (5 kDa and 20 kDa), polyethylene glycol (400 Da, 2 kDa, 6 kDa, 10 kDa, 20 kDa), propylene glycol monomethyl ether acetate (PGMEA), triarylsulfonium hexafluoroantimonate salts mixed with 50% propylene carbonate and sodium hydroxide (NaOH) were purchased from Sigma-Aldrich. Dimethyl sulfoxide (DMSO, 99.9%), methanol (99.9%), dimethyl formamide (DMF, 99.8%) and ethanol (99.9%) were purchased from Merck. For the photoresist filtration tests, SU-8 100 and SU-8 2075 from MicroChem brand were used in the experiments.

2.2 Preparation of the Membrane Casting Solution

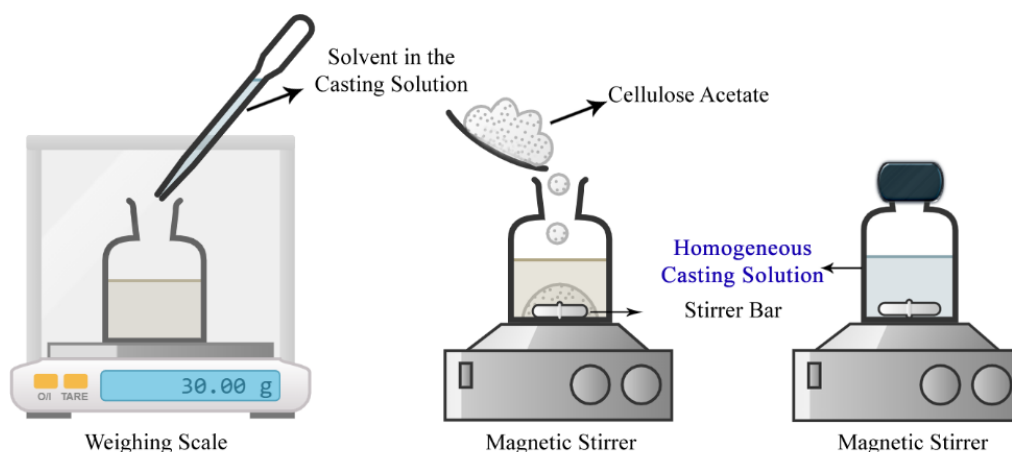


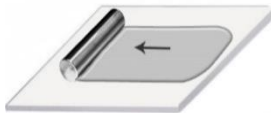
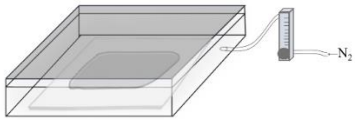
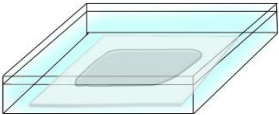

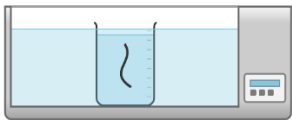

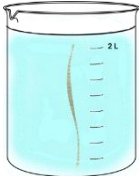
Figure 2.1. Casting solution preparation steps

In the membrane casting solutions, cellulose acetate (CA), dimethyl sulfoxide (DMSO), acetone and polyethylene glycol 400 Da (PEG400) were used as polymer, solvent, co-solvent and pore former agent, respectively. Before the casting procedure, cellulose acetate was dried under vacuum for at least two days. The contents except the polymer were mixed before the addition of the cellulose acetate, and a homogeneous mixture was obtained by using a stirrer. Then, cellulose acetate was added as the membrane polymer with a stirrer bar into the casting solutions as can be seen in the Figure 2.1 and the solution was mixed until it was homogeneous on the stirrer and roller if necessary.

2.3 Membrane Fabrication Procedure

The steps followed during the membrane fabrication are tabulated with the process illustrations and details in Table 2.1.

Table 2.1 Membrane fabrication steps

| | Process Scheme | Process Details |
|---------------------|---|--|
| CASTING |  | Cellulose acetate membranes were cast on the glass from the different casting solutions, with the stainless-steel casting bar having 250 μm casting thickness. |
| PRE-EVAPORATION |  | If the casting solution contained acetone as co-solvent, a pre-evaporation application was made in an N_2 bath with 0.6 L/min flow rate to the tank before the coagulation. |
| COAGULATION |  | The membranes were immersed into the non-solvent i.e., the water purified with reverse osmosis (RO) for the coagulation. |
| WASHING |  | The membranes were cleansed from the solvent by washing with RO water for 24 hours and changing the water three times in this process. |
| ANNEALING |  | For the annealed membranes, wet annealing was applied, and the membranes were annealed in the water bath at 85°C for 3 hours. This step was skipped for the other membranes. |
| ALKALINE HYDROLYSIS |  | The cellulose acetate membranes were put into the NaOH-water solution having 0.05 M concentration for the alkaline hydrolysis in order to obtain cellulose membranes. After 24 hours, the membranes were taken out of the alkaline solution. |
| WASHING |  | To stop the regeneration process and clean the membrane from the alkaline solution, the membranes were washed in the RO water for 24 hours. At the end, all the membranes were stored in the 20% ethanol- 80% water solution. |

The cellulose acetate and the cellulose membranes were fabricated according to the stated procedure and the membrane codes used in this study are listed in Table 2.2 and 2.3 according to the casting solution content and the fabrication steps.

Table 2.2 Membrane codes and casting solution compositions

| Membrane | Polymer % (CA) | Solvent % (DMSO) | Co-solvent % (Acetone) | Pore former % (PEG400) |
|-----------------|---------------------------|-----------------------------|-----------------------------------|-----------------------------------|
| CA20 | 20 | 80 | - | - |
| CA20P10 | 20 | 70 | - | 10 |
| CA25P10 | 25 | 65 | - | 10 |
| CA25P10A10 | 25 | 55 | 10 | 10 |
| CA30P10A10 | 30 | 50 | 10 | 10 |

Table 2.3 Membrane codes and applied processes during fabrication

| Membrane | Pre- evap. | Alkaline Hydrolysis | Annealing | Cool Coagulation Bath | Resulting Membrane Material |
|----------------------|-----------------------|--------------------------------|------------------|--------------------------------------|--|
| CA20 | - | - | - | - | CA |
| CA20P10 | - | - | - | - | CA |
| CA25P10 | - | - | - | - | CA |
| CA25P10A10 | + | - | - | - | CA |
| CA30P10A10 | + | - | - | - | CA |
| CA20-AH | - | + | - | - | Cellulose |
| CA20P10-AH | - | + | - | - | Cellulose |
| CA25P10-AH | - | + | - | - | Cellulose |
| CA25P10-AN- AH | - | + | + | - | Cellulose |
| CA25P10A10- AH | + | + | - | - | Cellulose |
| CA25P10A10- CC-AH | + | + | - | + | Cellulose |
| CA25P10A10- AN-AH | + | + | + | - | Cellulose |
| CA30P10A10- AH | + | + | - | - | Cellulose |

In summary, for the presented CAxPyAz type membrane codes; x,y and z show the percentages of the casting solution content for cellulose acetate, PEG400 and acetone, respectively. (-AH) code means the alkaline hydrolysis for the cellulose membranes and (-AN) code shows the annealing application. As explained in Table 2.1, the 30-minutes pre-evaporation step was only applied for the membranes containing acetone in their casting solutions.

2.4 Membrane Characterization and Performance Tests

The cellulose membranes were produced by tuning the casting solution content and the fabrication procedure. The characterization of the membranes was determined with the MWCO tests before the performance tests. In order to detect the membrane performances, the pure solvent permeances were measured and the rejection of the solutes was tested by the filtrations. For the blue dextran and SU-8 photoresist dead-end filtrations, Amicon stirred cell having 10 ml feed volume and Sterlitech HP4750 stainless steel cell were used, respectively. On the other hand, Sterlitech CF042A-FO, CF016A-FO acrylic and CF042-SS stainless steel crossflow membrane modules were used for the PEG filtrations of the MWCO tests. The schemes showing the dead-end and crossflow filtration systems are illustrated in the following Figure 2.2 and 2.3.

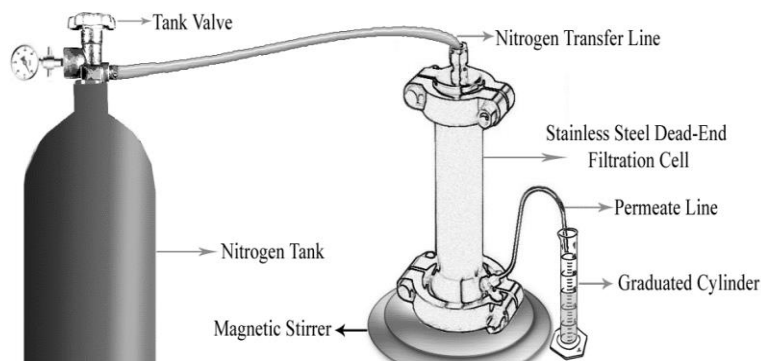


Figure 2.2. Dead-end filtration module

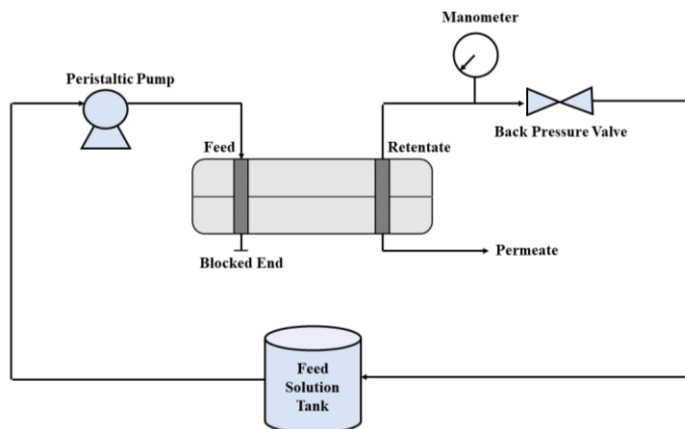


Figure 2.3. Crossflow filtration module

2.4.1 Solvent Permeance Tests

Pure solvent permeance performances of the membranes were tested before the filtration experiments. The collected permeate volume data per unit time were recorded at three different operation pressures until the fluxes were constant. The solvent flux values were calculated via the permeate volume against time and the active filtration area of the membrane. Finally, the pure solvent permeances (PSP) were calculated by the slope of the flux (J) vs. transmembrane pressure (TMP) graph. L/m².h.bar was used as the permeance unit in this study. The permeance calculation formula was shown below.

$$\text{Pure Solvent Permeance} = \frac{\text{Flux}}{\text{Transmembrane Pressure}}$$

Before the blue dextran and SU-8 photoresist filtrations, water and PGMEA solvent permeances were measured in the dead-end stirred cells, respectively. Additionally, the pure water, DMSO and methanol permeance tests were done before the MWCO tests via the crossflow filtration system.

2.4.2 Solute Rejection Tests

To detect the rejection performances of the membranes, different probes were used in the experiments. For the filtrations of Blue Dextran 5 kDa and Blue Dextran 20 kDa, Amicon stirred cell with 10 ml cell volume was used at 3 bar operational pressure with approximately 0.16 mM Blue Dextran 5 kDa and 0.04 mM Blue Dextran 20 kDa for the feed concentrations in water, separately. In the MWCO tests, the rejection performance data of the PEG probes were obtained. The feed solutions of the MWCO tests were prepared with 0.5 g/L concentration for each PEG probe in water. As the filtration system, Sterlitech CF042A-FO, CF016A-FO acrylic and CF042-SS stainless steel crossflow membrane modules were used for the MWCO tests and 0.3-0.5 bar pressure for water MWCO tests, 1 bar for solvent MWCO tests, were applied on the membrane.

For the SU-8 filtration tests, the synthetic feed solution preparation procedure was applied. In the beginning, SU-8 2075 resin was put onto approximately 2.5x2.5 cm² glass plate and the coating was done in a spin coater with the first ramp to 500 rpm with 100 rpm/s, the second ramp to 3000 rpm with 300 rpm/s, and the final spin speed application for 30 seconds. Then, the SU-8 on the glass was pre-baked at 65°C for 5 minutes and soft baked at 95°C for 20 minutes in a dark room to prevent light exposure on SU-8 material. The baking step was required to remove the solvent in the SU-8 resin. The whole procedure was performed by considering SU-8 coating instructions of MicroChem brand for SU-8 2075 with 100-micrometer coating thickness. After the coating process, the SU-8 coated glass plates were immersed in the PGMEA solvent to dissolve SU-8 and to prepare the synthetic SU-8 feed solution. This procedure mimics the photolithography process until the developing step. The nominal SU-8 concentration of the solution was determined by the calibration with the dissolved SU-8 in PGMEA from SU-8 coated glass with known nominal coating thickness and the feed solution was added into the filtration cell after the dilution of the SU-8 solution to the necessary photolithography waste solution concentration range.

In the solvent recovery tests of the photolithography wastes, SU-8 photoresist in PGMEA solvent with the 0.5-2.5 g/L concentration was used as the feed solution in the filtrations to mimic the real photolithography waste solution. In the filtration setup, Sterlitech HP4750 stainless steel cell was used and 10 bar pressure was applied for the SU-8 filtrations.

2.4.3 Molecular Weight Cut-off (MWCO) Tests



Figure 2.4. MWCO test in crossflow module

In order to detect the convenience of the cellulose membranes for the specific filtration applications, the characterization of the membranes was needed. For this study, Molecular Weight Cut-off (MWCO) tests were applied for the characterization procedure of the cellulose membranes fabricated by different methods and casting solutions. The crossflow module was used in the experiments as shown in Figure 2.4, and the operation pressure was controlled by a back-pressure valve. The applied pressure was 0.3 bar. Crossflow rate and velocity were 120 ml/min and 2.23 cm/s. The feed flow was supplied by the Watson Marlow brand peristaltic pump.

In the MWCO tests, the feed solution was prepared with different molecular weight PEG probes, each having 0.5 g/L concentration in the solution. In this study, PEG 400, 2000, 6000, 10000 and 20000 Da probes were added into the feed solutions. For the selection of molecular weights in the mixture, the peak overlaps in the GPC chromatograms were considered. At the beginning of the experiments, the feed solution analysis was done by Gel Permeation Chromatography (GPC) for

verification. Then, the permeate and retentate samples were taken into the GPC vials during the experiment and their concentrations were measured for further performance calculations.

2.5 Sorption Tests

To observe the interaction between the solute and the membrane polymer, the sorption tests were done. In this study, SU-8 sorption of the membranes was measured. Firstly, the cellulose membrane samples were sensitively wiped, and they were put into the 20 ml SU-8 photoresist – PGMEA solutions with known SU-8 concentrations. Then, the daily measurements of the SU-8 concentrations in the solution were done by using UV-VIS spectrophotometer until the solution concentrations reached the constant values. Whether the solute was sorbed or not was detected.

2.6 Swelling Tests

Before the performance tests of the membranes, the swelling test was applied to investigate the interaction between the solvent and the membrane polymer with CA20P10-AH, CA25P10A10-AN-AH and cellulose dense film cast from 20%CA 80% acetone solution with pre-evaporation followed by alkaline hydrolysis in 0.05 M NaOH_(aq) for 24 hours. The membranes were stored in 20% ethanol in ultra-pure water solution in this study. As the first step of the swelling test, the membranes were put out of the storage solution and completely dried. The dry weight values of the membranes were measured until they were constant. Then, the membrane samples were put into the solvent that was 20 ml in volume. The samples were weighed each day and the increase in the weight was recorded to observe the swelling behavior of different membranes. The daily measurements continued, and the swelling test was completed when the weights of the cellulose acetate and cellulose membrane samples were constant. In order to present the swelling behavior of the membranes quantitatively, the swelling ratio percentages were calculated, and the formula was shown below.

$$\text{Swelling Ratio \%} = \frac{(m_{\text{swollen membrane}} - m_{\text{dried membrane}})}{(m_{\text{dried membrane}})}.$$

2.7 Gel Permeation Chromatography (GPC)



Figure 2.5. MWCO test in crossflow module

The concentration analysis of the permeate and retentate samples collected during the filtration was performed by using Gel Permeation Chromatography (GPC) as shown in Figure 2.5. As can be seen in Figure 2.5, Agilent 1260 Infinity II GPC/SEC System was used with PolarGel-L type PL1120-6830 coded column for the analyses. In this system, the RI signal chromatograms were obtained with the refractive index detector (RID) and presented by the HPLC Online as the data output software. As the flow rate and operating temperature 1 ml/min and 30.5°C were used, respectively. The mobile phase of GPC was ultra pure water.

2.8 UV-VIS Spectrophotometry

The rejection calculations for the determination of the membrane performance were done by using the absorbance of the feed, retentate and permeate samples. The concentrations of the blue dextran and the SU-8 photoresist solutions in the filtration experiments were measured with Shimadzu UV- 1601 model UV-VIS Spectrophotometer. The solute concentrations were estimated with the calibration curves of each material by the raw absorbance data of the solute and the general mass balance was applied for the performance calculations. The absorbance measurement wavelength values were 277.5 nm and 620 nm for SU-8 and blue dextran probes, respectively.

2.9 ATR-FTIR Spectroscopy

The verification of the alkaline hydrolysis for the cellulose membranes was done by using the Attenuated Total Reflectance-Fourier Transform Spectroscopy (ATR-FTIR) analysis method with PerkinElmer UATR Two model ATR-FTIR analysis device in METU Chemical Engineering Department. For the ATR-FTIR method, the samples were dried in the fume hood and then under vacuum to eliminate the humidity effect on the peaks of the cellulosic bonds. Then, the absorbance measurements were done. For the determination of the extent of alkaline hydrolysis, the degree of deacetylation was determined by ATR-FTIR spectra of the membranes, and the required complete alkaline hydrolysis time was detected according to the disappearance of the peak coming from the acetate groups.

In addition, the cellulose membranes were dissolved in [EMIM]OAc and cast again from this solution for further verification of complete alkaline hydrolysis procedure to make sure that whole cross-section of the membrane was cellulose. Then, FTIR spectra of these membranes were analyzed.

2.10 Scanning Electron Microscopy (SEM)

Scanning electron microscopy was utilized to investigate the membrane structures and the morphologies cast from different casting solutions and exposed to various processes under the scope of this study. In METU facilities, the SEM analyses were performed with FEI Nanosem 430 model in METU Metallurgical and Materials Engineering Department and with QUANTA 400F model Field Emission type SEM in METU Central Laboratory.

In order to obtain clear SEM images, a preparation procedure was applied to the SEM membrane samples. For the scan of the membrane skin layers, the membranes were dried entirely and stored under vacuum. In the SEM analysis of the skin of the membranes, the active sides of the membranes were captured. In the membrane cross-sectional SEM analysis, an additional procedure was required. Therefore, the membranes that were frozen in the liquid nitrogen were broken in order to prevent the cross-sectional defects stemming from the cutting procedure. Then, the samples were stuck on the holder by the conductive type tape and finally, Au-Pd coating was applied for both skin and cross-sectional scans.

2.11 Elemental Analysis

For the photoacid generator content detection in SU-8 photoresist, elemental analysis method was used. The solvent content in the SU-8 resin was evaporated before the analysis to eliminate the misleading possibility of the elements in the solvent. The Elemental Analysis of the SU-8 resin sample was done via LECO, CHNS-932 device in the METU Central Laboratory and the atomic weight percentages of C, H and S elements were obtained.

2.12 Photolithography Process Details

In photolithography; the glass slide was coated by the SU-8 photoresist, the solvents in the resin were evaporated by the soft baking, the regions exposed to UV were crosslinked by the effect of the PAG, the non-crosslinked SU-8 was cleaned by the PGMEA. In Table 2.4, the photolithography process steps with applied experimental details were listed.

Table 2.4 Photolithography process steps and details

| Process Step | Process Details |
|---|---|
| SU-8 Spin Coating (for 110 μm thickness) | 1 st ramp to 500 rpm with 100 rpm/s acceleration and holding at this speed 5-10 seconds, then a 2 nd ramp to 2000 rpm with 300 rpm/s and holding for 30 seconds |
| Pre-bake & Soft bake | Pre-bake at 5 minutes at 65°C and soft bake at 20 minutes at 95°C |
| UV Exposure | UV exposure with i-line 365 nm radiometer (440 mJ/cm ²) for 11 seconds |
| Post Exposure Bake | Heating for 1 minute at 65°C and then 10 minutes at 95°C |
| Developer Bath | Immersing the sample to the PGMEA bath and waiting for 10 minutes |
| Rinsing and Drying | Briefly rinsing with isopropanol and then drying with a gently stream of nitrogen |

CHAPTER 3

RESULTS AND DISCUSSION

3.1 Alkaline Hydrolysis of Cellulose Acetate Membranes

In this study, cellulose membranes are formed from cellulose acetate membranes by alkaline hydrolysis. Compared to fabrication of cellulose membranes directly from cellulose solutions, this method provides easier ways for tuning the membrane morphology. This method is advantageous compared to the production using ionic liquids because of the high viscosity and cost of ionic liquids.

For the alkaline hydrolysis procedure of the cellulose acetate membranes, the optimization of the experimental conditions was done with the CA20 membrane. Four different NaOH concentration levels were specified in 0.001-0.05 M range, and the samples of the CA20 membrane were put into the NaOH solutions for alkaline hydrolysis. The extent of alkaline hydrolysis was monitored via Attenuated Total Reflectance – Fourier Transform Infrared (ATR-FTIR) spectroscopy analysis by the O-H bonds of the cellulose and the C=O double bonds of the acetate groups in the structure of cellulose acetate.

According to the FTIR results shown in Figure 3.1. and 3.2 for a completely regenerated membrane by alkaline hydrolysis, it was observed that the stretching vibration of the C=O double bond peak of the acetate group at approximately 1740 cm^{-1} disappeared, and the O-H bond peak of the hydroxyl group at 3000-3600 cm^{-1} wavenumber range representing the cellulose came up in the FTIR spectra.

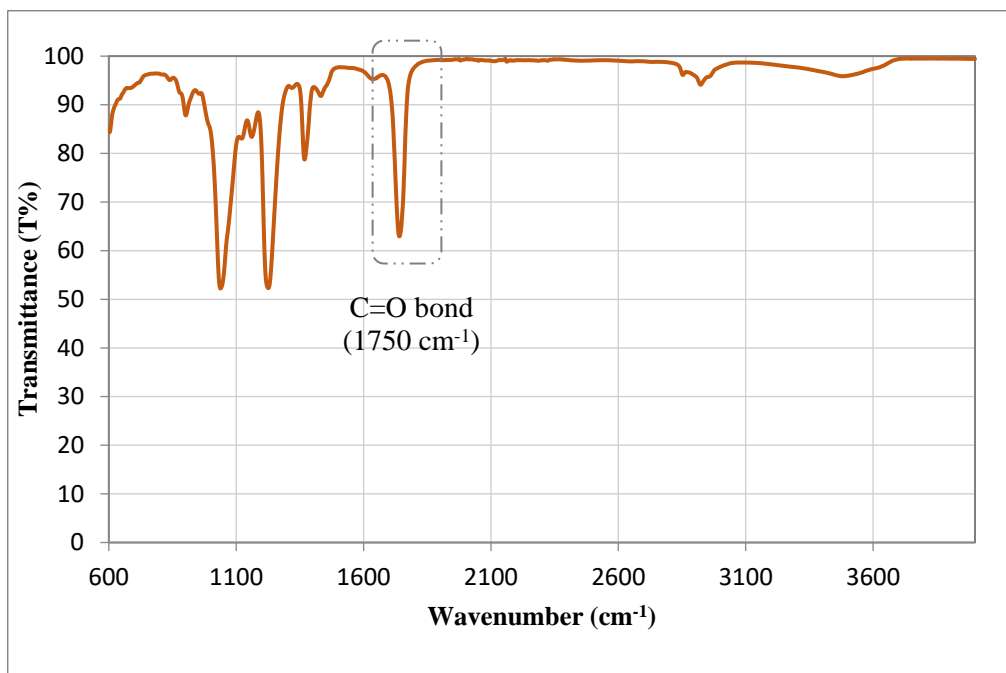


Figure 3.1. FTIR Spectrum of the Cellulose Acetate Membrane Sample

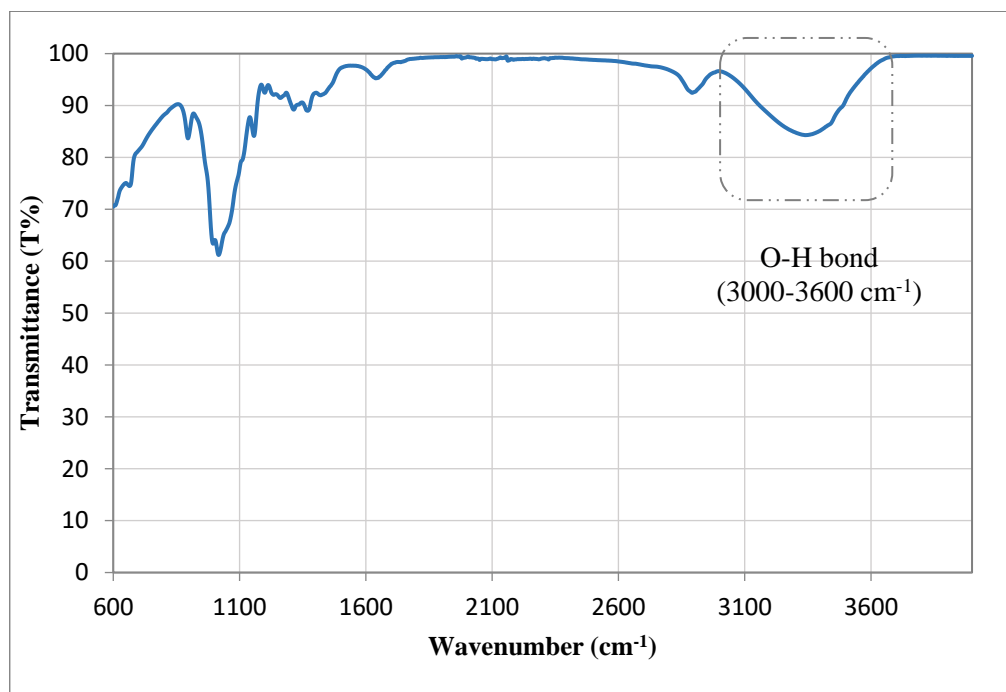


Figure 3.2. FTIR Spectrum of the Cellulose Membrane Sample Obtained in Aqueous 0.05 M NaOH Solution

The results of the different alkaline hydrolysis conditions were tabulated in Table 3.1, and the O-H/C=O peak area ratios, representing the completion of alkaline hydrolysis, increased with increasing NaOH concentration and the alkaline hydrolysis duration. The complete alkaline hydrolysis was obtained with 0.05 M NaOH solution in the shortest time as one day. While the process was completed for 0.01 M NaOH solution in three days, the procedure couldn't result in complete alkaline hydrolysis in 0.001 and 0.005 M NaOH solutions. As an additional observation, the membranes were deformed in the alkaline hydrolysis medium having NaOH concentration greater than 0.05 M like 0.1 M.

Table 3.1 ATR-FTIR Spectra O-H /C=O Peak Area Ratios of the Cellulose Membranes Fabricated via Alkaline Hydrolysis at Different NaOH Concentration Solutions

| Duration of Alkaline Hydrolysis | O-H /C=O Peak Area Ratios for Varying NaOH Concentrations (M) | | | |
|---------------------------------|---|---------|--------|--------|
| | 0.001 M | 0.005 M | 0.01 M | 0.05 M |
| 1 Day | 1.8 | 90 | 316 | ∞ |
| 2 Day | 2.6 | 128 | 1838 | ∞ |
| 3 Day | 3.3 | 167 | ∞ | ∞ |
| 4 Day | 4.0 | 150 | ∞ | ∞ |

To verify that the complete alkaline hydrolysis was done on the surface and the inner structure of all membranes, CA30P10A10-AH membrane as the most dense membrane in this study, was dissolved in [EMIM]OAc and then cast again in order to analyze whole cross-section of the membrane sample. The ATR-FTIR spectra were determined and the peak coming from the acetate group was not observed as shown in Figure 3.3.

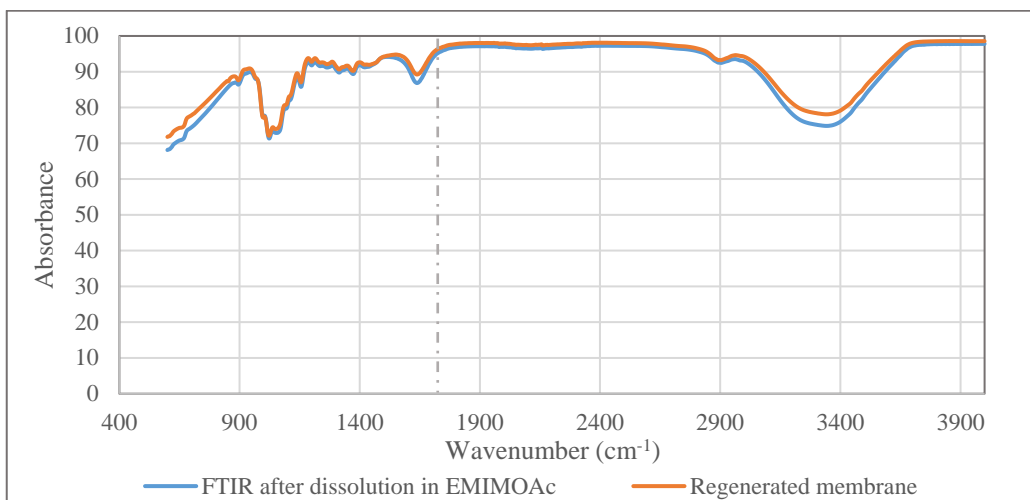


Figure 3.3. ATR-FTIR spectra of CA30P10A10-AH

So, the alkaline hydrolysis procedure was verified with two different measurement techniques and the alkaline hydrolysis was applied with 0.05 M NaOH aqueous solution in this study.

In the literature, FTIR and ATR-FTIR methods were used for the verification of the alkaline hydrolysis process. Tulos et al. applied alkaline hydrolysis to cellulose acetate fibers with 1.0 M NaOH-Ethanol solution for different application durations as 90 and 180 minutes. After the alkaline hydrolysis, they checked with FTIR and ATR-FTIR for different alkaline hydrolysis time ranges and saw that small peaks belonging CA were still visible in the spectrum after 90 minutes while the peaks coming from CA were absent after 180 minutes.¹⁶³ In the study of İmir et al., different alkaline hydrolysis concentrations and solvents were also tested, and 0.05 M NaOH – water medium exposure of one day to the cellulose acetate membrane was used for complete alkaline hydrolysis.⁶⁰ In another study, Liu et al. used aqueous and ethanolic 0.05 M NaOH solution for the fabrication of regenerated cellulose fibers.⁴⁸ When the experimental results were compared with the literature data and the studies done in our research group, the alkaline hydrolysis data were consistent with literature, and the deacetylation of the cellulose acetate membrane was completely achieved in 0.05 M NaOH-water solution within one day.

3.2 Membrane Morphology

To observe the morphology of the membrane surface and cross-section of the cellulose membranes, scanning electron microscopy (SEM) method was used. It was observed that all membranes have symmetrical, nodular and low porosity structures as shown in Figure 3.4. Although the porous structure of membranes are not obvious in the SEM images, the permeance performances of the membranes show that they have a porous structure.

In the cross-section images, it can be seen that the skin layer of the ISA type cellulose membrane cast from casting solutions having lower polymer concentration is more distinct, implying a higher extent of asymmetry in the membrane. In the literature, similar observations were reported in the studies of Ali et al. and Tiron et al. with PVDF and PS membranes.^{164,165}

| | x2500 | x20000 |
|---------------|-------|--------|
| CA20PI0-AH | | |
| CA20-AH | | |
| CA25PI0-AH | | |
| CA25PI0-AN-AH | | |

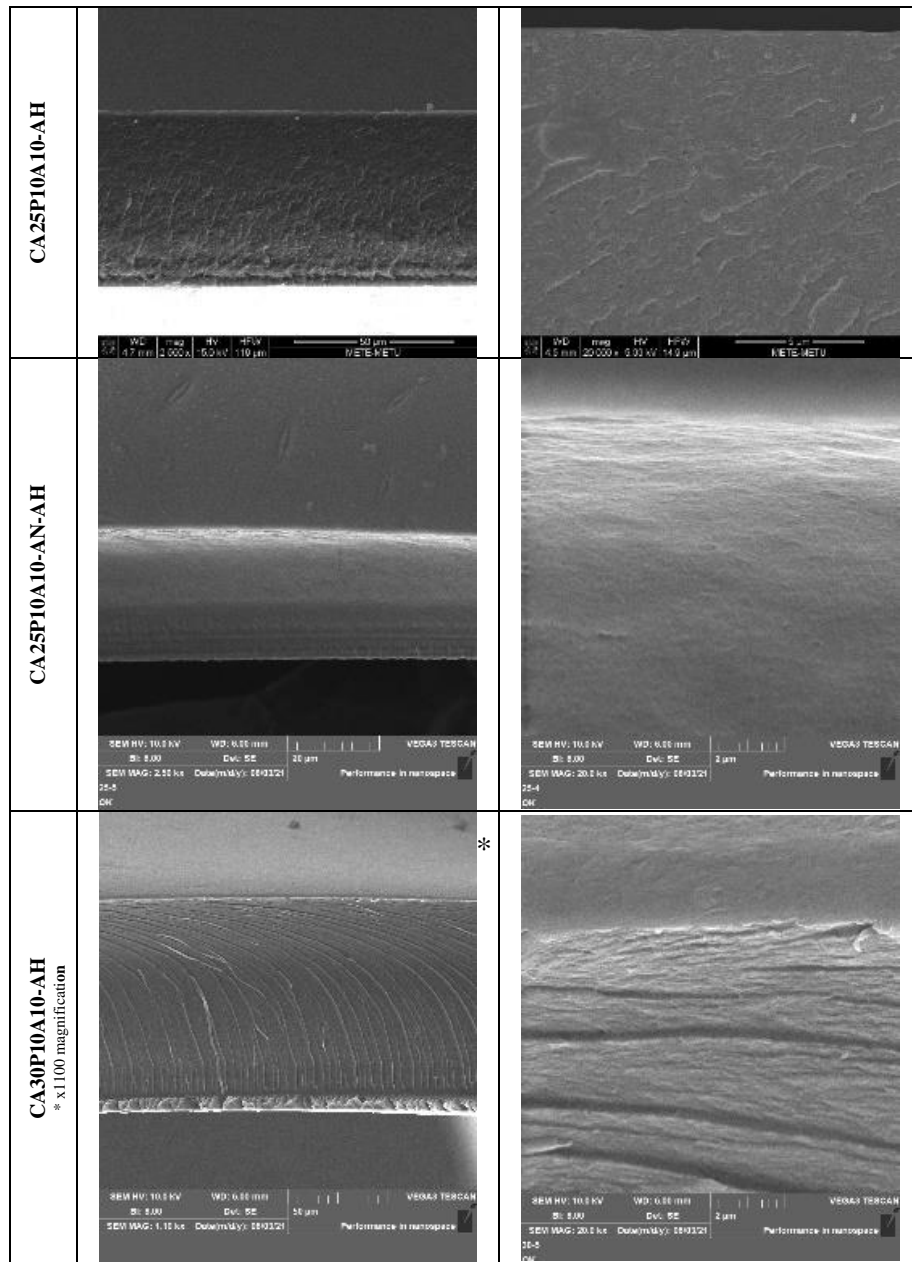


Figure 3.4. Cross-sectional SEM images of membranes

3.3 Membrane Characterization and Performance Tests

3.3.1 Effect of the Alkaline Hydrolysis of the PWP and Blue Dextran (20 kDa) Rejections

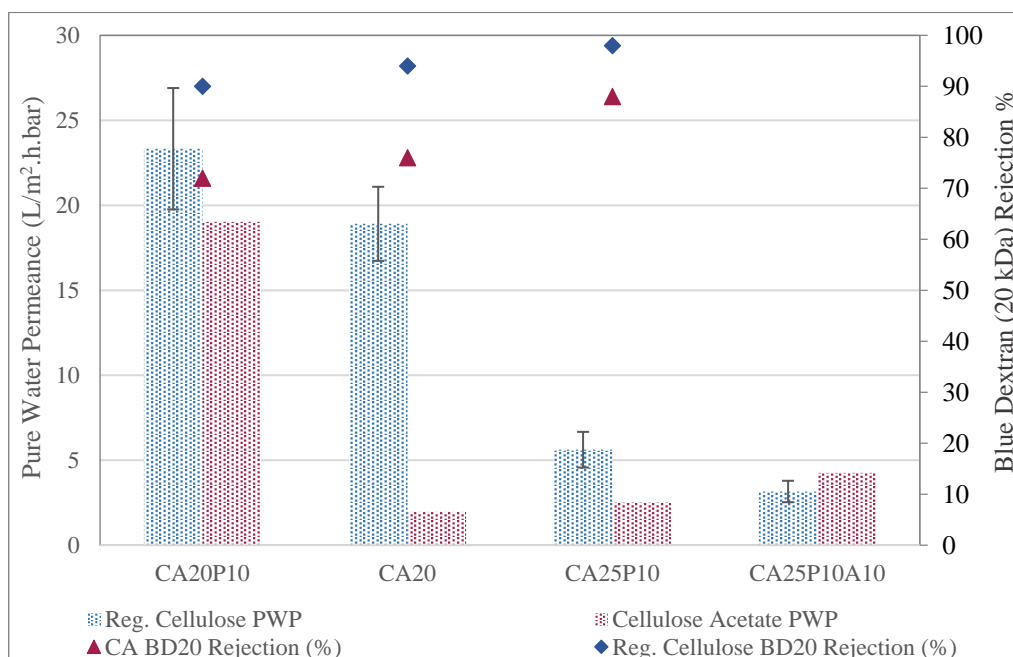


Figure 3.5. Pure water permeance comparison of cellulose acetate and cellulose membranes

To investigate the effect of the alkaline hydrolysis procedure on the membrane, the pure water permeance (PWP) and rejection performances of the cellulose acetate and cellulose membranes were illustrated in Figure 3.5. When the data in the chart are considered, the pure water permeances of the membranes generally increased after the alkaline hydrolysis. Similar observations were also done by Ćimir et al.⁶⁰ Firstly, the difference may stem from the different swelling characteristics of the cellulose acetate and cellulose membranes. According to the studies of Durmaz et al., cellulose film swells approximately 20 times more than cellulose acetate does in water and the permeance becomes higher by the swollen polymer matrix.³⁹ Additionally, Košutić et al. observed the permeance increase with the alkaline hydrolysis of the cellulose

acetate RO membranes in study on the research on the effect of the hydrolysis on performance, pore size distribution and effective number of pores. In the study, sodium bicarbonate/sodium carbonate solution was used for the alkaline hydrolysis with 90 h duration under 17 bar applied pressure. They explained the permeance increase after alkaline hydrolysis with the closing of a part of the small network pores and accompanying an increase in the other pores on the membrane skin.¹⁶⁶ As a result, swelling and the change in the pore network caused an increase in the permeance. As an additional observation, the membranes cast from the solution including PEG400 resulted in less permeance increase while the greatest permeance difference was observed for CA20 as a membrane not containing PEG400. In the membranes cast from the solutions containing PEG, the pores can be considered as more well-connected so this may cause less permeance difference by not allowing a comparable change in the pore structure of the membranes due to the enlarged pore connection network.

As shown in Figure 3.5, the Blue Dextran (20 kDa) rejections generally increased for the membranes after alkaline hydrolysis. At this point, the swelling behavior difference of cellulose acetate and cellulose should be considered. Durmaz et al. showed that cellulose swells 20 times higher than cellulose acetate does.⁶¹ Therefore, the swollen polymer matrix can cause narrowed pores as well as increased water permeation through the swollen matrix in the membranes by resulting in higher rejection values.

3.3.2 Effect of the Morphology Tuning Factors on the Pure Water Permeance and MWCO of Cellulose Membranes

In this study; the effect of polymer composition, pore former agent use, co-solvent content and pre-evaporation in the casting solution, coagulation bath temperature and annealing on pure water permeance and MWCO was investigated.

The simultaneous illustration of the pure water permeance and MWCO values of the membranes are shown in Figure 3.6.

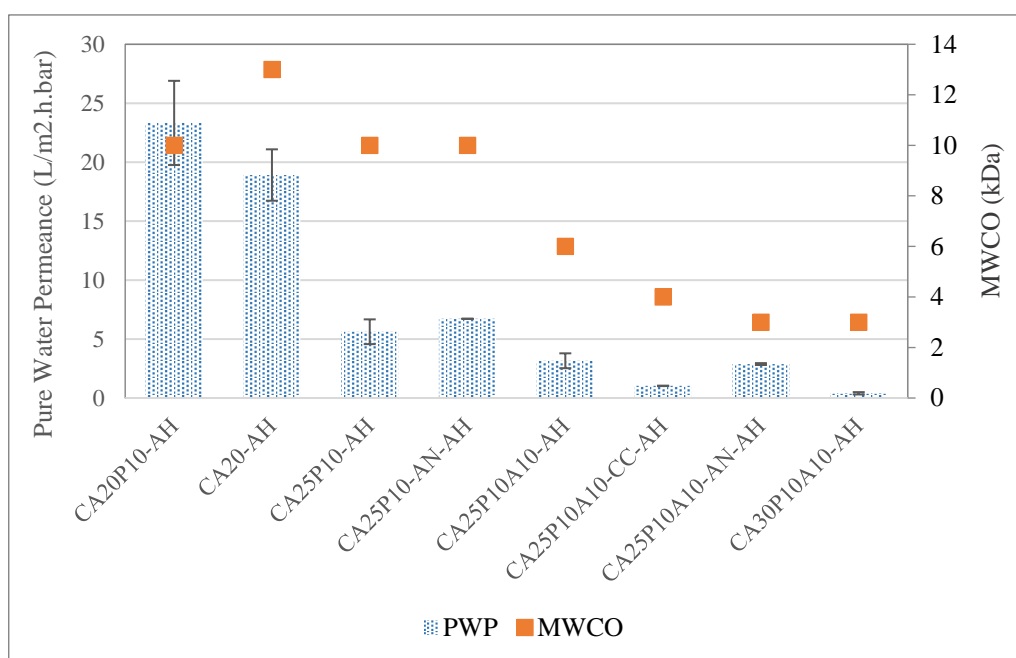


Figure 3.6. Pure water permeance and Average MWCO trend of the membranes

In MWCO tests, probes having similar molecular structures and available in a wide range of molecular weight values, which are PEGs having different molecular weights as 400, 2000, 6000, 10000 and 20000 Da, were used. The MWCO curves were plotted according to the best fit of the PEG rejection as a function of PEG molecular weight in Figure 3.7. As illustrated in the figure, the MWCO values in water were mainly in the range of 3-10 kDa. Then, the best candidate membranes

were selected for the photolithography waste purification according to their separation performance.

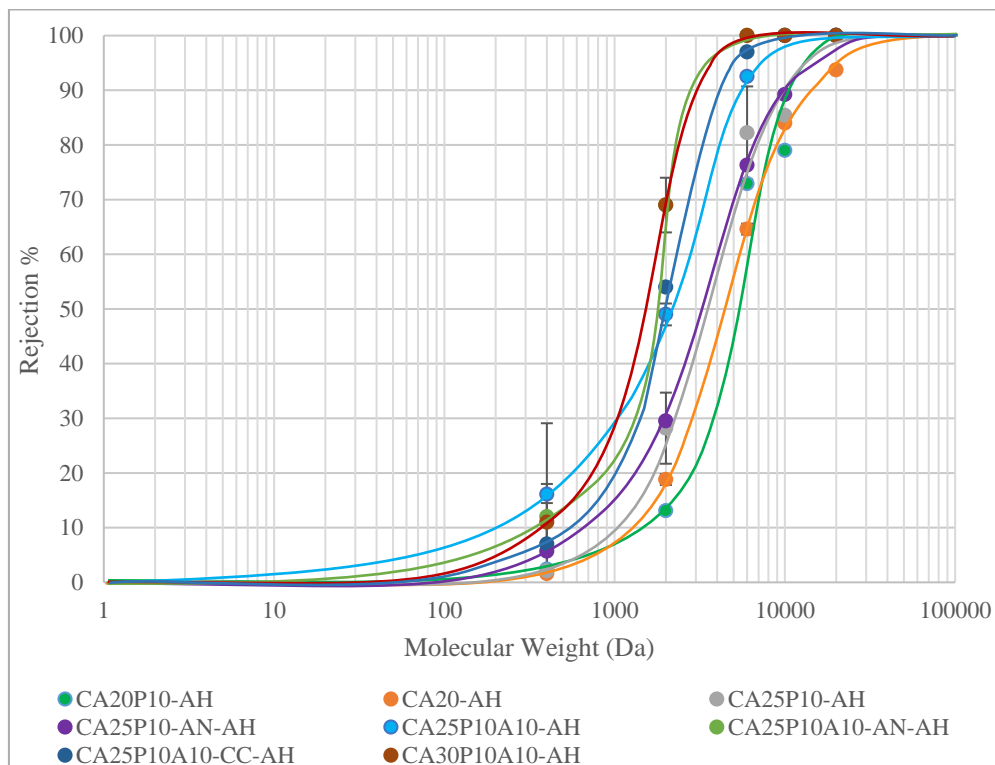


Figure 3.7. MWCO curves of cellulose membranes

The polymer content of the casting solutions was kept in 20%-30% cellulose acetate range. To get high rejection performance with the SU-8 photoresist, the production of tight ultrafiltration membranes was aimed. According to the literature, the membranes fabricated from the casting solutions having high polymer content results in denser membranes.^{22,55-59,167} The general trend in the experimental permeance data obtained in this study was similar, and the permeances decreased with the increase of polymer content of the casting solution. It was observed that the MWCO value of the membrane decreased from approximately 10 kDa to 3 kDa by the increase in the cellulose acetate concentration from 20% to 30% in the casting solution.

As another morphology tuning factor, the effect of the pore former agent use in the casting solution was also investigated. The main aim of the pore former addition is

to increase the permeance of the membranes fabricated via phase inversion method without decreasing the rejection of the membrane by the highly soluble character of pore former additives in the non-solvent (water) of the phase inversion. The pore-former agent molecules leave the casting solution phase leaving well-interconnected pores in the membrane structure.¹⁶⁸ When the pore-former additive composition in the casting solution increases, the permeance increases and mostly the rejection decreases a little.^{70,168,169} In the literature, the pore former agents like polyethylene glycol (PEG) and polyvinylpyrrolidone (PVP) were used to tune the morphology of the polymeric membranes like cellulose acetate or polyethersulfone.^{70,168} It was stated that pore former agent addition like PEG and PVP caused a permeance increase stemming from higher porosity for CA, PS etc. polymeric membranes.¹⁷⁰⁻¹⁷⁵ The aim of the use of pore-former agents is to enhance the permeance of the membrane; but if the porosity increases together with the pore size, the permeance-rejection trade-off becomes an issue. In this study, PEG400 was added as the pore former to the casting solutions, because the pore formers with high molecular weight have higher tendency to remain in the membrane structure after coagulation and PEG was preferred instead of PVP due to the higher rejection decrease for the membranes cast from solutions with PVP in literature.⁷⁰ In the casting solutions 10% PEG400 content was used since more PEG use in the casting solution weakens the membrane mechanically.¹⁷² If the CA20P10-AH and CA20-AH membrane permeance performance data in Figure 3.6. are compared, it can be seen that the PEG400 addition led to an increase in the permeance with no change in MWCO.

A co-solvent addition and the pre-evaporation step of it before coagulation were also studied in the literature to produce membranes with dense skin layers by increasing the polymer concentration of the casting solution with pre-evaporation. Kim et al. searched for the effect of acetone usage as a co-solvent on the performances of flat sheet and hollow fiber cellulose acetate membranes from cellulose acetate and 1-ethyl-3-methylimidazolium acetate solutions, and observed that BSA and γ -globulin rejections were increased to 91% and 98% levels by stating that co-solvent use led to high polymer concentrations and more selectivity.⁷¹ Similarly, in this research,

acetone was used as the co-solvent of the cellulose acetate. An improvement in the MWCO performance similar to the studies in the literature was observed with the 10% acetone addition into the membrane casting solution with a 30-minute pre-evaporation procedure under N₂ stream. A decrease in the permeance was observed by the comparison of CA25P10-AH and CA25P10A10-AH membrane permeance performances. As can be seen in Figure 3.6, the decrease in MWCO from 10 kDa to 6 kDa and decrease in the permeance approximately from 5 to 3 L/m².h.bar for CA25P10-AH and CA25P10A10-AH membranes, respectively.

For the membranes fabricated via the phase inversion method, the coagulation bath temperature is one of the factors affecting the membrane morphology and the porosity. In two different studies of Saljoughi et al., it was stated that the cool coagulation bath temperature resulted in a decrease in PWP and increase in human serum albumin (HSA) and insulin rejections with a denser structure for cellulose acetate membranes.^{169,170} In this study, the effect of coagulation bath temperature was observed with the CA25P10A10-AH and CA25P10A10-CC-AH membranes. In a similar way, the permeance results of CA25P10A10-AH was higher than the permeance of CA25P10A10-CC-AH membrane and the MWCO of the membranes were 5 kDa and 4 kDa, respectively.

Annealing of the cellulose acetate membranes is one of the methods to produce denser membranes because annealing causes a decrease in the free volume between the polymer chains. By this way, it was possible to obtain denser cellulose ultrafiltration membranes via the annealing application on the cellulose acetate membrane before alkaline hydrolysis. Mahendran et al. applied an annealing procedure to the cellulose acetate membranes in the range of 70-90°C and an increase in the BSA rejection from 95% to 100% with a permeance decrease was observed with the change in the pore size and distribution. They observed that the annealing application resulted in the fabrication of denser cellulose acetate membranes and the decrease in the permeance was also detected especially when the applied temperature was higher than 70°C.¹⁰⁷ In another study, the effect of annealing temperature of

cellulose acetate reverse osmosis membranes on performance was shown in Figure 3.8.

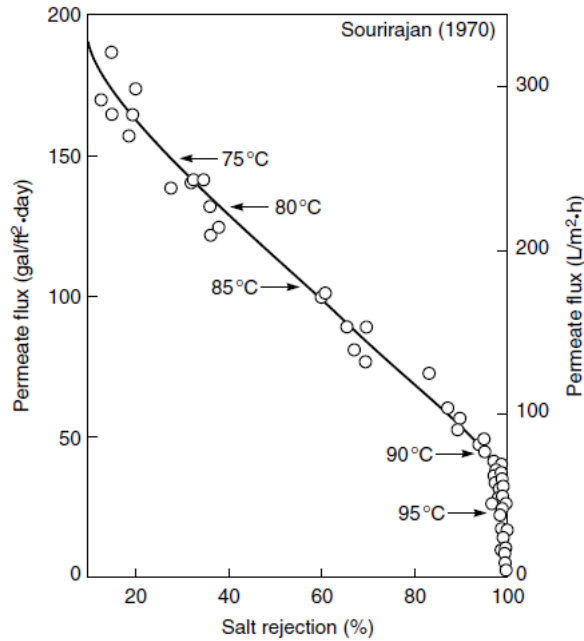


Figure 3.8. Effect of annealing on permeate flux and salt rejection cellulose acetate reverse osmosis membranes ⁵

For this purpose in this study, CA25P10-AN-AH and CA25P10A10-AN-AH membranes were fabricated via annealing application at 85°C for 3 hours in water before the alkaline hydrolysis process i.e., the annealing was applied to cellulose acetate membranes. Generally, it was observed that annealing did not change the permeance significantly while PEG rejections increased in MWCO tests. The membranes in this study were mainly in tight UF membrane range. Hence, annealing made membrane filtration range closer to the NF range. Although pore flow is the main transport mechanism in the UF membranes, tight UF membranes closer to the NF range may be under the effect of the combination of pore flow and solution diffusion model due to the tightened polymer matrix of the membrane by thermal annealing. During filtration, water can pass through both the membrane pores and the polymer matrix, although PEG molecules would dominantly pass through the

membrane pores due to the low diffusion coefficient of PEG in membrane material. So, it can be speculated that upon annealing while pores became smaller, the final cellulose matrix may have become more open for water transport, hence balancing the reduced water flow through the smaller pores.

The main purpose of tuning was to fabricate a cellulose membrane which is suitable for the photolithography waste purification. From this aspect, the critical performance improvement was achieved with the CA25P10A10-AN-AH by the use annealing while the permeance and separation performance of CA25P10-AN-AH membrane were similar to the data of CA25P10-AH membrane as the not annealed version of it

As a general result, increasing polymer content in the casting solution, co-solvent usage with the pre-evaporation step before coagulation, decrease of the coagulation bath temperature to 0°C and the annealing application decreased the MWCO value of the cellulose membranes. According to the literature, drying of the membranes is one of the methods to increase the rejection of the membrane by pore collapsing but it causes a significant decrease in the permeance.^{46,176} That is why the drying procedure of the cellulose membranes produced in this study was not a preferred method to increase the rejection.

3.3.3 Pure Solvent Permeance and MWCO Test Performance of Cellulose Membranes in Different Solvents

The transport through the membrane is mainly affected by the interactions between the solute, solvent and the membrane. Hence, the effect of the solvent type on the pure solvent permeance and the MWCO of the membrane was examined after the MWCO determination process in water. From this point of view, the relations between the solvent type, swelling ratio, solvent viscosity, permeance and the MWCO performance were investigated. For this purpose, the experiments were performed with CA25P10A10-AN-AH and CA20P10-AH membranes. CA25P10A10-AN-AH was one of the membranes having lowest MWCO values being more practical to fabricate and resulted in the best SU-8 filtration performance and used in the experiments of solvent recovery from photolithography waste. On the other hand, CA20P10-AH was a more open membrane with larger pores. The pure solvent permeance of CA25P10A10-AN-AH is shown in Figure 3.9.

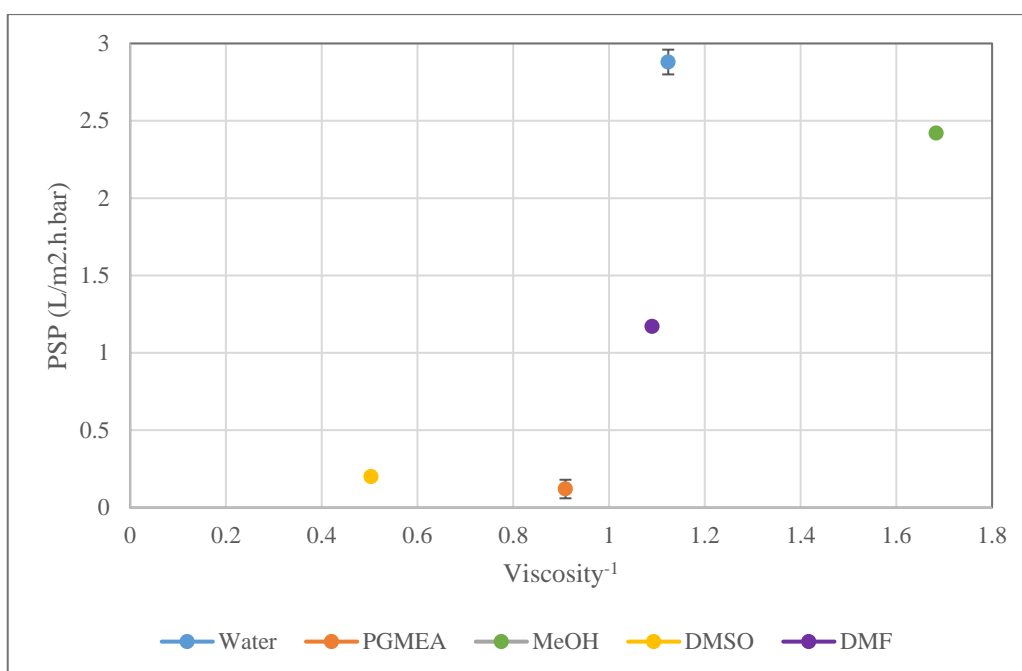


Figure 3.9. Pure solvent permeance vs. viscosity⁻¹ data for CA25P10A10-AN-AH membrane

The membranes for which pore flow model is dominant, permeance is inversely proportional to the reciprocal of solvent viscosity. Drioli et al. stated that solvent viscosity is inversely proportional to the permeance for porous membranes for which pore-flow model is dominant and that is explained this by Darcy's law.¹⁷⁷ On the other hand, for dense membranes where solution-diffusion is effective, permeance typically varies in direct proportion to the swelling of the membranes in the solvent. In many cases, both mechanisms are effective. Vankelecom et al. stated that solvent transport through nanofiltration membranes depend on viscosity, porosity and swelling with the experiments carried out with commercial MPF 50, which is commercial composite membrane having silicone top layer, and PDMS solvent resistant nanofiltration membranes.¹⁷⁸ In that study, it was shown that the solvent permeance is inversely proportional with solvent viscosity and directly proportional with swelling with experiments carried out with methanol, isopropanol, acetone, ethyl acetate and toluene.

Stamatialis et al. studied permeance of oil/toluene and TOABr/toluene feed mixtures and hydrophobic PDMS based PAN supported and more hydrophilic PEO-PDMS-PEO based PAN supported membranes.¹⁷⁹ As a result, they found that pure solvent permeances are mainly dependent on the solvent viscosity and membrane swelling by showing there is a linear relation between PSP and swelling of the membrane/solvent viscosity ratio.

The same analysis was done for CA20P10-AH membrane by the addition of DMSO permeance data to the experimental data carried out in our research group by Çağlayan et al. (Figure 3.10).¹⁸⁰ Similar results were observed with the results of CA25P10A10-AN-AH membrane by observing water was over the trend and PGMEA was under the trend. Although the membrane is more porous than CA25P10A10-AN-AH, it appears that pore flow and solution-diffusion mechanisms are simultaneously effective for this membrane as well. The SEM images (Figure 3.4) which show quite dense and low-porosity membrane cross-sections support this behavior.

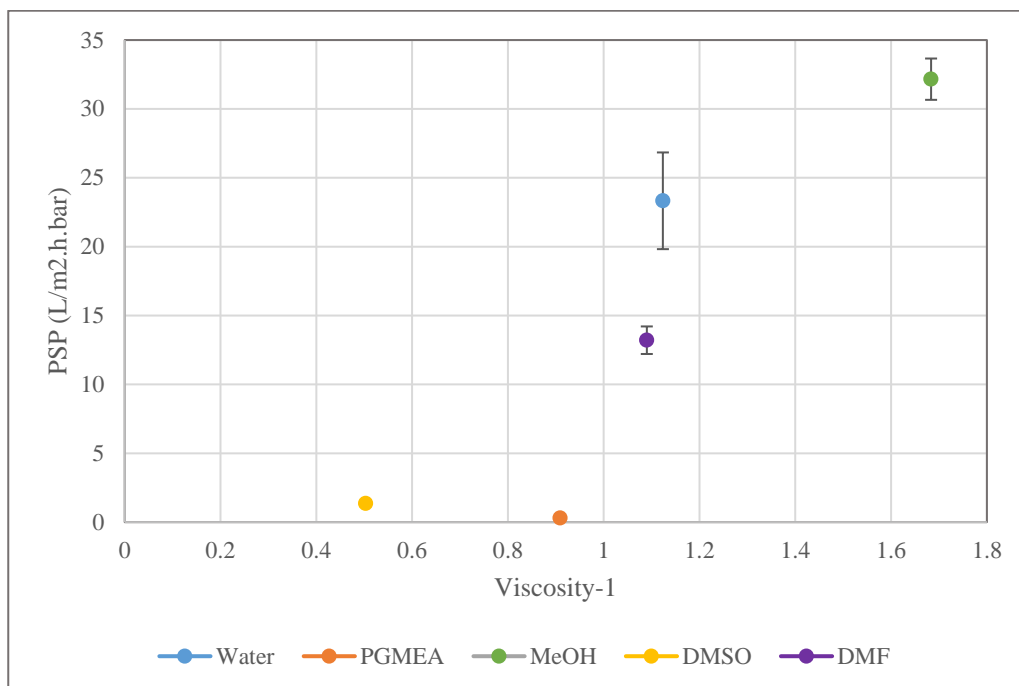


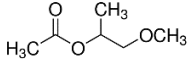
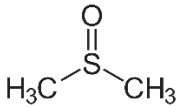
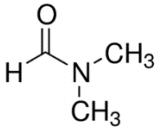
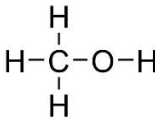
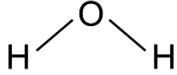
Figure 3.10. Pure solvent permeance vs. viscosity⁻¹ data for CA20P10-AH membrane

If the pure solvent permeance results are compared with literature, it can be seen that the permeance results are reasonable when compared to the cellulose OSN membrane permeance results. In the study of Konca et al., DMSO permeance of the cellulose OSN membrane was measured as 0.13 L/m².h.bar.⁴⁷ In another study, Anokhina et al. tested the DMF permeance of cellulose composite OSN membranes and it was measured as 0.28 L/m².h.bar.⁴⁴

In our study, permeance of five different solvents, which are water, methanol, dimethyl formamide, dimethyl sulfoxide and PGMEA, were investigated. Overall, the pure solvent permeance was inversely proportional with the solvent viscosity, but the permeances of water and PGMEA were out of the general linear trend. The reason behind this exceeding behavior for water may be related to high swelling ratio of the cellulose membrane in water (Table 3.2), which allows water to flow through both the pores and the swollen polymer matrix to a larger extent than the rest of the solvents. On the other hand, among all solvents tested, PGMEA is the bulkiest, which

may have slowed down its diffusion through the polymer matrix. As a general conclusion, it appears that both pore flow and solution-diffusion are effective in solvent permeance of the membranes, where for the solution diffusion mechanism, both the solubility of the solvent, indicated in the membranes' swelling in the solvent, as well as its diffusion coefficient in the membrane matrix appears to affect the permeance.

Table 3.2. Solvent chemical structure, viscosity, swelling ratio of dense cellulose film, molecular weight, molar volume and pure solvent permeance data

| Solvent | Chemical Structure | Viscosity (cP) | Swelling Ratio % | Molecular Weight (g/mol) | Molar Volume (cm ³ /mol) | PSP (L/m ² .h.bar) |
|----------|---|----------------|------------------|--------------------------|-------------------------------------|-------------------------------|
| PGMEA |  | 1.10 | 19 | 132 | 137 | 0.12 |
| DMSO |  | 1.99 | 32 | 78 | 71 | 0.20 |
| DMF |  | 0.92 | 2 | 73 | 77 | 1.17 |
| Methanol |  | 0.59 | 8 | 32 | 40 | 2.40 |
| Water |  | 0.89 | 110 | 18 | 18 | 2.88 |

Following the permeance tests, the MWCO tests were performed and the comparison of the membrane performances in the solvents with different properties were analyzed. The related MWCO curves are shown in Figure 3.11.

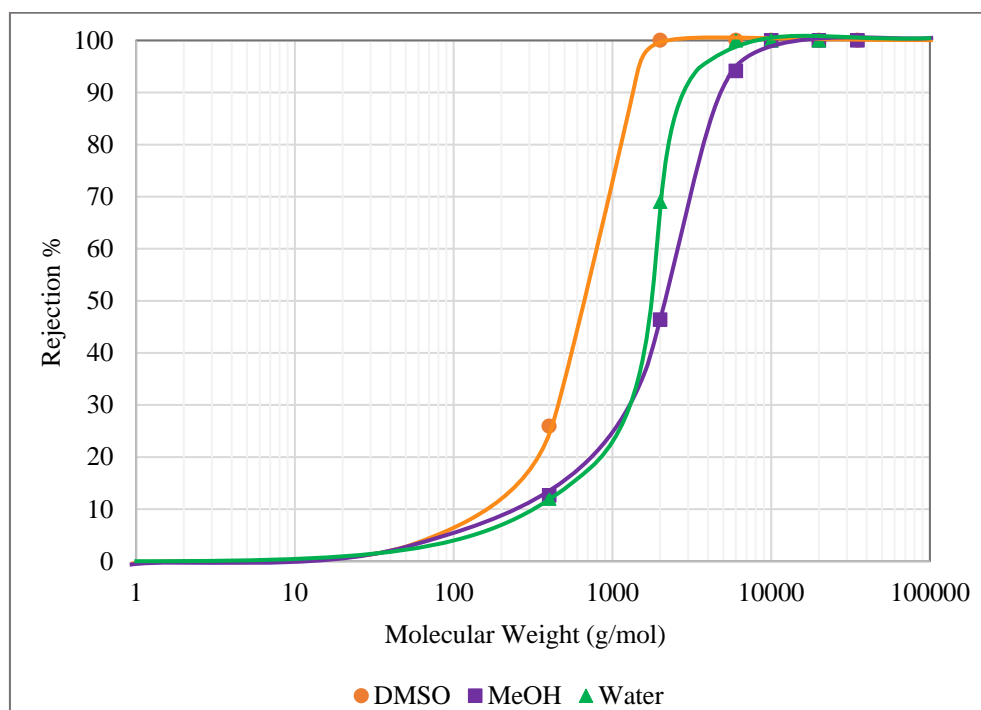


Figure 3.11. MWCO test results in different solvents

The solvent types were determined according to their PEG dissolution quality to obtain consistent results with the same probes. The MWCO values were measured as 1.3 kDa, 3 kDa and 5 kDa in DMSO, water and methanol, respectively.

In literature, Anokhina et al. stated that the enhancement in the rejection character of the cellulose NF membrane stemmed from the narrowed pore structure due to the swollen membrane polymer via the MWCO tests performed with different aprotic solvents.¹⁸¹ In that study, DMSO, NMP, DMFA, THF and acetone solvents were used and higher than 90% Remazol Brilliant Blue R rejections were obtained with the cellulose membranes giving higher than 100% swelling ratios by resulting in 230% swelling in DMSO at most.

In the studies of Koops et al. and Bhanushali et al., it was stated that the rejection performance was mainly affected by the solute size, shape and the solute affinity to membrane material and the preferential transport was observed in water for the membrane materials having high affinity like cellulose acetate's affinity to water due to the -OH groups of cellulose acetate and strong hydrogen bonding of water.^{182,183}

Additionally, Darvishmanesh stated that solvent affects the effective solute size in that particular solvent and the effective size is dependent on solvent type because of hydration of solute by solvent and solvation.¹⁸⁴ Therefore, the rejection is affected by the solute size in the solvent. Similarly, Shen et al. stated that the rejection of reverse osmosis membranes, for which solution-diffusion model is dominant, is dependent on the hydrated solute size by the hydration shell of water molecules and hydrogen bonding between organic solute molecules and membrane material.¹⁸⁵ In the UF membranes in our study, while the solvent can pass through the membrane in both swollen polymer matrix and pores, PEG probes are expected to pass primarily through the pores. While water swells the membrane matrix the most, the lowest MWCO is observed in DMSO. Hence, it appears that neither the narrowing of pores nor the preferential permeation of solvent through the polymer matrix can explain the change in MWCO in the three solvents studied.

We analyzed the PEG coil sizes in the solvents via DLS using PEG 20 kDa. The coil diameter decreased in the order DMSO (11.3 nm) > Water (8.3 nm) > Methanol (6.6 nm) as shown in Figure 3.12. The related MWCO values are 1.3, 3 and 5 kDa, respectively. Hence, the size of the PEG chains in these solvents may explain the variation in MWCO of the membrane in these three solvents.

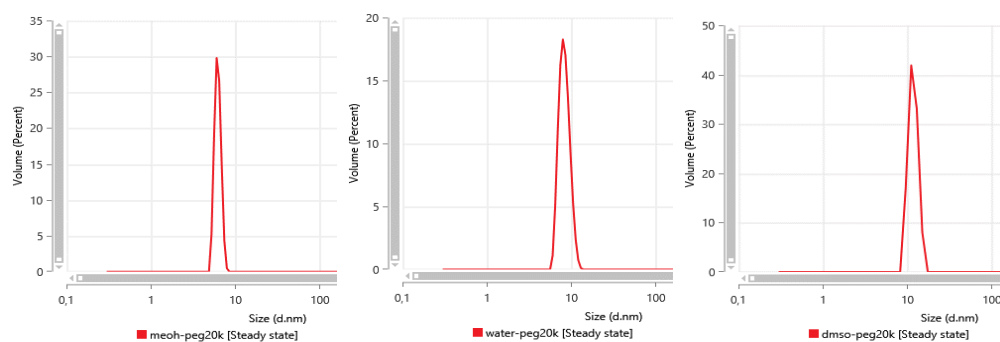


Figure 3.12. DLS results of PEG20K in Methanol (left), Water (Middle) and DMSO (right)

Solvent viscosity has also been related to solute rejections in literature.¹⁷⁸ The MWCO values in DMSO (1.99 cP), water (0.89 cP) and methanol (0.59 cP) were 1.3 kDa, 3 kDa and 5 kDa, respectively. From this point of view, the MWCO value of the membrane decreased with the increase in the viscosity. Vankelecom et al. correlated this behavior with the physico-chemical approach by stating that the viscosity reflects also the dual interactions of the moving molecules, and although viscosity is a bulk property, it also shows the friction amount during permeation.¹⁷⁸ It was also explained that viscosity should be regarded as a property showing the mutual interactions between the migrating molecules and the interactions of them with the wall in both porous and non-porous systems. Hence, rejection in solvents with high viscosity was expected to increase.

3.4 Photolithography Waste Purification

In this study, SU-8 was used as the photoresist which is an epoxy based negative photoresist. The main components of photoresists are base resin polymer, photoacid generator and casting solvent. The casting solvent makes spin coating process possible. Then, the solvent is evaporated by the soft baking before the exposure step. After soft baking, the photoresist which is exposed to UV radiation transforms with the initiation of triaryl sulfonium based salt photoacid generator (PAG) and if the photoresist is positive type, it becomes soluble in the developer solution, and on the other hand, the photoresist is crosslinked and becomes insoluble in developer if it is negative photoresist.

According to the SU-8 series, photoresist contains different casting solvent like gamma-butyrolactone or cyclopentanone. After the soft bake the solvents were removed from the photoresist and only SU-8 photoresist and triarylsulfonium hexafluoroantimonate PAG remain on the coated surface.

The aim of this study was to obtain recovered solvent having high purity required for photolithography by the filtration of SU-8 photoresist and PGMEA developer solvent mixture with cellulose membranes.

3.4.1 SU-8 Resin Elemental Analysis for Photo Acid Generator Concentration Detection

For the determination of the exact amount of photoacid generator in SU-8 due to the observation of the UV-VIS peak overlap of the photoacid generator triarylsulfonium hexafluoroantimonate salts and the SU-8 photoresist, elemental analysis of the SU-8 resin after solvent evaporation was carried out. By considering the size of the photoacid generator, it was assumed that the PAG salts were not rejected by the membrane and the PAG concentrations in the permeate and feed side would be equal. For the analysis of the PAG content of the SU-8 resin, the solvent was evaporated from the resin and the elemental analysis are done for C, H and S elements. At this point, the most distinctive element was S, because there was S only in the chemical structure of PAG. The result of elemental analysis is shown in Table 3.3.

Table 3.3 SU-8 resin elemental analysis percentages

| Sample | C% | H% | S% |
|--------------------------------------|-------|------|------|
| SU-8 Resin after Solvent Evaporation | 72.48 | 6.94 | 0.35 |

Accordingly, considering the S content of the PAG salts, the photoacid generator content was calculated as 3.4% in the resin and the photoacid generator content range in the literature and the MicroChem Chemicals company datasheets were 1-5%. So, the obtained atomic percentage results and the estimation of the photoacid generator content ratio, shown in Appendix D in detail, was consistent with the manufacturer specification.

3.4.2 SU-8 and Photo Acid Generator UV-VIS Spectra

For the concentration determination of SU-8 and the photoacid generator, UV-VIS spectrophotometry was utilized. To correctly detect the concentration of the SU-8 photoresist, the investigation of the peak overlaps was needed. The detection of the effect of the photoacid generator triarylsulfonium hexafluoroantimonate salt on the SU-8 photoresist UV_VIS spectrum was necessary, so the determination of the pure photoacid generator (PAG) spectrum was needed. Triarylsulfonium hexafluoroantimonate salt as the photoinitiator is available in the market as 50% triarylsulfonium hexafluoroantimonate salt- 50% propylene carbonate mixture. Therefore, the propylene carbonate solvent was firstly evaporated and then the PAG salt was dissolved in PGMEA. In this way, the UV spectrum analysis of the pure PAG, obtained by the evaporation of the solvent from PAG-propylene carbonate mixture, was done. The spectra of the pure PAG aligned to the SU-8 concentration according to the elemental analysis and SU-8 feed, permeate solutions' spectra are illustrated in Figure 3.13.

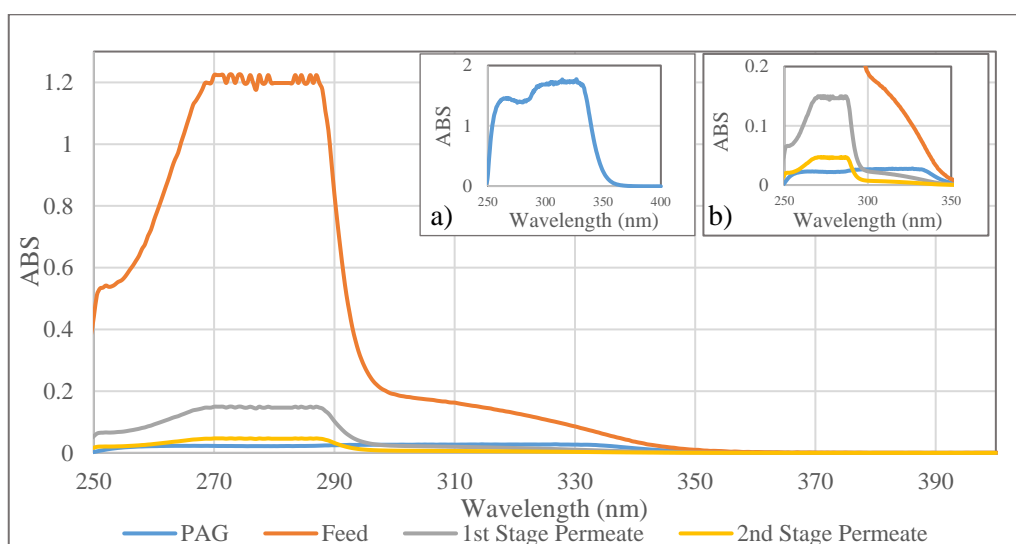


Figure 3.13. UV-VIS spectra of PAG salt (in PGMEA) proportional to SU-8 concentration, SU-8 feed, 1st and 2nd stage permeates of SU-8 filtration, 0.025 wt% PAG salt in PGMEA (a), zoomed version of the main spectra (b)

The measured PAG mixture spectrum was compared with the data of Sigma Aldrich Chemical Company and the experimental data were consistent.¹⁸⁶

When the UV-VIS spectrums of the SU-8 and PAG salt were evaluated, an overlap was observed due to the aromatic groups in the structures of both. As stated previously, the PAG content in the SU-8 photoresist resin was detected as 3.4% via elemental analysis. So, an analysis was carried out by considering the concentration of photoresist and photoacid generator in the filtration limits. The pure PAG spectrum was obtained with the evaporation of solvent in PAG-propylene carbonate mixture and then the dissolution of it in PGMEA. By this method, the solution was prepared with PAG in PGMEA and the spectra of PAG and SU-8 were compared with each other according to the required concentrations in the photoresist resin. The PAG molecules are so small according to the pores of the membranes produced for this project, so it was assumed that the PAG concentration in both feed and permeate samples were the same because of the lack of rejection. It means that the absorbance stemming from the PAG was almost the same in all feed, retentate, permeate samples. That is why the absorbance at 277.5 nm coming from the PAG was calculated according to the maximum SU-8 concentration in the photolithography waste. The SU-8 concentration of the photolithography waste of developer bath is approximately in the range of 0.5-2.5 g/L. Thus, 2.5 g/L was chosen as the reference concentration for this overlap comparison, and this was also the concentration at which the synthetic waste filtrations were performed to measure the purification degree at highest impurity level. For the accuracy in UV-VIS measurements, a dilution with 1:20 ratio was done for all the samples by using pure PGMEA and the dilution ratio was not changed from one sample to another to keep consistency for all the materials and impurities affecting the absorbance at that wavelength. According to this analysis, the absorbance of SU-8-PAG mixture was approximately 1.226 and the absorbance of PAG was 0.022 in diluted samples for the filtration simulations performed at the maximum concentration in the limitations. Therefore, it was assumed that the SU-8 measurement was not significantly affected by the PAG absorbance due to the negligible error coming from the PAG, but the rejection errors

coming from the PAG may be more effective on the permeate analyses of 2nd stage SU-8 filtrations due to the low SU-8 concentration according to the constant PAG concentration assumption.

3.4.3 Pure PGMEA Permeance of the Membranes

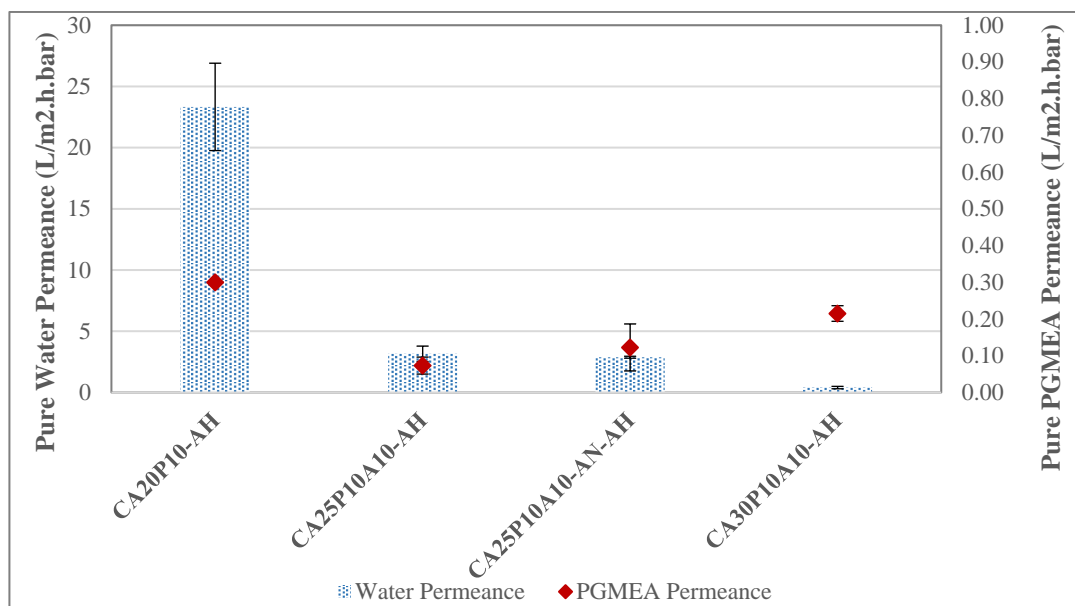


Figure 3.14. Water and PGMEA permeance comparison of the membranes

The pure PGMEA permeance results were compared with the pure water permeance values of the same membranes in Figure 3.14. Although the permeance changes with the membranes of the different casting solutions are obvious for the pure water permeance measurements, the PGMEA permeance performances change very little for different membranes at 10^{-1} L/m².h.bar order of magnitude level. The reasons behind this result can be considered as different polymer-solvent interactions, swelling behavior of cellulose in water and PGMEA, different solvent viscosities. For CA30P10A10-AH membrane, the result was a little different from the other membranes and the reason of the further decrease in water permeance may be the combined effect of denser membrane structure caused by higher polymer composition in casting solution and the possibility of narrowed pore structure due to the more swollen polymer matrix in water according to PGMEA.

3.4.4 PGMEA Permeance and SU-8 Rejection Performance During SU-8 Filtration Tests

After the determination of the pure PGMEA permeance, the SU-8 photoresist filtration tests were done at 10 bar in the stainless-steel dead-end filtration cell for the photolithography waste removal simulation. The feed concentration was kept approximately at 1.5 ± 1 g/L SU-8 in PGMEA concentration to simulate the real photolithography wastes. According to the permeance data recorded during the filtration tests, the permeance decreased slightly during the filtration due to concentration polarization.

The comparison of the SU-8 filtration results and the MWCO test performance of the same membranes in water are shown in Figure 3.15. As can be observed, the membranes having lower MWCO values resulted in higher SU-8 rejection values and similar SU-8 rejection values were measured for the membranes with similar MWCO performances. Additionally, SU-8 sorption measurements are done in PGMEA and sorption was not observed. So, there is no effect of sorption on SU-8 rejection determination.

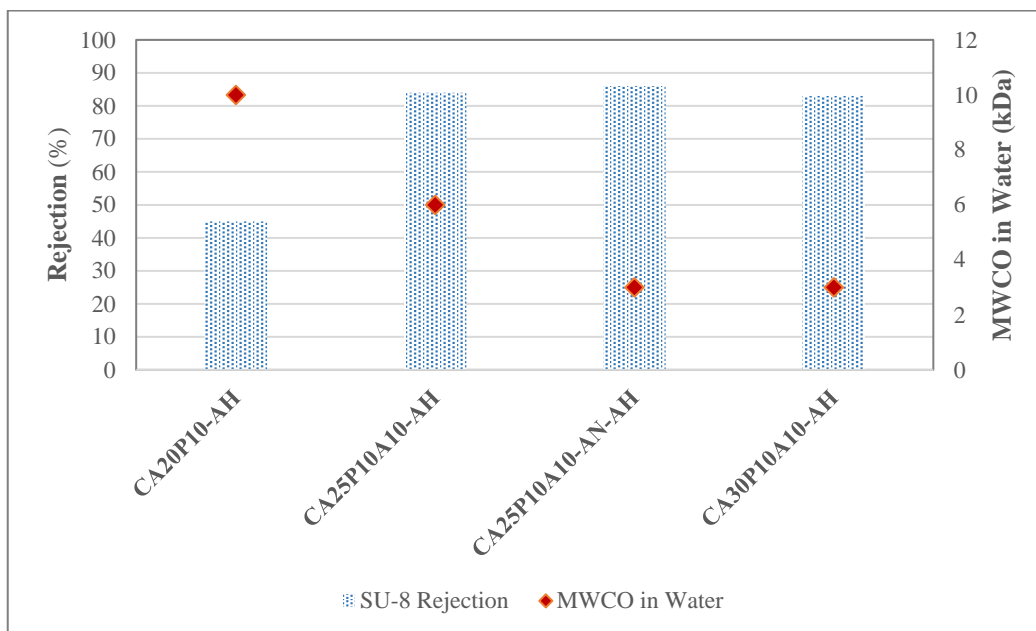


Figure 3.15. SU-8 rejections and water MWCO values of the membranes

In this study, synthetic photolithography waste solutions were prepared and purified with the cellulose membranes. Single-stage and two-stage filtrations were performed and the solvents with 99.95% and 99.99% purity level, which was calculated according to the SU-8 concentrations of the permeates, were respectively obtained by the membrane filtration applications.

For CA30P10A10-AH membrane, the permeance and filtration rejection performances are illustrated in Figure 3.14 and 3.15 for 40% solvent recovery ratios for both filtration stages. Next, from the membranes having the same rejection performance, the membranes with higher PGMEA permeance for higher solvent recovery ratio were used by aiming to obtain recovered solvents in larger amount considering a better representation of large-scale applications. The performance data of the filtrations were illustrated in the form of data versus % solvent recovery ratio.

For this purpose, the SU-8 filtrations with high solvent recovery ratios, as 80% and 70% for 1st and 2nd filtration stages respectively, were performed with CA25P10A10-AH and CA25P10A10-AN-AH membranes. These membranes were selected due to the low MWCO values in water MWCO tests and accompanying more reasonable permeance performance compared to the CA30P10A10-AH membrane. The results of CA25P10A10-AH membrane were shown in Figure 3.16. and 3.17.

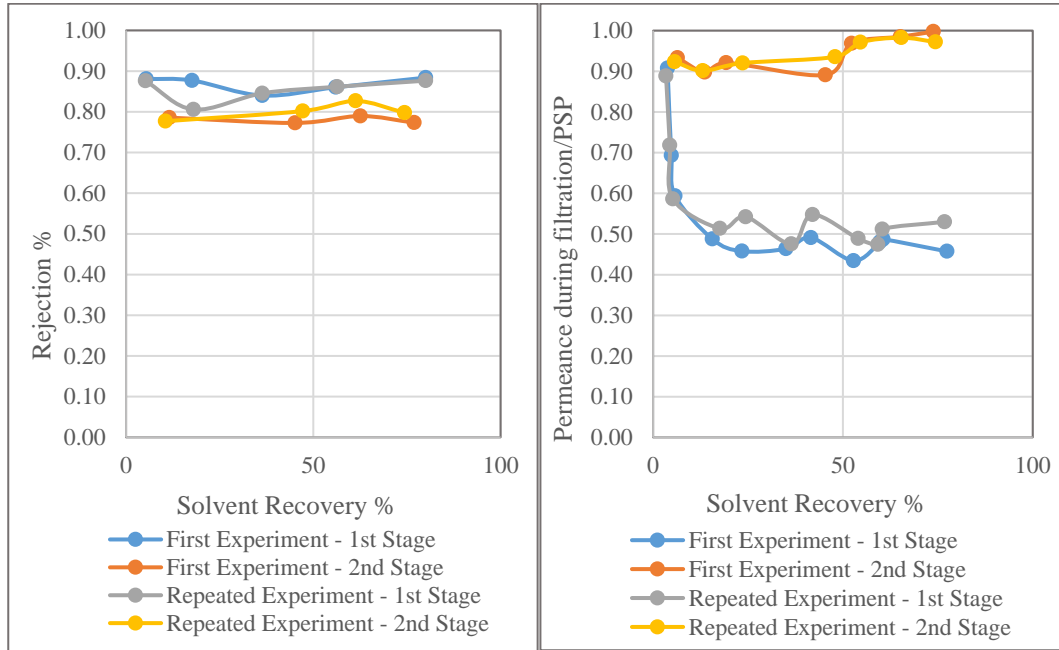


Figure 3.16. SU-8 rejection and PGMEA permeance of CA25P10A10-AH membrane during filtration

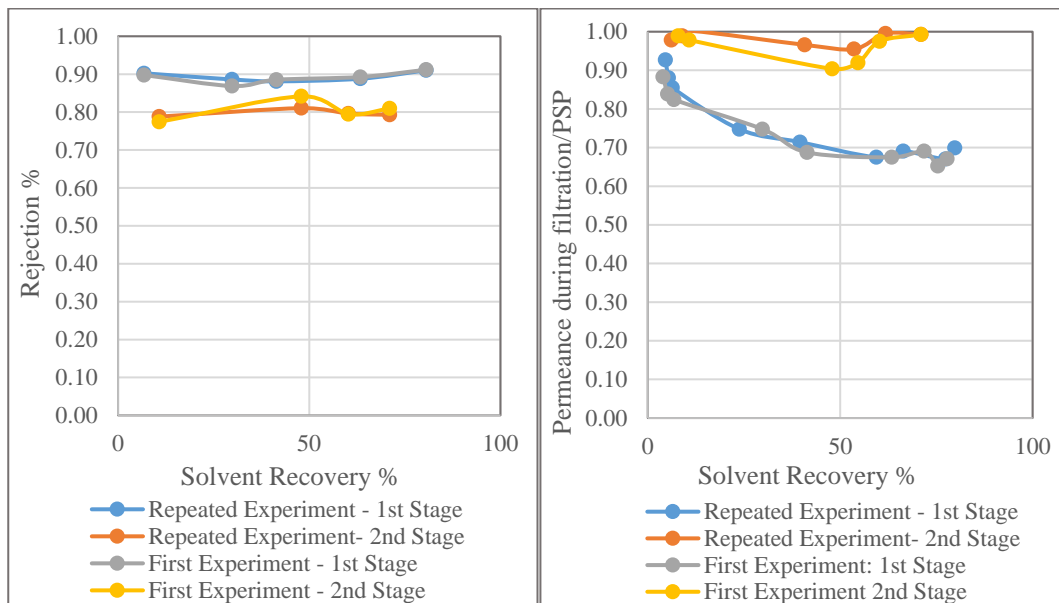


Figure 3.17. SU-8 rejection and PGMEA permeance of CA25P10A10-AN-AH membrane during filtration

As a result of the filtration experiments carried out with two different membranes, higher rejection values were generally observed for both stages with CA25P10A10-AN-AH membrane which is the annealed type of CA25P10A10-AH membrane. As another observation, the rejections were measured lower for the 2nd stage filtrations and it can be related with the increased effect of PAG on SU-8 concentration detection due to the lower SU-8 concentration in the second stage permeates of all SU-8 filtration tests. Thus, the manipulating effect of PAG on apparent SU-8 rejection was calculated for CA25P10A10-AN-AH membrane filtrations. For the 1st and 2nd stages of filtrations, change from nominal rejection to real rejection was calculated, and in the 1st stage, rejection changed from 91% into 91.4% and for the 2nd stage, rejection changed from 79% into 82%, according to the assumption of no rejection for PAG salts. So, it can be seen that the PAG effect was higher in the samples having low SU-8 concentrations and this may show the SU-8 rejection lower than the reality for especially 2nd stage filtrations.

Additionally, SU-8 rejections may have been affected by the slight fouling in the 1st filtration stages, causing an increase in the rejection. The experiments were repeated and consistent results were obtained. For the permeance during filtration, further decline was observed for CA25P10A10-AH membrane compared to the CA25P10A10-AN-AH membrane performance. The reason of this result may be the denser skin layer of annealed membrane by resulting in less fouling behavior.

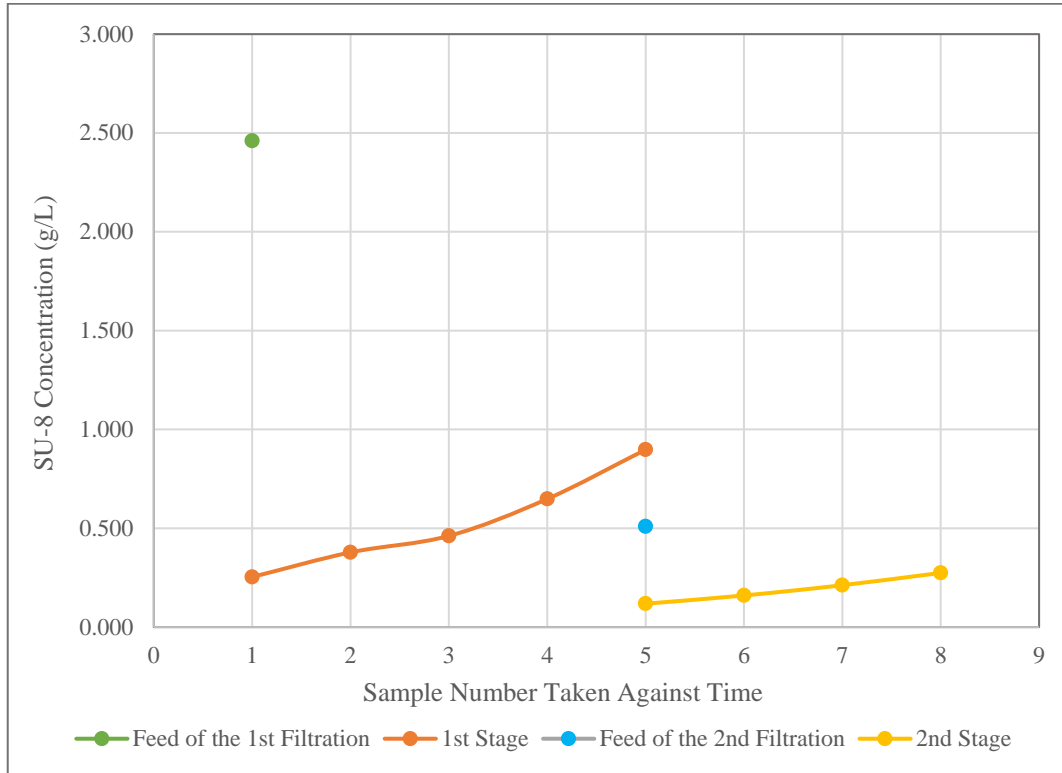


Figure 3.18. SU-8 concentration path during filtration

In the light of this information, the required purity level was obtained in the experiments performed with synthetic photolithography waste solutions. The best rejection performance was obtained with CA25P10A10-AN-AH with approximately 90% and 80% rejection levels for 1st and 2nd stage of filtrations, respectively. The concentration path from feed to permeate was illustrated in Figure 3.18. The concentration of the photolithography waste from the developer bath is approximately 2.5 g/L and the starter feed concentration is adjusted to that value for this reason. In total, 56% of the solvent with 0.18 g/L SU-8 concentration was recovered with two stage filtration.

As a summarizing chart, the rejection and permeance performances for both stages were illustrated in Figure 3.19. For CA25P10A10-AH and CA25P10A10-AN-AH membranes, the 1st and 2nd stage filtration solvent recovery% levels were approximately 80% and 70%, respectively. On the other hand, 1st and 2nd stage

filtration solvent recovery% levels were approximately 40% for CA30P10A10-AH membrane. As can be seen, the highest rejections were measured with CA25P10A10-AN-AH membrane with reasonable permeance when compared with the other membranes. Hence, CA25P10A10-AN-AH membrane was used in the further SU-8 filtration experiments and the photolithography tests.

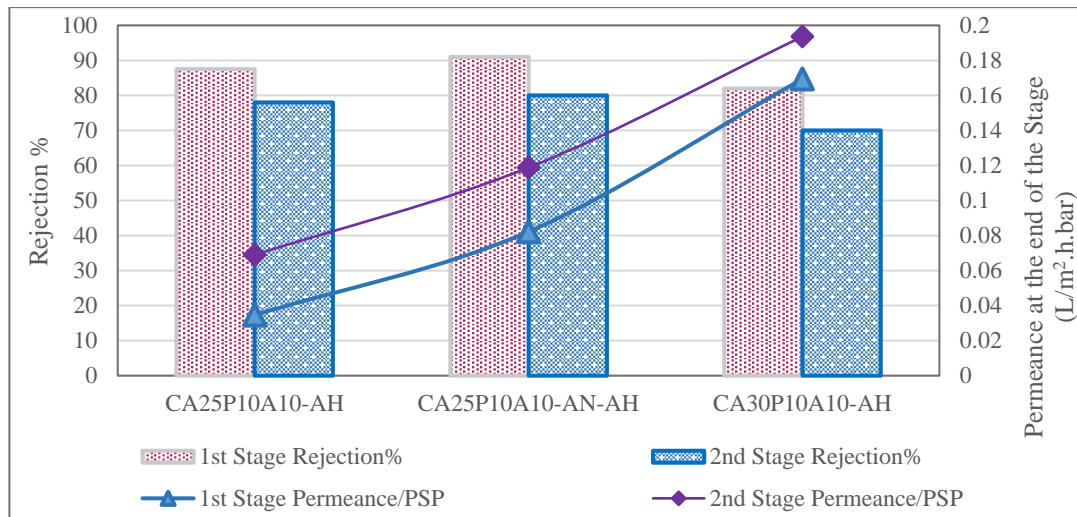


Figure 3.19. SU-8 rejection and Permeance/PSP data at the end of filtration stages

3.4.5 Photolithography Performance of the Recovered Solvent

Finally, the photolithography performance of the recycled solvent by cellulose membrane filtration was tested. As photolithography steps up to the rinsing step; surface cleaning with acetone, SU-8 photoresist spin coating, soft baking for casting solvent evaporation, UV exposure with photomask, post-exposure bake, immersion into PGMEA developer bath and rinsing step with isopropanol were applied, in order.

The recorded microscope images of the starry pattern were shown in Figure 3.20.

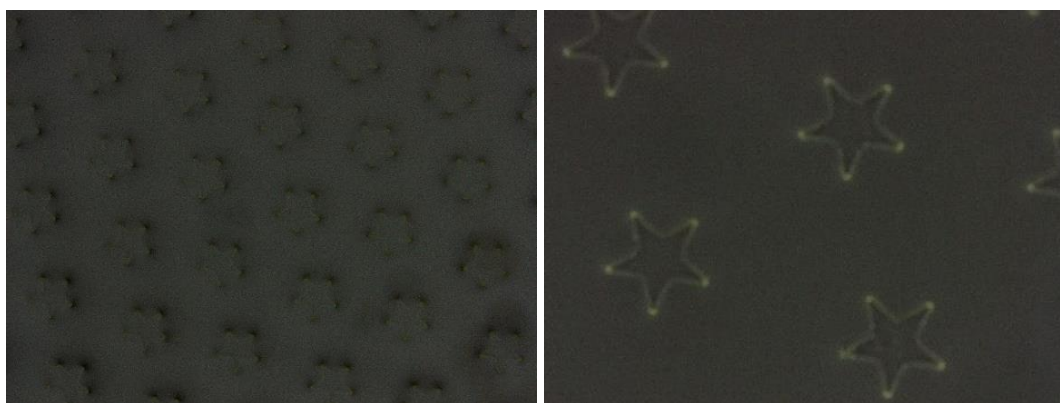


Figure 3.20. Starry imprinted surface via photolithography before UV exposure

In the photolithography test, the imprinted patterns obtained with fresh PGMEA and recycled PGMEA solvent developer bath were compared. In Figure 3.21. for comparison, the image on the upper left side belongs to the sample of fresh PGMEA developer bath and the image on the upper right side belongs to the sample from recycled solvent bath. Additionally, the image at the bottom shows the pattern of the recycled solvent bath from wider angle. In Figure 3.22, SEM images of the imprinted starry patterns with fresh and recycled solvents are shown. As can be seen, it was observed that the results were promising.

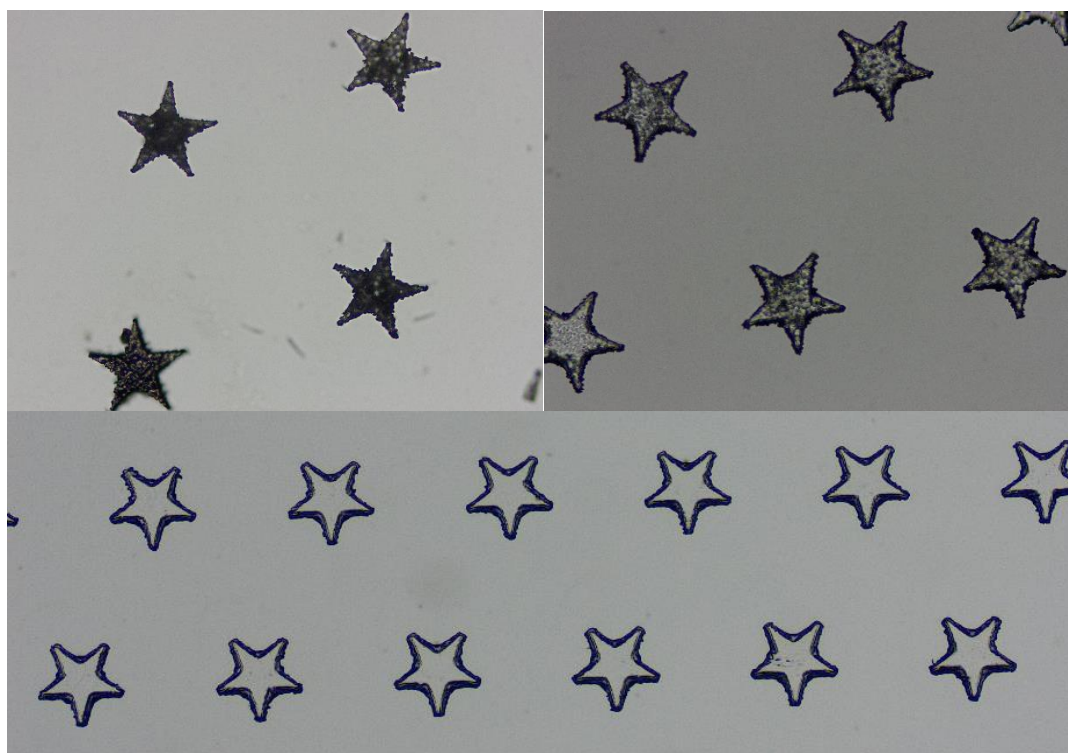


Figure 3.21. Microscope images of starry pattern after developer bath step with recycled solvent (upper right and bottom) and fresh PGMEA solvent (upper left)

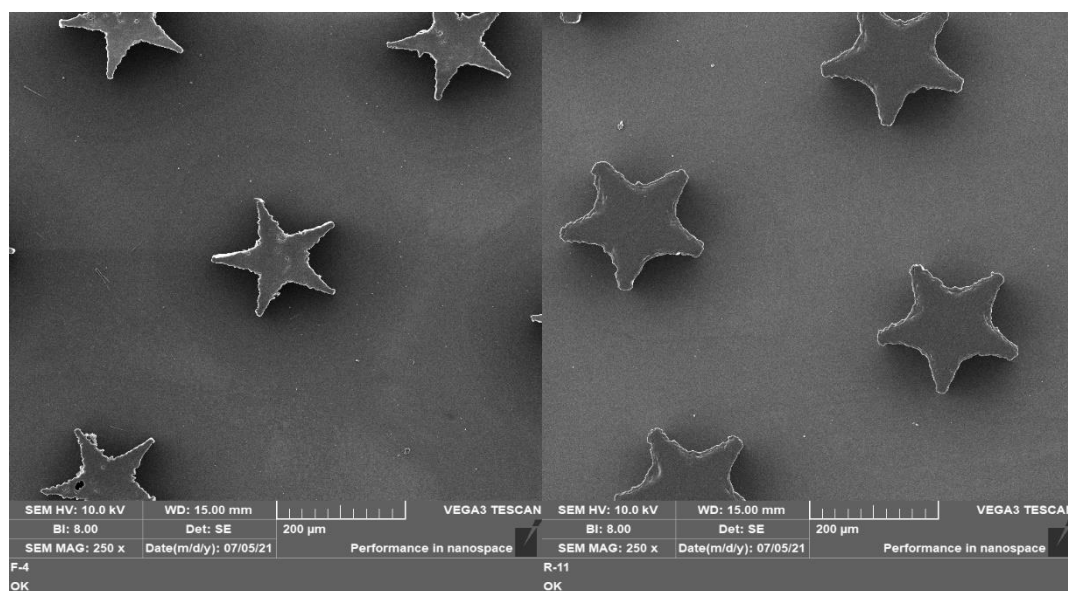


Figure 3.22. SEM images of starry pattern imprinted by fresh developer solvent (left) and recycled solvent (right)

The quantification of the error in pattern quality was determined via perimeter and concave angle measurements from the SEM images as shown in Figure 3.23. The five edge stars of photomask having 108° concave angles, used in photolithography have 100 micrometers radius hence approximately 727 micrometers perimeter. The perimeters of stars in SEM images were measured as $821\ \mu\text{m}$ and $842\ \mu\text{m}$ for fresh and recycled solvent cases, respectively. The related concave angles are measured as 108° and 120° . For the concave angle of the fresh solvent case, there was no error with 108° according to the photomask pattern. The reason behind the change in the pattern quality may be the remaining PAG salts on the edges of the stars. Considering that in the actual developer bath, the triarylsulfonium salts will partly decompose, as shown in Figure 1.11, better pattern fidelity may be expected.

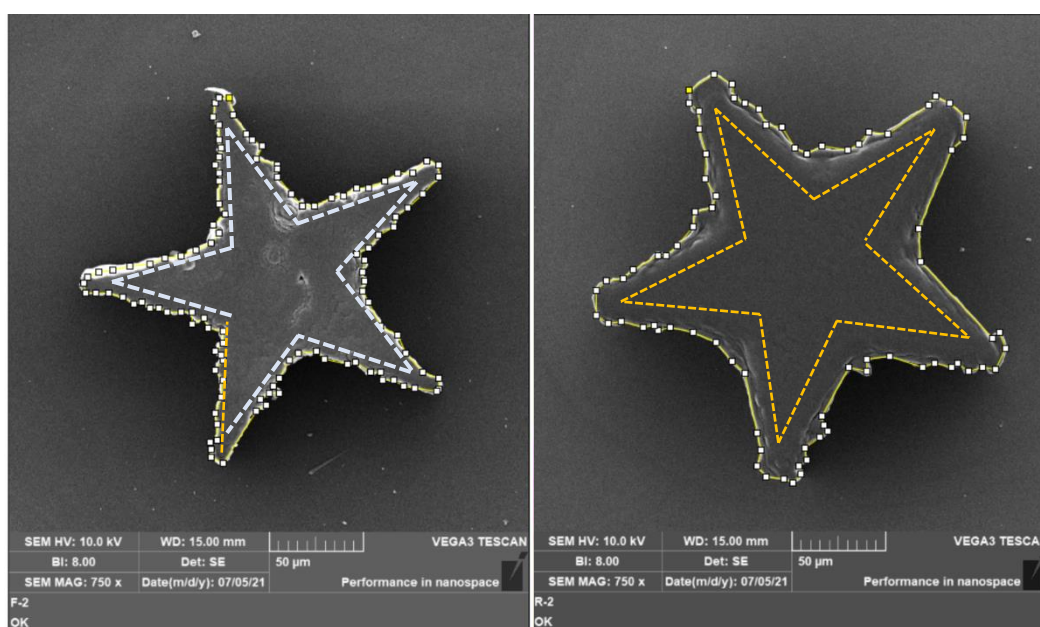


Figure 3.23. Starry pattern imprinted by fresh developer solvent (left) and recycled solvent (right) at x750 magnification

CHAPTER 4

CONCLUSION

In this study, cellulose ultrafiltration flat sheet membranes were fabricated for the solvent recovery from photolithography waste. Cellulose membranes were produced via alkaline hydrolysis of cellulose acetate membranes. Alkaline hydrolysis degree was analyzed with ATR-FTIR spectra of the samples regenerated in NaOH-water solutions having different concentrations and complete alkaline hydrolysis durations were determined for different concentrations. As a result, alkaline hydrolysis of the membranes were done in 0.05 M NaOH solutions for 24 h. In the first part of the study, the morphology tuning parameters of cellulose ultrafiltration membranes were varied and the performance of membranes was investigated with permeance and rejection tests. As the morphology tuning factors of the polymeric membranes; casting solution polymer composition, pore-former addition, co-solvent usage, annealing and coagulation bath temperature were evaluated. Firstly, all of the membranes were tested by water permeance tests and molecular weight cut-off (MWCO) tests with PEG probes. By this way, MWCO levels of the membranes were determined and the MWCO of the membranes were generally in 3-10 kDa range. The tightest UF membranes with the lowest MWCO values were obtained with CA30P10A10-AH and CA25P10A10-AN-AH membranes having approximately 3 kDa MWCO level. On the other hand, permeance of CA25P10A10-AN-AH membrane was higher.

In the second part of the study, PGMEA solvent recovery from the SU-8 photolithography wastes were done with cellulose ultrafiltration membranes. To mimic the photolithography wastes, SU-8 mixtures were prepared in PGMEA and then, the filtration was done with the fabricated cellulose membranes. The recycled

solvent was obtained with two stage filtration via CA25P10A10-AN-AH membrane. At the end of the 1st and 2nd stages of the filtration, approximately 90% and 80% SU-8 rejections were obtained. The permeate mixture of the 2nd stage filtration was reused in SU-8 photolithography. In the photolithography, starry patterned photomask was used and the change in pattern quality was evaluated by the comparison of fresh and recycled solvent cases. Microscope and SEM images of the patterns showed that the results of recycled solvent case was promising. For the quantification of the change in quality, the perimeter and concave angles of the stars in the fresh solvent and recycled solvent cases were compared. As a result, 3% star perimeter from 821 μm to 842 μm and 11% concave angle errors from 108° to 120° were observed in recycled solvent case compared to the fresh solvent case.

REFERENCES

1. Marchetti, P., Jimenez Solomon, M. F., Szekely, G. & Livingston, A. G. Molecular separation with organic solvent nanofiltration: A critical review. *Chemical Reviews* (2014) doi:10.1021/cr500006j.
2. King, C. J. *Separation Processes, Second Edition. Center for Studies in Higher Education* (1980).
3. Afonso, C. A. M. & Crespo, J. G. *Green Separation Processes: Fundamentals and Applications. Green Separation Processes: Fundamentals and Applications* (2006). doi:10.1002/3527606602.
4. Nunes, S. P. *et al.* Thinking the future of membranes: Perspectives for advanced and new membrane materials and manufacturing processes. *Journal of Membrane Science* vol. 598 117761 (2020).
5. Baker, R. W. *Membrane Technology and Applications. Membrane Technology and Applications* (John Wiley and Sons, 2012). doi:10.1002/9781118359686.
6. L.J. ZEMAN, ZYDNEY, A. L. & Dekker, M. Microfiltration and Ultrafiltration - Principles and Applications. *Chemie Ing. Tech.* (1996) doi:10.1002/cite.330691022.
7. Pore Size, Pore Size Distribution, and Roughness at the Membrane Surface. in *Synthetic Polymeric Membranes* 101–139 (Springer Berlin Heidelberg, 2007). doi:10.1007/978-3-540-73994-4_5.
8. LOEB, S. & SOURIRAJAN, S. Sea Water Demineralization by Means of an Osmotic Membrane. in 117–132 (1963). doi:10.1021/ba-1963-0038.ch009.
9. Basile, A. & Favvas, E. P. *Current trends and future developments on (Bio-) membranes: Carbon dioxide separation/capture by using membranes.*

Current Trends and Future Developments on (Bio-) Membranes: Carbon Dioxide Separation/Capture by using Membranes (Elsevier, 2018). doi:10.1016/C2016-0-04760-5.

10. Organic Solvents | NIOSH | CDC. <https://www.cdc.gov/niosh/topics/organsolv/default.html>.
11. Vane, L. *SUSTAINABLE & HEALTHY COMMUNITIES RESEARCH PROGRAM Actionable Science for Communities Techniques for Separating Organic Solvents to Facilitate Reuse and Remanufacturing (3.63 Task 2)*.
12. Pulido, B. A., Waldron, C., Zolotukhin, M. G. & Nunes, S. P. Porous polymeric membranes with thermal and solvent resistance. *J. Memb. Sci.* **539**, 187–196 (2017).
13. White, L. S. & Nitsch, A. R. Solvent recovery from lube oil filtrates with a polyimide membrane. *J. Memb. Sci.* **179**, 267–274 (2000).
14. De Smet, K., Aerts, S., Ceulemans, E., Vankelecom, I. F. J. & Jacobs, P. A. Nanofiltration-coupled catalysis to combine the advantages of homogeneous and heterogeneous catalysis. *Chem. Commun.* 597–598 (2001) doi:10.1039/b009898l.
15. Vankelecom, I. F. J. Polymeric membranes in catalytic reactors. *Chem. Rev.* **102**, 3779–3810 (2002).
16. Scarpello, J. T., Nair, D., Freitas Dos Santos, L. M., White, L. S. & Livingston, A. G. The separation of homogeneous organometallic catalysts using solvent resistant nanofiltration. *J. Memb. Sci.* **203**, 71–85 (2002).
17. Sheth, J. P., Qin, Y., Sirkar, K. K. & Baltzis, B. C. Nanofiltration-based diafiltration process for solvent exchange in pharmaceutical manufacturing. *J. Memb. Sci.* **211**, 251–261 (2003).
18. Bhosle, B. M., Subramanian, R. & Ebert, K. Deacidification of model

- vegetable oils using polymeric membranes. *Eur. J. Lipid Sci. Technol.* **107**, 746–753 (2005).
19. See Toh, Y. H., Lim, F. W. & Livingston, A. G. Polymeric membranes for nanofiltration in polar aprotic solvents. *J. Memb. Sci.* **301**, 3–10 (2007).
 20. Hořda, A. K., Aernouts, B., Saeys, W. & Vankelecom, I. F. J. Study of polymer concentration and evaporation time as phase inversion parameters for polysulfone-based SRNF membranes. *J. Memb. Sci.* **442**, 196–205 (2013).
 21. Valtcheva, I. B., Kumbharkar, S. C., Kim, J. F., Bhole, Y. & Livingston, A. G. Beyond polyimide: Crosslinked polybenzimidazole membranes for organic solvent nanofiltration (OSN) in harsh environments. *J. Memb. Sci.* **457**, 62–72 (2014).
 22. da Silva Burgal, J., Peeva, L. G., Kumbharkar, S. & Livingston, A. Organic solvent resistant poly(ether-ether-ketone) nanofiltration membranes. *J. Memb. Sci.* (2015) doi:10.1016/j.memsci.2014.12.035.
 23. Mertens, M., Van Goethem, C., Thijs, M., Koeckelberghs, G. & Vankelecom, I. F. J. Crosslinked PVDF-membranes for solvent resistant nanofiltration. *J. Memb. Sci.* (2018) doi:10.1016/j.memsci.2018.08.051.
 24. Polotskaya, G. A., Meleshko, T. K., Gofman, I. V., Polotsky, A. E. & Cherkasov, A. N. Polyimide ultrafiltration membranes with high thermal stability and chemical durability. *Sep. Sci. Technol.* **44**, 3814–3831 (2009).
 25. Yuan, S. *et al.* Nano/microstructure decorated thin film composite poly(arylene sulfide sulfone) membrane constructed by induced fouling in organic solvent ultrafiltration. *Chem. Eng. J.* **348**, 180–190 (2018).
 26. Yang, C. *et al.* Preparation and characterization of acid and solvent resistant polyimide ultrafiltration membrane. *Appl. Surf. Sci.* (2019) doi:10.1016/j.apsusc.2019.03.226.

27. Yin, Z., Ma, Y., Tanis-Kanbur, B. & Chew, J. W. Fouling behavior of colloidal particles in organic solvent ultrafiltration. *J. Memb. Sci.* **599**, 117836 (2020).
28. Yin, Z., Yeow, R. J. E., Ma, Y. & Chew, J. W. Link between interfacial interaction and membrane fouling during organic solvent ultrafiltration of colloidal foulants. *J. Memb. Sci.* **611**, 118369 (2020).
29. Luis, P. *Fundamental Modeling of Membrane Systems: Membrane and Process Performance. Fundamental Modeling of Membrane Systems: Membrane and Process Performance* (Elsevier, 2018). doi:10.1016/C2016-0-02489-0.
30. Pulido, B., Chisca, S. & Nunes, S. P. Solvent and thermal resistant ultrafiltration membranes from alkyne-functionalized high-performance polymers. *J. Memb. Sci.* (2018) doi:10.1016/j.memsci.2018.07.025.
31. de Melo, J. R. M., Tres, M. V., Steffens, J., Vladimir Oliveira, J. & Di Luccio, M. Desolventizing organic solvent-soybean oil miscella using ultrafiltration ceramic membranes. *J. Memb. Sci.* (2015) doi:10.1016/j.memsci.2014.10.029.
32. Yuan, S. *et al.* Nano/microstructure decorated thin film composite poly (arylene sulfide sulfone) membrane constructed by induced fouling in organic solvent ultrafiltration. *Chem. Eng. J.* (2018) doi:10.1016/j.cej.2018.04.183.
33. Jin, W. *et al.* Crosslinkable polyaryletherketone ultrafiltration membranes with solvent-resistant improvement. *Mater. Today Commun.* **21**, 100696 (2019).
34. Yousefi, N., Jones, M., Bismarck, A. & Mautner, A. Fungal chitin-glucan nanopapers with heavy metal adsorption properties for ultrafiltration of organic solvents and water. *Carbohydr. Polym.* **253**, 117273 (2021).
35. Tohidian, E., Dehban, A., Zokaee Ashtiani, F. & Kargari, A. Fabrication and

- characterization of a cross-linked two-layer polyetherimide solvent-resistant ultrafiltration (SRUF) membrane for separation of toluene–water mixture. *Chem. Eng. Res. Des.* **168**, 59–70 (2021).
36. Kostag, M. & El Seoud, O. A. Sustainable biomaterials based on cellulose, chitin and chitosan composites - A review. *Carbohydr. Polym. Technol. Appl.* **2**, 100079 (2021).
 37. Wang, S., Lu, A. & Zhang, L. Recent advances in regenerated cellulose materials. *Progress in Polymer Science* vol. 53 169–206 (2016).
 38. Medronho, B. & Lindman, B. Brief overview on cellulose dissolution/regeneration interactions and mechanisms. *Advances in Colloid and Interface Science* vol. 222 502–508 (2015).
 39. Durmaz, E. N. & Zeynep Çulfaz-Emecen, P. Cellulose-based membranes via phase inversion using [EMIM]OAc-DMSO mixtures as solvent. *Chem. Eng. Sci.* **178**, 93–103 (2018).
 40. Sukma, F. M. & Çulfaz-Emecen, P. Z. Cellulose membranes for organic solvent nanofiltration. *J. Memb. Sci.* **545**, 329–336 (2018).
 41. Boluk, Y. Acid-base interactions and swelling of cellulose fibers in organic liquids. *Cellulose* **12**, 577–593 (2005).
 42. Fidale, L. C., Ruiz, N., Heinze, T. & El Seoud, O. A. Cellulose swelling by aprotic and protic solvents: What are the similarities and differences? *Macromol. Chem. Phys.* **209**, 1240–1254 (2008).
 43. Philipp, B., Schleicher, H. & Wagenknecht, W. Influence of cellulose structure on the swelling of cellulose in organic liquids. *J. Polym. Sci. Polym. Symp.* **42**, 1531–1543 (1973).
 44. Anokhina, T., Ignatenko, V., Ilyin, S., Antonov, S. & Volkov, A. Fabrication of cellulose-based composite membranes for organic solvent nanofiltration. *J.*

- Phys. Conf. Ser.* **1099**, 012039 (2018).
45. Falca, G., Musteata, V. E., Behzad, A. R., Chisca, S. & Nunes, S. P. Cellulose hollow fibers for organic resistant nanofiltration. *J. Memb. Sci.* **586**, 151–161 (2019).
 46. Sukma, F. M. *CELLULOSE MEMBRANES FOR ORGANIC SOLVENT NANOFILTRATION A THESIS SUBMITTED TO THE GRADUATE SCHOOL OF NATURAL AND APPLIED SCIENCES OF MIDDLE EAST TECHNICAL UNIVERSITY.* (2016).
 47. Konca, K. & Çulfaz-Emecen, P. Z. Effect of carboxylic acid crosslinking of cellulose membranes on nanofiltration performance in ethanol and dimethylsulfoxide. *J. Memb. Sci.* **587**, 117175 (2019).
 48. Liu, H. & Hsieh, Y. Lo. Ultrafine fibrous cellulose membranes from electrospinning of cellulose acetate. *J. Polym. Sci. Part B Polym. Phys.* **40**, 2119–2129 (2002).
 49. Yamashita, Y. & Endo, T. Deterioration behavior of cellulose acetate films in acidic or basic aqueous solutions. *J. Appl. Polym. Sci.* **91**, 3354–3361 (2004).
 50. Sofi, H. S. *et al.* Regenerated cellulose nanofibers from cellulose acetate: Incorporating hydroxyapatite (HAp) and silver (Ag) nanoparticles (NPs), as a scaffold for tissue engineering applications. *Mater. Sci. Eng. C* **118**, (2021).
 51. Son, W. K., Youk, J. H., Lee, T. S. & Park, W. H. Electrospinning of ultrafine cellulose acetate fibers: Studies of a new solvent system and deacetylation of ultrafine cellulose acetate fibers. *J. Polym. Sci. Part B Polym. Phys.* **42**, 5–11 (2004).
 52. Feng, C., Wang, R., Shi, B., Li, G. & Wu, Y. Factors affecting pore structure and performance of poly(vinylidene fluoride-co-hexafluoro propylene) asymmetric porous membrane. *J. Memb. Sci.* **277**, 55–64 (2006).

53. Bottino, A., Capannelli, G. & Munari, S. FACTORS AFFECTING THE STRUCTURE AND PROPERTIES OF ASYMMETRIC POLYMERIC MEMBRANES. in 163–178 (Plenum Press, 1986). doi:10.1007/978-1-4899-2019-5_17.
54. Hołda, A. K. & Vankelecom, I. F. J. Understanding and guiding the phase inversion process for synthesis of solvent resistant nanofiltration membranes. *J. Appl. Polym. Sci.* **132**, 42130 (2015).
55. Liu, Y., Koops, G. H. & Strathmann, H. Characterization of morphology controlled polyethersulfone hollow fiber membranes by the addition of polyethylene glycol to the dope and bore liquid solution. *J. Memb. Sci.* **223**, 187–199 (2003).
56. Strathmann, H., Kock, K., Amar, P. & Baker, R. W. The formation mechanism of asymmetric membranes. *Desalination* **16**, 179–203 (1975).
57. Strathmann, H. & Kock, K. The formation mechanism of phase inversion membranes. *Desalination* **21**, 241–255 (1977).
58. Madaeni, S. S. & Taheri, A. H. Effect of Casting Solution on Morphology and Performance of PVDF Microfiltration Membranes. *Chem. Eng. Technol.* **34**, 1328–1334 (2011).
59. Sani, N. A. A., Lau, W. J. & Ismail, A. F. Influence of polymer concentration in casting solution and solvent-solute-membrane interactions on performance of polyphenylsulfone (PPSU) nanofiltration membrane in alcohol solvents. *J. Polym. Eng.* **34**, 489–500 (2014).
60. Āmir, Z. *CELLULOSE MEMBRANES VIA ALKALINE HYDROLYSIS OF CELLULOSE ACETATE MEMBRANES AND THEIR APPLICATION IN ORGANIC SOLVENTS A THESIS SUBMITTED TO THE GRADUATE SCHOOL OF NATURAL AND APPLIED SCIENCES OF MIDDLE EAST TECHNICAL UNIVERSITY.* (2019).

61. Durmaz, E. N. *INVESTIGATION OF PHASE INVERSION BEHAVIOR OF CELLULOSE-IONIC LIQUID SOLUTIONS IN RELATIONSHIP WITH MEMBRANE FORMATION A THESIS SUBMITTED TO THE GRADUATE SCHOOL OF NATURAL AND APPLIED SCIENCES OF MIDDLE EAST TECHNICAL UNIVERSITY.* (2017).
62. Tsai, J. T. *et al.* Retainment of pore connectivity in membranes prepared with vapor-induced phase separation. *J. Memb. Sci.* **362**, 360–373 (2010).
63. Yeow, M. L., Liu, Y. T. & Li, K. Morphological study of poly(vinylidene fluoride) asymmetric membranes: Effects of the solvent, additive, and dope temperature. *J. Appl. Polym. Sci.* **92**, 1782–1789 (2004).
64. Guillen, G. R., Pan, Y., Li, M. & Hoek, E. M. V. Preparation and characterization of membranes formed by nonsolvent induced phase separation: A review. *Ind. Eng. Chem. Res.* **50**, 3798–3817 (2011).
65. Li, Q., Xu, Z.-L. & Yu, L.-Y. Effects of mixed solvents and PVDF types on performances of PVDF microporous membranes. *J. Appl. Polym. Sci.* **115**, 2277–2287 (2010).
66. Ma, Y. *et al.* Preparation and characterization of PSf/clay nanocomposite membranes with PEG 400 as a pore forming additive. *Desalination* **286**, 131–137 (2012).
67. Roy, K. J., Anjali, T. V. & Sujith, A. Asymmetric membranes based on poly(vinyl chloride): effect of molecular weight of additive and solvent power on the morphology and performance. *J. Mater. Sci.* **52**, 5708–5725 (2017).
68. Panda, S. R. & De, S. Effects of polymer molecular weight, concentration, and role of polyethylene glycol as additive on polyacrylonitrile homopolymer membranes. *Polym. Eng. Sci.* **54**, 2375–2391 (2014).
69. Chou, W. L., Yu, D. G., Yang, M. C. & Jou, C. H. Effect of molecular weight and concentration of PEG additives on morphology and permeation

- performance of cellulose acetate hollow fibers. *Sep. Purif. Technol.* **57**, 209–219 (2007).
70. Arthanareeswaran, G. & Kumar, S. A. Effect of additives concentration on performance of cellulose acetate and polyethersulfone blend membranes. *J. Porous Mater.* **17**, 515–522 (2010).
71. Kim, D. L., Le, N. L. & Nunes, S. P. The effects of a co-solvent on fabrication of cellulose acetate membranes from solutions in 1-ethyl-3-methylimidazolium acetate. *J. Memb. Sci.* **520**, 540–549 (2016).
72. Nguyen, T. P. N., Yun, E. T., Kim, I. C. & Kwon, Y. N. Preparation of cellulose triacetate/cellulose acetate (CTA/CA)-based membranes for forward osmosis. *J. Memb. Sci.* **433**, 49–59 (2013).
73. Bokhorst, H., Altena, F. W. & Smolders, C. A. Formation of asymmetric cellulose acetate membranes. *Desalination* **38**, 349–360 (1981).
74. Nunes, S. P., Galembeck, F. & Barelli, N. Cellulose acetate membranes for osmosedimentation: Performance and morphological dependence on preparation conditions. *Polymer (Guildf)*. **27**, 937–943 (1986).
75. Schwarz, H. H. & Hicke, H. G. Influence of casting solution concentration on structure and performance of cellulose acetate membranes. *J. Memb. Sci.* **46**, 325–334 (1989).
76. Murphy, D. & de Pinho, M. N. An ATR-FTIR study of water in cellulose acetate membranes prepared by phase inversion. *J. Memb. Sci.* **106**, 245–257 (1995).
77. Arthanareeswaran, G., Thanikaivelan, P., Srinivasn, K., Mohan, D. & Rajendran, M. Synthesis, characterization and thermal studies on cellulose acetate membranes with additive. *Eur. Polym. J.* **40**, 2153–2159 (2004).
78. Ferjani, E., Ellouze, E. & Ben Amar, R. Treatment of seafood processing

- wastewaters by ultrafiltration-nanofiltration cellulose acetate membranes. *Desalination* **177**, 43–49 (2005).
79. Duarte, A. P., Bordado, J. C. & Cidade, M. T. Cellulose acetate reverse osmosis membranes: Optimization of preparation parameters. *J. Appl. Polym. Sci.* **103**, 134–139 (2007).
 80. Arthanareeswaran, G., Thanikaivelan, P., Raguime, J. A., Raajenthiren, M. & Mohan, D. Metal ion separation and protein removal from aqueous solutions using modified cellulose acetate membranes: Role of polymeric additives. *Sep. Purif. Technol.* **55**, 8–15 (2007).
 81. Arthanareeswaran, G., Sriyamuna Devi, T. K. & Raajenthiren, M. Effect of silica particles on cellulose acetate blend ultrafiltration membranes: Part I. *Sep. Purif. Technol.* **64**, 38–47 (2008).
 82. Saljoughi, E. & Mohammadi, T. Cellulose acetate (CA)/polyvinylpyrrolidone (PVP) blend asymmetric membranes: Preparation, morphology and performance. *Desalination* **249**, 850–854 (2009).
 83. Cano-Odena, A. *et al.* Optimization of cellulose acetate nanofiltration membranes for micropollutant removal via genetic algorithms and high throughput experimentation. *J. Memb. Sci.* **366**, 25–32 (2011).
 84. Nolte, M. C. M., Simon, P. F. W., del Toro, M. A., Gerstandt, K. & Calmano, W. Cellulose acetate reverse osmosis membranes made by phase inversion method: Effects of a shear treatment applied to the casting solution on the membrane structure and performance. *Sep. Sci. Technol.* **46**, 395–403 (2011).
 85. Medina-Gonzalez, Y., Aimar, P., Lahitte, J. F. & Remigy, J. C. Towards green membranes: Preparation of cellulose acetate ultrafiltration membranes using methyl lactate as a biosolvent. *Int. J. Sustain. Eng.* **4**, 75–83 (2011).
 86. Ghaemi, N. *et al.* Separation of nitrophenols using cellulose acetate nanofiltration membrane: Influence of surfactant additives. *Sep. Purif.*

- Technol.* **85**, 147–156 (2012).
87. Rana, D. *et al.* Comparison of cellulose acetate (CA) membrane and novel CA membranes containing surface modifying macromolecules to remove pharmaceutical and personal care product micropollutants from drinking water. *J. Memb. Sci.* **409–410**, 346–354 (2012).
 88. Krason, J. & Pietrzak, R. Membranes obtained on the basis of cellulose acetate and their use in removal of metal ions from liquid phase. *Polish J. Chem. Technol.* **18**, 104–110 (2016).
 89. Afzal, A. *et al.* Synergistic effect of functionalized nanokaolin decorated MWCNTs on the performance of cellulose acetate (CA) membranes spectacular. *Nanomaterials* **6**, 79 (2016).
 90. Waheed, H., Hussain, A. & Farrukh, S. Fabrication, characterization and permeation study of ultrafiltration dialysis membranes. *Desalin. Water Treat.* **57**, 24799–24806 (2016).
 91. Zhou, J., Chen, J., He, M. & Yao, J. Cellulose acetate ultrafiltration membranes reinforced by cellulose nanocrystals: Preparation and characterization. *J. Appl. Polym. Sci.* **133**, (2016).
 92. Rakhshan, N. & Pakizeh, M. The effect of functionalized SiO₂ nanoparticles on the morphology and triazines separation properties of cellulose acetate membranes. *J. Ind. Eng. Chem.* **34**, 51–60 (2016).
 93. Da Silva Pereira, B. *et al.* Water permeability increase in ultrafiltration cellulose acetate membrane containing silver nanoparticles. in *Materials Research* vol. 20 887–891 (Universidade Federal de Sao Carlos, 2017).
 94. Sprick, C., Chede, S., Oyanedel-Craver, V. & Escobar, I. C. Bio-inspired immobilization of casein-coated silver nanoparticles on cellulose acetate membranes for biofouling control. *J. Environ. Chem. Eng.* **6**, 2480–2491 (2018).

95. Mulijani, S., Iswantini, D., Wicaksono, R. & Notriawan, D. Optical Sensor based Chemical Modification as a Porous Cellulose Acetate Film and Its Application for Ethanol Sensor. in *IOP Conference Series: Materials Science and Engineering* vol. 333 012014 (Institute of Physics Publishing, 2018).
96. Vaulina, E., Widyaningsih, S., Kartika, D. & Romdoni, M. P. The Effect of Cellulose Acetate Concentration from Coconut Nira on Ultrafiltration Membrane Characters. in *IOP Conference Series: Materials Science and Engineering* vol. 349 012020 (Institute of Physics Publishing, 2018).
97. Mulyati, S. *et al.* The effect of poly ethylene glycol additive on the characteristics and performance of cellulose acetate ultrafiltration membrane for removal of Cr(III) from aqueous solution. in *IOP Conference Series: Materials Science and Engineering* vol. 352 012051 (Institute of Physics Publishing, 2018).
98. Nu, D. T. T., Hung, N. P., Van Hoang, C. & Van der Bruggen, B. Preparation of an asymmetric membrane from sugarcane bagasse using DMSO as green solvent. *Appl. Sci.* **9**, 3347 (2019).
99. Marbelia, L. *et al.* Preparation of patterned flat-sheet membranes using a modified phase inversion process and advanced casting knife construction techniques. *J. Memb. Sci.* **597**, 117621 (2020).
100. Han, M. J. & Nam, S. T. Thermodynamic and rheological variation in polysulfone solution by PVP and its effect in the preparation of phase inversion membrane. *J. Memb. Sci.* **202**, 55–61 (2002).
101. Rahimpour, A. & Madaeni, S. S. Polyethersulfone (PES)/cellulose acetate phthalate (CAP) blend ultrafiltration membranes: Preparation, morphology, performance and antifouling properties. *J. Memb. Sci.* **305**, 299–312 (2007).
102. Saljoughi, E., Sadrzadeh, M. & Mohammadi, T. Effect of preparation variables on morphology and pure water permeation flux through asymmetric

- cellulose acetate membranes. *J. Memb. Sci.* **326**, 627–634 (2009).
103. Mozia, S., Tomaszewska, M. & Morawski, A. W. Studies on the effect of humic acids and phenol on adsorption- ultrafiltration process performance. *Water Res.* **39**, 501–509 (2005).
 104. Costa, A. R. & De Pinho, M. N. Effect of membrane pore size and solution chemistry on the ultrafiltration of humic substances solutions. *J. Memb. Sci.* **255**, 49–56 (2005).
 105. Schwarz, H. H., Richau, K. & Hicke, H. G. Annealing effect in porous cellulose acetate membranes. *J. Memb. Sci.* **34**, 283–296 (1987).
 106. Aburideh, H. *et al.* THERMAL ANNEALING EFFECT ON MORPHOLOGY AND PERFORMANCE OF POLYSULFONE-CELLULOSE ACETATE MEMBRANES: APPLICATION FOR WATER DEFLUORIDATION. *CELLULOSE CHEMISTRY AND TECHNOLOGY Cellulose Chem. Technol* vol. 53 (2019).
 107. Mahendran, R., Malaisamy, R. & Mohan, D. Preparation, characterization and effect of annealing on performance of cellulose acetate/sulfonated polysulfone and cellulose acetate/epoxy resin blend ultrafiltration membranes. *Eur. Polym. J.* **40**, 623–633 (2004).
 108. Tahun, M. *et al.* Fouling Evaluation of Modified Cellulose Acetate Asymmetric Membranes for Various Brackish Water Treatment. (2017).
 109. Khan, S. *et al.* Synthesis and characterization of low molecular weight cut off ultrafiltration membranes from cellulose propionate polymer. *Desalination* **128**, 57–66 (2000).
 110. Yuan, G. L., Xu, Z. L. & Wei, Y. M. Characterization of PVDF-PFSA hollow fiber UF blend membrane with low-molecular weight cut-off. *Sep. Purif. Technol.* **69**, 141–148 (2009).

111. Yehl, C. J. & Zydney, A. L. Characterization of dextran transport and molecular weight cutoff (MWCO) of large pore size hollow fiber ultrafiltration membranes. *J. Memb. Sci.* **622**, (2021).
112. Idris, A., Mat Zain, N. & Noordin, M. Y. Synthesis, characterization and performance of asymmetric polyethersulfone (PES) ultrafiltration membranes with polyethylene glycol of different molecular weights as additives. *Desalination* **207**, 324–339 (2007).
113. Capello, C., Wernet, G., Sutter, J., Hellweg, S. & Hungerbühler, K. A comprehensive environmental assessment of petrochemical solvent production. *Int. J. Life Cycle Assess.* **14**, 467–479 (2009).
114. European Commission. Directive 2008/98/EC on waste (Waste Framework Directive) - Environment - European Commission. <https://ec.europa.eu/environment/waste/framework/>.
115. Waste and Circular Economy | EU Science Hub. <https://ec.europa.eu/jrc/en/research-topic/waste-and-recycling>.
116. ESRG - European Solvent Recycler Group. *Europe's Green Agenda*. <http://library1.nida.ac.th/termpaper6/sd/2554/19755.pdf> (2020).
117. Raymond, M. J., Slater, C. S. & Savelski, M. J. LCA approach to the analysis of solvent waste issues in the pharmaceutical industry. *Green Chem.* **12**, 1826–1834 (2010).
118. Capello, C. *et al.* CASE STUDY • PETROCHEMICAL SOLVENT PRODUCTION ROUTES A comprehensive environmental assessment of petrochemical solvent production. *Int J Life Cycle Assess* **14**, 467–479 (2009).
119. Tozzi, P. V. *et al.* Life cycle assessment of solvent extraction as a low-energy alternative to distillation for recovery of N-methyl-2-pyrrolidone from process waste. *Green Process. Synth.* **7**, 277–286 (2018).

120. Amelio, A., Genduso, G., Vreysen, S., Luis, P. & Van Der Bruggen, B. Guidelines based on life cycle assessment for solvent selection during the process design and evaluation of treatment alternatives. *Green Chem.* **16**, 3045–3063 (2014).
121. ESRG - European Solvent Recycler Group. *Carbon footprint of recycled solvents at the sectoral level compared to virgin solvents Study for the European Solvent Recycler Group (ESRG) ETHOS Environment · Technology · Society*. www.esrg-online.eu (2018).
122. European Environment Agency. circular-economy-system-diagram (693×970). <https://www.eea.europa.eu/soer/2020/soer-2020-visuals/circular-economy-system-diagram> (2019).
123. Kirchherr, J., Reike, D. & Hekkert, M. Conceptualizing the circular economy: An analysis of 114 definitions. *Resources, Conservation and Recycling* vol. 127 221–232 (2017).
124. ECHA - European Chemicals Agency. Consumers and SCIP - ECHA. <https://echa.europa.eu/consumers-and-scip>.
125. European Commission. New Circular Economy Strategy - Environment - European Commission. <https://ec.europa.eu/environment/circular-economy/> (2020).
126. Hartmut Stahl, C. M. (Oeko-I. e. V. . Study to support the Commission in gathering structured information and defining of reporting obligations on waste oils and other hazardous waste. https://esrg.de/media/PDF/EU_STUDY_WasteOil_Solvents_Oeko_final-report_for_publication.pdf (2020).
127. Micronas. *Environmental Statement*. (2010).
128. Martinez-Duarte, R. & Madou, M. J. *8 SU-8 Photolithography and Its Impact on Microfluidics*.

129. KMG Chemicals. Solvents & GenSolve™ Blends. <https://kmgchemicals.com/our-businesses/electronic-chemicals/products/solvents-solvent-blends/>.
130. Micro Chemicals. *Fundamentals of Microstructuring PHOTORESIST REMOVAL*. www.microchemicals.com/downloads/application_notes.html.
131. EHCA. Information on Chemicals. <https://echa.europa.eu/information-on-chemicals>.
132. Maratek Environmental. Solvent Waste Recycling & Recovery Services. <https://www.maratekenvironmental.com/solutions/solvent-waste-recycling-recovery-disposal-service/>.
133. Veolia North America. Solvent Recycling's Key Role in the Circular Economy. <http://blog.veolianorthamerica.com/solvent-recycling-key-role-circular-economy> (2019).
134. Veolia North America. Recycled Solvents For Sale | Veolia North America. <https://www.veolianorthamerica.com/what-we-do/waste-capabilities/recycled-solvents-sale>.
135. Industrial Technology Research Institute (ITRI). Green Technology for Electronic Grade Solvent Recycling. https://www.itri.org.tw/english/ListStyle.aspx?DisplayStyle=01_content&SiteID=1&MmmID=1037333532432522160&MGID=1073047612264160133.
136. Chaniago, Y. D., Harvianto, G. R., Bahadori, A. & Lee, M. Enhanced recovery of PGME and PGMEA from waste photoresistor thinners by heterogeneous azeotropic dividing-wall column. *Process Saf. Environ. Prot.* **103**, 413–423 (2016).
137. Vikalp Group. Recycled Products. <https://vikalpgroup.com/recycled-products/#squelch-taas-toggle-shortcode-content-0>.

138. SHINKO ORGANIC CHEMICAL INDUSTRY LTD. Solvent Recycle. <https://www.shinkoyuki.co.jp/en/jutaku/recycle/index.html>.
139. KMG Chemicals. Electronic Chemicals. <https://kmgchemicals.com/our-businesses/electronic-chemicals/>.
140. KMG Chemicals. Manufacturing & Services. <https://kmgchemicals.com/our-businesses/electronic-chemicals/manufacturing-services/>.
141. KMG Chemicals. Sustainability. <https://kmgchemicals.com/corporate-responsibility/sustainability/>.
142. IBM. *Hazardous Waste Facility Permit*. <https://dec.vermont.gov/sites/dec/files/documents/Final2014IBMPermitOneDocument.pdf> (2014).
143. Infineon Technologies. *Our Sustainability Targets*. (2018).
144. Vandezande, P. Periodic Report Summary - SOLVER (Solvent purification and recycling in the process industry using innovative membrane technology). *SOLVER Report Summary* http://cordis.europa.eu/result/rcn/61706_en.html (2014).
145. Grand View Search. Aprotic Solvents Market Size & Analysis | Global Industry Report, 2025. <https://www.grandviewresearch.com/industry-analysis/aprotic-solvents-market> (2016).
146. Merck Global. Cyrene: a cleaner alternative to harmful organic solvents - Research. <https://www.merckgroup.com/en/research/science-space/envisioning-tomorrow/scarcity-of-resources/cyrene.html>.
147. MENAFN. Global Propylene Glycol Methyl Ether Acetate (PGMEA) Market Size Worth Around USD 216.5 million by 2026, from USD 142.3 million in 2020, at a CAGR of 7.2% During 2020-2026 with Top Countries Data. <https://menafn.com/1101170711/Global-Propylene-Glycol-Methyl-Ether->

Acetate-PGMEA-Market-Size-Worth-Around-USD-2165-million-by-2026-from-USD-1423-million-in-2020-at-a-CAGR-of-72-During-2020-2026-with-Top-Countries-Data (2020).

148. Shell. Propylene glycol methyl ether (PGME) and Propylene glycol methyl ether acetate (PGMEA) [MethylPROXITOL and MethylPROXITOL acetate] Product Stewardship Summary. (2011).
149. Solvents Use in Microchip Production. <https://solvents.americanchemistry.com/Solvents-Explained/Benefits/solvents-use-in-microchip-production.html>.
150. Markets | KMG Chemicals. <https://kmgchemicals.com/our-businesses/electronic-chemicals/markets/>.
151. Applications. <https://www.gersteltec.ch/applications/#app2>.
152. Bratton, D., Yang, D., Dai, J. & Ober, C. K. Recent progress in high resolution lithography. *Polymers for Advanced Technologies* vol. 17 94–103 (2006).
153. Optical Lithography - an overview. *Nanocoatings and Ultra-Thin Films* <https://www.sciencedirect.com/topics/materials-science/optical-lithography> (2011).
154. Zahn, J. D. *Methods in Bioengineering - Biomicrofabrication and BioMicrofluidics*. *Bioengineering* (2010).
155. Pinto, V., Sousa, P., Cardoso, V. & Minas, G. Optimized SU-8 Processing for Low-Cost Microstructures Fabrication without Cleanroom Facilities. *Micromachines* **5**, 738–755 (2014).
156. Reznikova, E. F., Mohr, J. & Hein, H. Deep photo-lithography characterization of SU-8 resist layers. in *Microsystem Technologies* vol. 11 282–291 (Springer, 2005).
157. Treliant Fang. US7005233B2 - Photoresist formulation for high aspect ratio

- plating - Google Patents. <https://patents.google.com/patent/US7005233> (2006).
158. Hurditch, R. *Fast drying thick film negative photoresist*. www.microchem.com/resourceS/Su8 (2002).
 159. Dentinger, P. M., Clift, W. M. & Goods, S. H. Removal of SU-8 photoresist for thick film applications. in *Microelectronic Engineering* vols 61–62 993–1000 (Elsevier, 2002).
 160. Teh, W. H., Dürig, U., Drechsler, U., Smith, C. G. & Güntherodt, H.-J. Effect of low numerical-aperture femtosecond two-photon absorption on (SU-8) resist for ultrahigh-aspect-ratio microstereolithography. *J. Appl. Phys.* **97**, 054907 (2005).
 161. Abgrall, P., Conedera, V., Camon, H., Gue, A.-M. & Nguyen, N.-T. SU-8 as a structural material for labs-on-chips and microelectromechanical systems. (2007) doi:10.1002/elps.200700333.
 162. Bertsch, A. & Renaud, P. Special Issue: 15 Years of SU8 as MEMS Material. **6**, 790–792 (1997).
 163. Tulos, N., Harbottle, D., Hebden, A., Goswami, P. & Blackburn, R. S. Kinetic Analysis of Cellulose Acetate/Cellulose II Hybrid Fiber Formation by Alkaline Hydrolysis. (2019) doi:10.1021/acsomega.9b00159.
 164. Ali, I. *et al.* Assessment of blend PVDF membranes, and the effect of polymer concentration and blend composition. *Membranes (Basel)*. **8**, (2018).
 165. Geanina Tiron, L. *et al.* *Influence of Polymer Concentration on Membrane Performance in Wastewater Treatment*. <http://www.revmaterialeplastice.ro> (2018) doi:10.37358/MP.18.1.4971.
 166. Košutić, K. & Kunst, B. Effect of hydrolysis on porosity of cellulose acetate reverse osmosis membranes. *J. Appl. Polym. Sci.* **81**, 1768–1775 (2001).

167. Wang, H. H. *et al.* A novel green solvent alternative for polymeric membrane preparation via nonsolvent-induced phase separation (NIPS). *J. Memb. Sci.* **574**, 44–54 (2019).
168. Kim, J. H. & Lee, K. H. Effect of PEG additive on membrane formation by phase inversion. *J. Memb. Sci.* **138**, 153–163 (1998).
169. Saljoughi, E., Amirilargani, M. & Mohammadi, T. Effect of poly(vinyl pyrrolidone) concentration and coagulation bath temperature on the morphology, permeability, and thermal stability of asymmetric cellulose acetate membranes. *J. Appl. Polym. Sci.* **111**, 2537–2544 (2009).
170. Saljoughi, E., Amirilargani, M. & Mohammadi, T. Effect of PEG additive and coagulation bath temperature on the morphology, permeability and thermal/chemical stability of asymmetric CA membranes. *Desalination* **262**, 72–78 (2010).
171. Chakrabarty, B., Ghoshal, A. K. & Purkait, M. K. Effect of molecular weight of PEG on membrane morphology and transport properties. *J. Memb. Sci.* **309**, 209–221 (2008).
172. Ma, Y. *et al.* Effect of PEG additive on the morphology and performance of polysulfone ultrafiltration membranes. *Desalination* **272**, 51–58 (2011).
173. Gebru, K. A. & Das, C. Effects of solubility parameter differences among PEG, PVP and CA on the preparation of ultrafiltration membranes: Impacts of solvents and additives on morphology, permeability and fouling performances. *Chinese J. Chem. Eng.* **25**, 911–923 (2017).
174. Farjami, M., Vatanpour, V. & Moghadassi, A. Influence of the various pore former additives on the performance and characteristics of the bare and EPVC/boehmite nanocomposite ultrafiltration membranes. *Mater. Today Commun.* **21**, 100663 (2019).
175. Lv, C. *et al.* Enhanced permeation performance of cellulose acetate

- ultrafiltration membrane by incorporation of Pluronic F127. *J. Memb. Sci.* **294**, 68–74 (2007).
176. da Silva Burgal, J., Peeva, L., Marchetti, P. & Livingston, A. Controlling molecular weight cut-off of PEEK nanofiltration membranes using a drying method. *J. Memb. Sci.* **493**, 524–538 (2015).
177. Drioli, E., Giorno, L. & Macedonio, F. *Membrane engineering*. (De Gruyter, 2018).
178. Vankelecom, I. F. J. *et al.* Physico-chemical interpretation of the SRNF transport mechanism for solvents through dense silicone membranes. *J. Memb. Sci.* **231**, 99–108 (2004).
179. Stamatialis, D. F., Stafie, N., Buadu, K., Hempenius, M. & Wessling, M. Observations on the permeation performance of solvent resistant nanofiltration membranes. *J. Memb. Sci.* **279**, 424–433 (2006).
180. Çağlayan, P. *ChE499 Topics in Chemical Engineering II - Project Report*. (2020).
181. Anokhina, T. S. *et al.* Cellulose composite membranes for nanofiltration of aprotic solvents. *Pet. Chem.* **56**, 1085–1092 (2016).
182. Koops, G. H., Yamada, S. & Nakao, S. I. Separation of linear hydrocarbons and carboxylic acids from ethanol and hexane solutions by reverse osmosis. *J. Memb. Sci.* **189**, 241–254 (2001).
183. Bhanushali, D., Kloos, S. & Bhattacharyya, D. Solute transport in solvent-resistant nanofiltration membranes for non-aqueous systems: Experimental results and the role of solute-solvent coupling. *J. Memb. Sci.* **208**, 343–359 (2002).
184. Darvishmanesh, S., Buekenhoudt, A., Degève, J. & Van der Bruggen, B. General model for prediction of solvent permeation through organic and

- inorganic solvent resistant nanofiltration membranes. *J. Memb. Sci.* (2009)
doi:10.1016/j.memsci.2009.02.013.
185. Shen, M., Keten, S. & Lueptow, R. M. Rejection mechanisms for contaminants in polyamide reverse osmosis membranes. *J. Memb. Sci.* **509**, 36–47 (2016).
186. Aldrich Chemical Co, A. *Aldrich Polymer Products Application & Reference Information*. www.sigma-aldrich.com.

APPENDICES

A. Calibration Graphs

Gel Permeation Chromatography and PEG Probe Calibrations

In the Gel Permeation Chromatography analyses of the MWCO test samples, the specific measurement conditions and settings were used for all measurements. 1.0 ml/min, 30.5°C and water were used as the flow rate, analysis temperature and the mobile phase, respectively. Whereas HPLC Online software was used for the observation of the live analysis and the management of the settings, HPLC Offline program was used to detect the chromatograms, probe retention times, peak areas and to export the graphs for the peak deconvolution if necessary.

In the GPC device, there are four main units as IsoPump, Sampler, Column Compartment and RID unit. Before the GPC analysis of a sample, the purge valve of the RID unit was opened and it was kept for at least 1 hour. Then, the purge valve was closed and the samples in the GPC vials were placed into the Automatic Liquid Sampler (ALS) compartment holders. The pre-defined method with the specific conditions for the analysis of the MWCO test samples was loaded. When all the units were in ready position, the analysis sequence was given to the software with the coordinates of the GPC vials in the ALS compartment. After the analysis, the RI signal vs. retention time data was exported in the HPLC Offline software.

To determine the retention time vs. molecular weight relation, the calibration was done with Agilent EasiCal Pre-prepared Calibration Kits at the start-up step and the relation equation was obtained. The graph showing this relation was illustrated in the Figure A.1 and the equation was found as $\log(\text{MW})=8.308-0.5644 \times \text{RT}$. In the equation, MW and RT represent the molecular weight and the retention time, respectively.

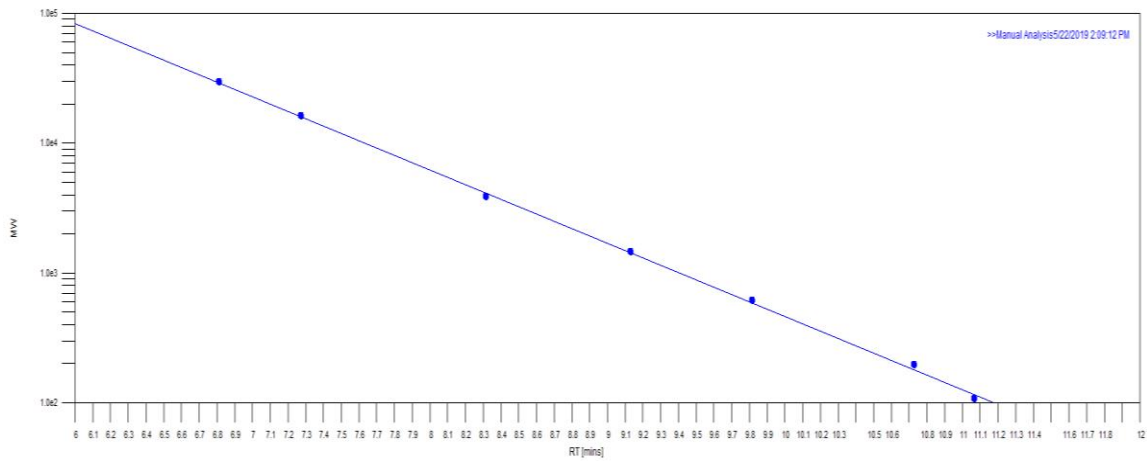


Figure A.1. MW(Da) vs. RT(min) relation graph for the GPC calibration

The concentration of the MWCO test samples was determined by the concentration vs. GPC unit area calibrations for the PEG probes and the calibration graphs were shown in Figure A.2-6.

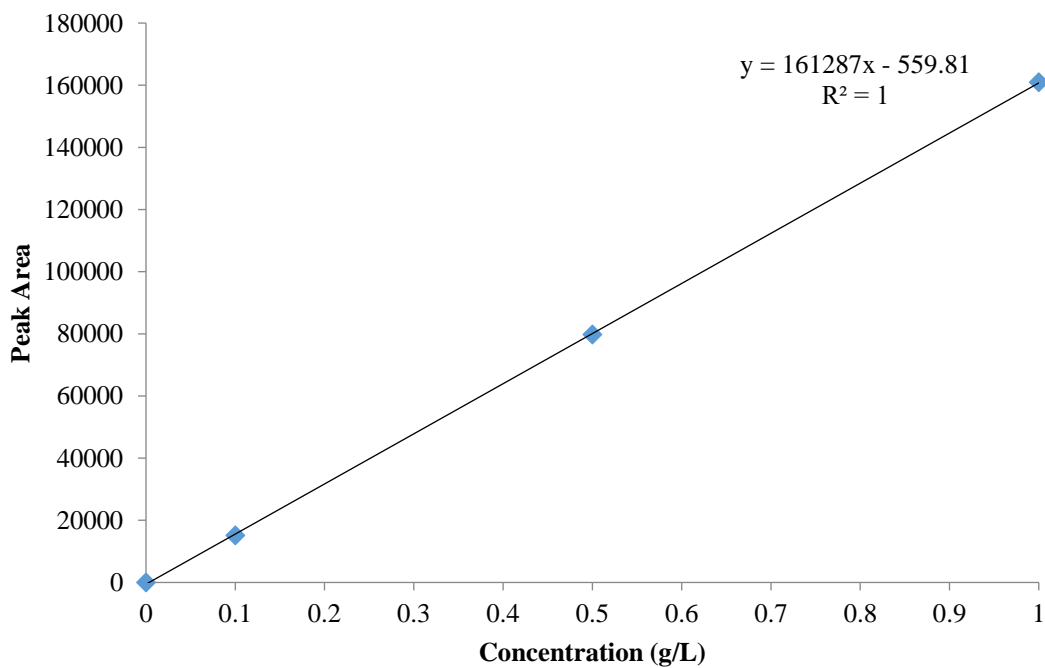


Figure A.2. PEG 400 Da calibration graph

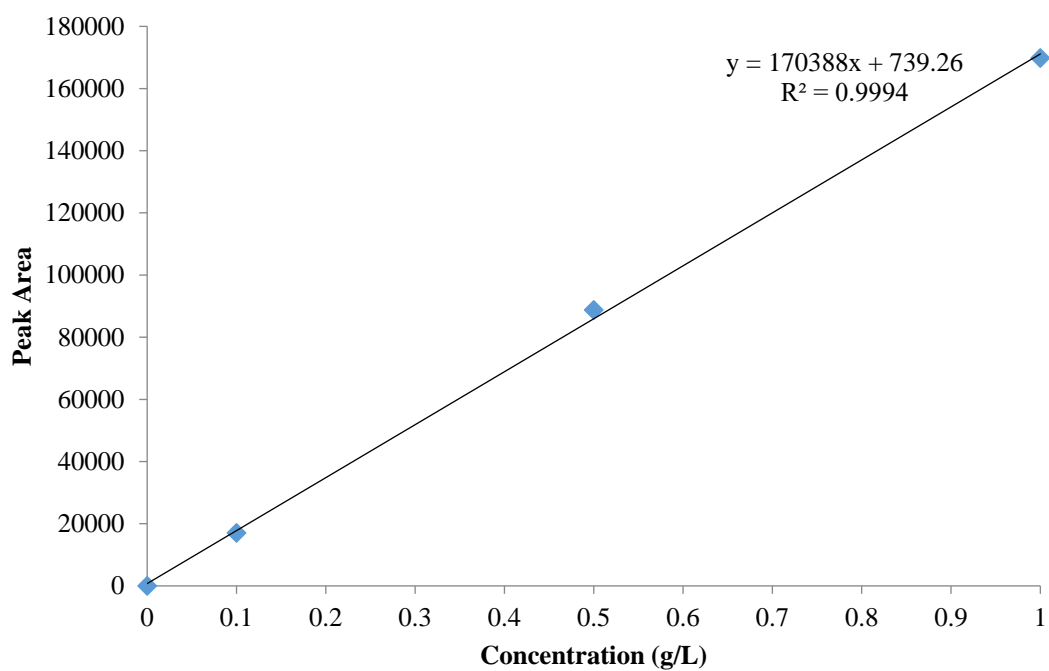


Figure A.3. PEG 2 kDa calibration graph

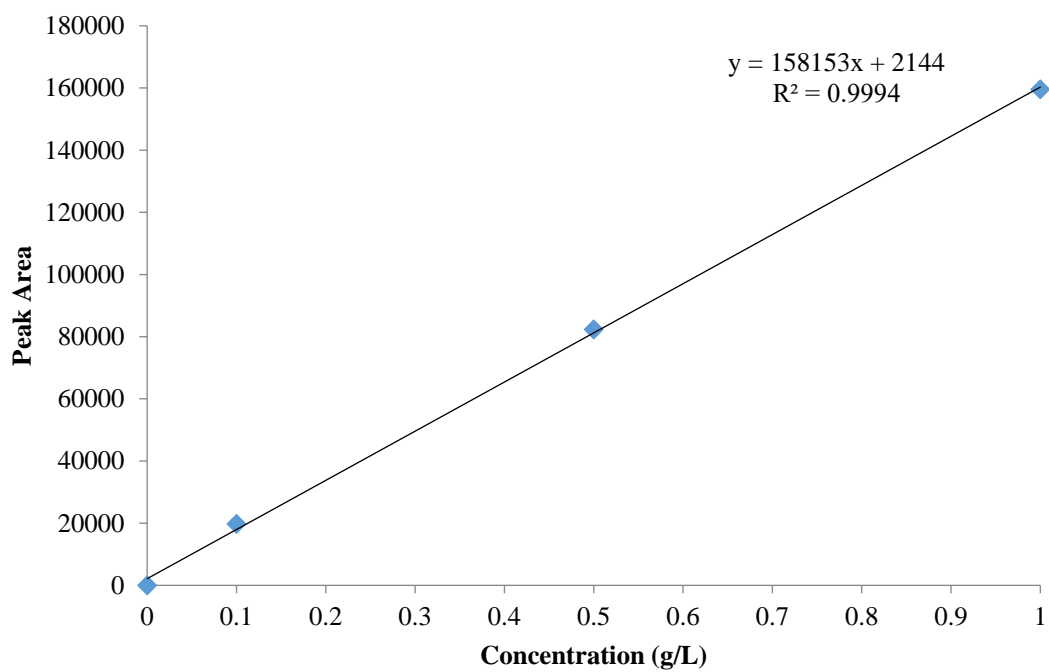


Figure A.4 PEG 6 kDa calibration graph

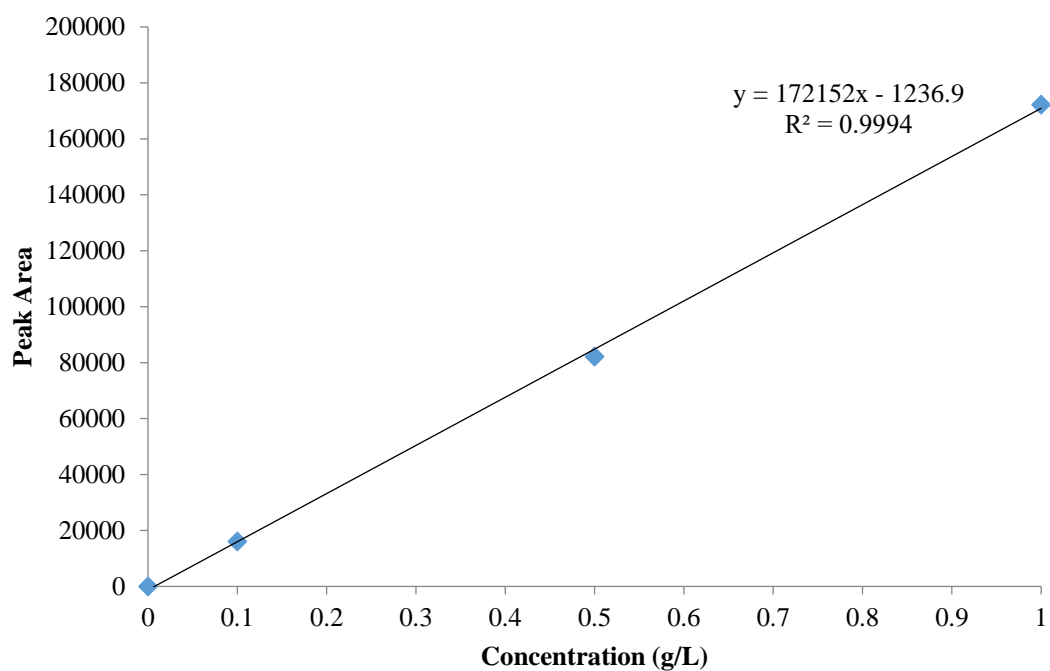


Figure A.5. PEG 10 kDa calibration graph

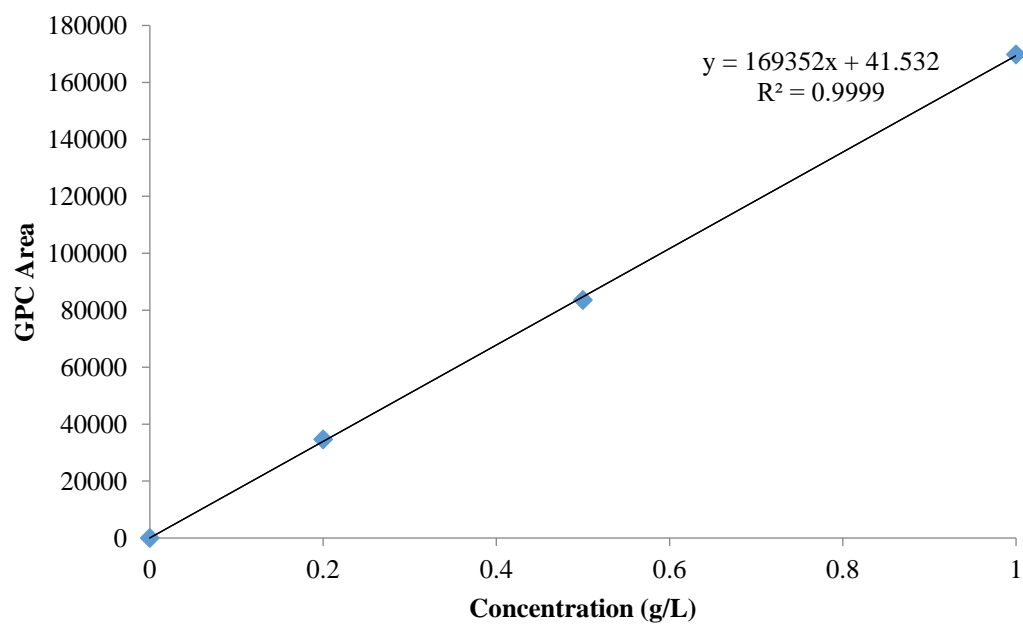


Figure A.6. PEG 20 kDa calibration graph

Blue Dextran Calibrations

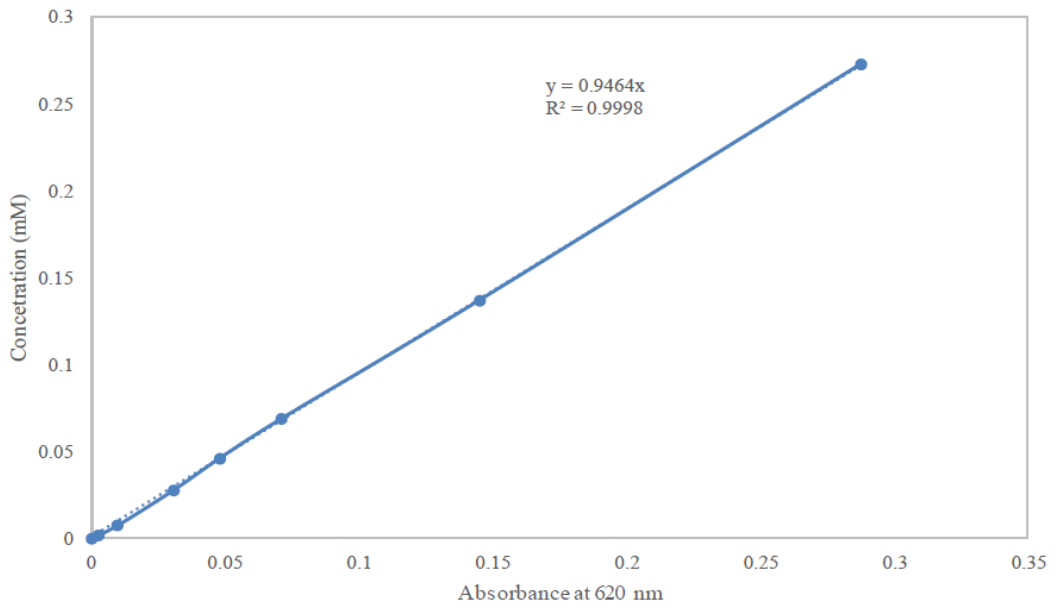


Figure A.7. Blue Dextran 5 kDa calibration at 620 nm

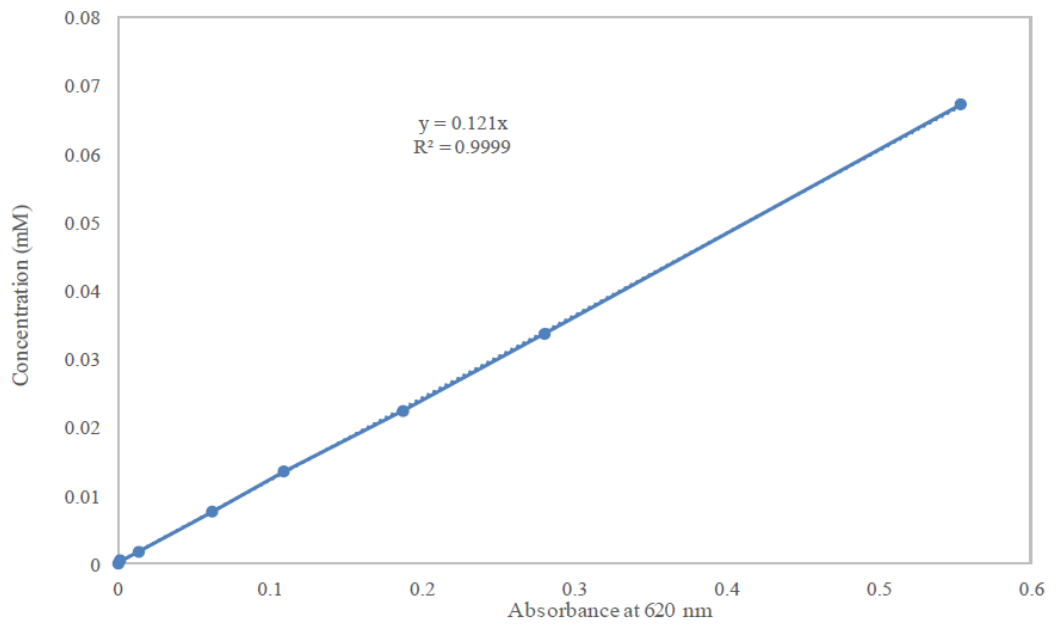


Figure A.8. Blue Dextran 20 kDa calibration at 620 nm

SU-8 Calibration and SU-8 & PAG UV-VIS Spectra

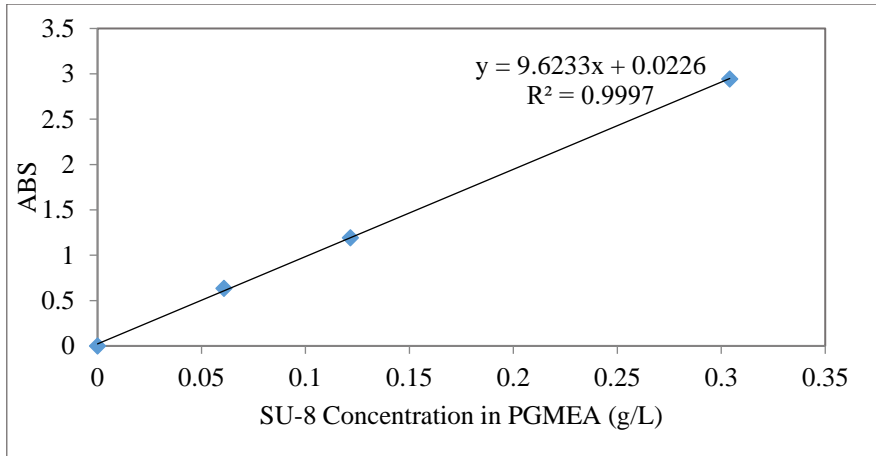


Figure A.9. SU-8 Calibration at 277.5 nm

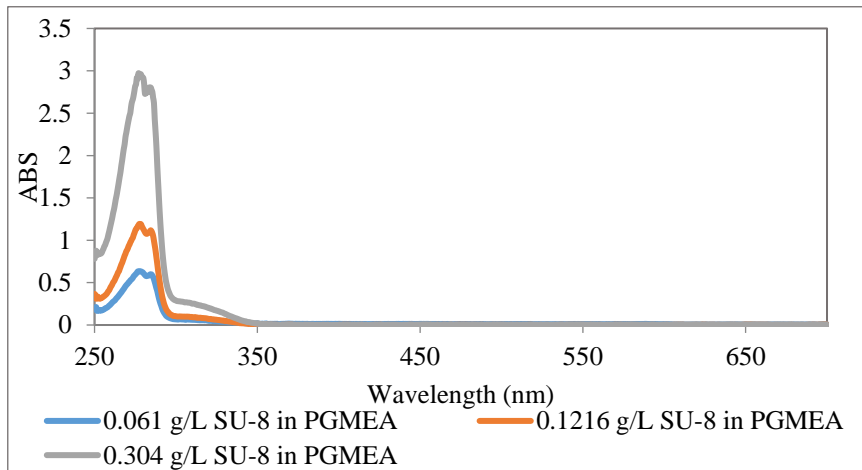


Figure A.10. SU-8 Solutions UV-VIS Spectra

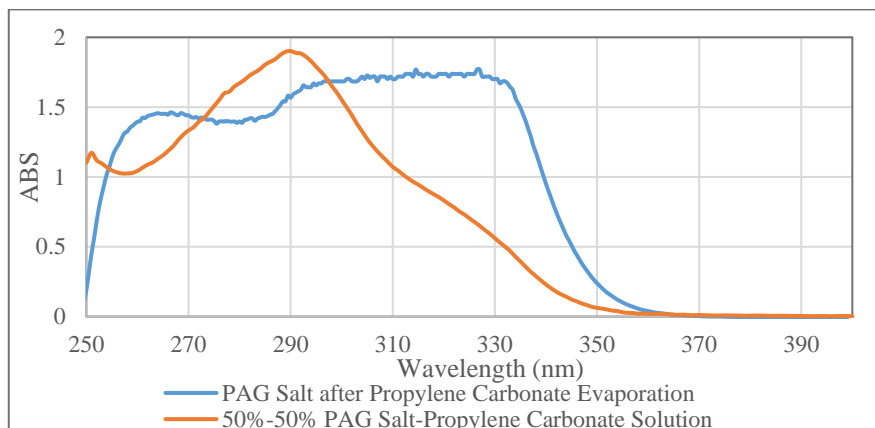


Figure A.11. PAG Salt UV Spectrum (0.025 wt % PAG/PGMEA and 0.2405 g PAG in Liter PGMEA)

B. Membrane Rejection Sample Calculation

Initial feed concentration: 0.0414 mM

Table B.1. Rejection calculation data

| V_{Feed} (ml) | $V_{Permeate}$ (ml) | $V_{Retentate}$ (ml) | C_{Feed} (mM) | $C_{Permeate}$ (mM) | $C_{Retentate}$ (mM) | Rejection (%) |
|--------------------|------------------------|-------------------------|--------------------|------------------------|-------------------------|------------------|
| 10 | 1.5 | 8.5 | 0.0412 | 0.0023 | 0.0480 | 95 |
| 8.5 | 1.5 | 7 | 0.0480 | 0.0018 | 0.0579 | 97 |
| 7 | 2 | 5 | 0.0579 | 0.0016 | 0.0805 | 98 |

The sample rejection calculation was done for the results of Blue Dextran 20 kDa filtration with CA25P10-AH membrane. The feed concentration of each step was calculated by the material balance and the retentate concentration of a step was the feed concentration of the next step. As a result, the difference between the actual and calculated concentrations stemmed from the dye sorption by the membrane.

$$C_{Feed} = \frac{C_{Permeate} * V_{permeate} + C_{Retentate} * V_{Retentate}}{V_{Feed}}$$

$$C_{Feed,3} = \frac{0.0016 * 2 + 0.0805 * 5}{7} = 0.0579 \text{ mM}$$

$$C_{Feed,2} = \frac{0.0018 * 1.5 + 0.0579 * 7}{8.5} = 0.0480 \text{ mM}$$

$$C_{Feed,1} = \frac{0.0023 * 1.5 + 0.0480 * 8.5}{10} = 0.0412 \text{ mM}$$

$$Rejection \% = \left(1 - \frac{C_{Permeate}}{(C_{Feed} + C_{Retentate})/2}\right) x 100$$

$$Rejection_1 \% = \left(1 - \frac{0.0023}{(0.0412 + 0.0480)/2}\right) x 100 = 95\%$$

$$Rejection_2 \% = \left(1 - \frac{0.0018}{(0.0480 + 0.0579)/2}\right) x 100 = 97\%$$

$$Rejection_3 \% = \left(1 - \frac{0.0016}{(0.0579 + 0.0805)/2}\right) x 100 = 98\%$$

C. Membrane Surface SEM Images

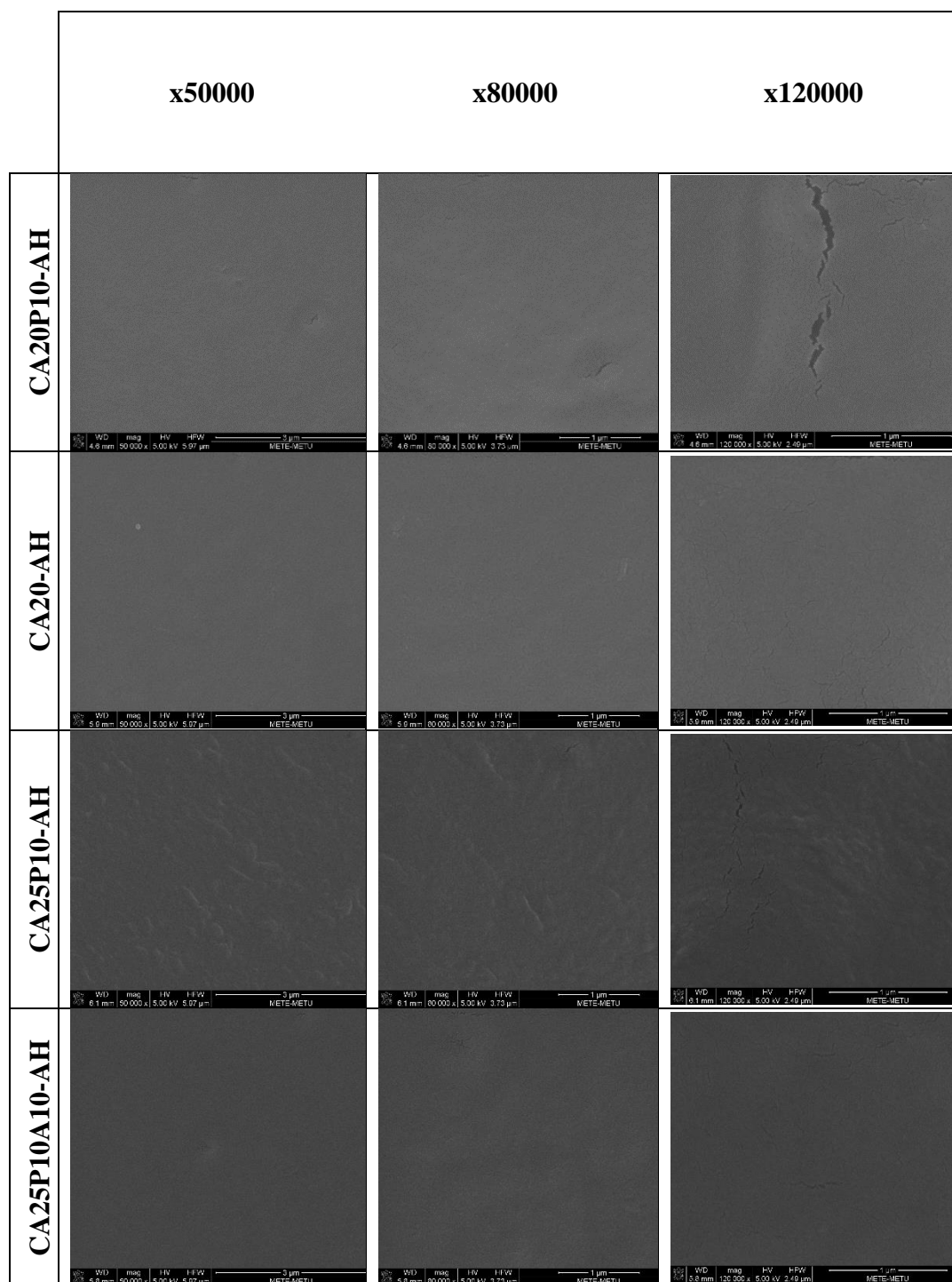


Figure C.1. SEM surface images of the membranes

D. Elemental Analysis PAG Concentration Calculation

In the calculations, elemental analysis results shown in Table 3.3 were used.

Basis: 100 g SU-8 and PAG mixture

$$\frac{0.35 \text{ g S}}{32 \frac{\text{g S}}{\text{mol S}}} \cdot 12 \frac{\text{mol C}}{\text{mol S}} = 0.13 \text{ mol C coming from PAG}$$

$$\frac{72.48 \text{ g C}}{12 \frac{\text{g C}}{\text{mol C}}} = 6.04 \text{ mol C existing in the whole mixture}$$

$$\frac{(6.04 - 0.13) \text{ mol C}}{87 \frac{\text{mol C}}{\text{mol SU8}}} = 0.068 \text{ mol SU-8}$$

$$\frac{0.35 \text{ g S}}{32 \frac{\text{g S}}{\text{mol S}}} \cdot \frac{1 \text{ mol PAG}}{5 \text{ mol S}} = 0.002 \text{ mol PAG}$$

$$0.002 \text{ mol PAG} \times 1635 \text{ g/mol} = 3.27 \text{ g PAG}$$

$$(0.068) \text{ mol SU8} \times 1400 \text{ g/mol} = 95 \text{ g SU-8}$$

$$\% \text{Ratio of PAG to SU8} = \frac{3.27}{95} \cdot 100 = 3.4\%$$

E. SU-8 Calibration Mixture Concentration Calculation and Mixture Preparation

SU-8 coating thickness: 100 micrometers

Coated glass size: 2.5 cm x 2.5 cm

By multiplying the coating thickness with the area, the coated SU-8 volume was obtained.

$$(6.25 \text{ cm}^2 \text{ coated area}) \times (0.01 \text{ cm coating thickness}) = 0.0625 \text{ cm}^3 \text{ SU-8}$$

Then, the weight of SU-8 film was calculated by using SU-8 density.

$$(0.0625 \text{ cm}^3) \times 1.2 \text{ g/cm}^3 = 0.075 \text{ g SU-8}$$

To prepare a SU-8 mixture having 2.5 g/L concentration, the coated SU-8 film was dissolved in 30 ml PGMEA. So, 2.5 g/L photoresist mixture was prepared in PGMEA.

F. Blue Dextran Rejection Results

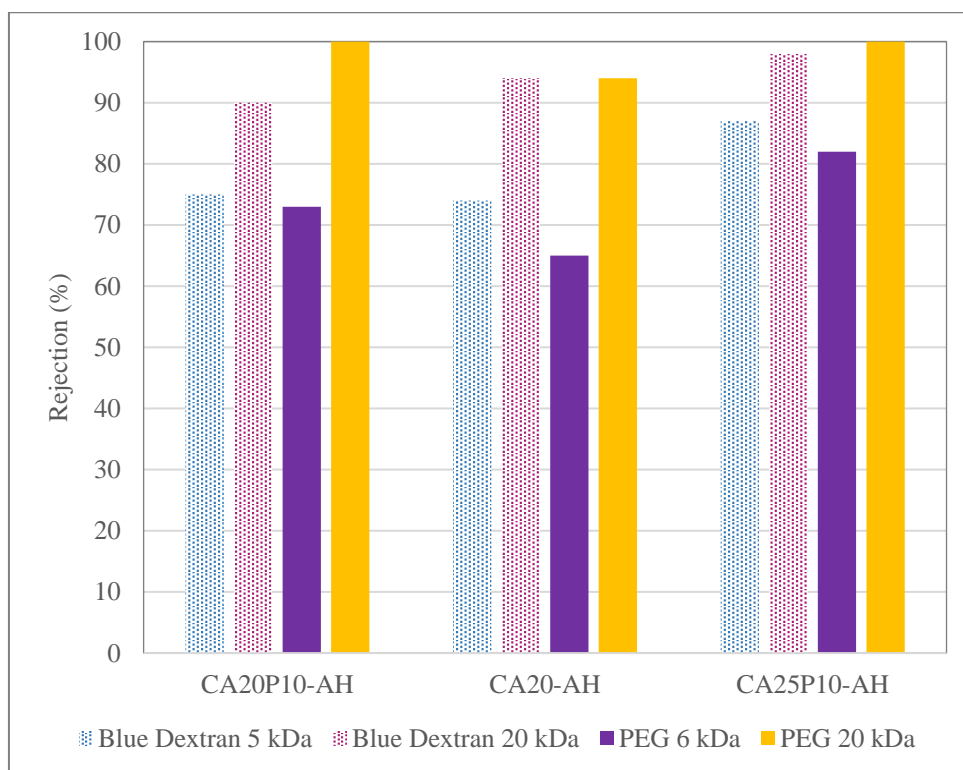


Figure F.11. Blue dextran and PEG probes' rejection comparison

In addition to the MWCO tests with PEG probes of different molecular weight values, the cellulose membrane rejection performances of Blue Dextran 5 and 20 kDa probes were measured with CA20P10-AH, CA20-AH and CA25P10-AH membranes. As can be seen in Figure F.1., the rejection generally increases with the increasing polymer content of the membrane casting solution. The increasing polymer ratio of the casting solution results in denser membranes, so better rejection performance was expected. In addition, Blue Dextran 5 kDa rejections were almost the same for CA20P10-AH and CA20-AH membranes, but the Blue Dextran 20 kDa rejection was higher for CA20-AH. The result can be explained in terms of the content of the pore former agent – PEG400. When the results of CA20P10-AH and CA25P10-AH membranes were compared as the membranes having the same PEG400 concentration in the casting solution and different polymer compositions, it

was observed that the rejection was increased for all the probes with increasing polymer composition. As another point, PEG 6 kDa rejections were lower than Blue Dextran 5 kDa rejections for these membranes and it can be explained by the sorption because the sorption blue dextran 5 kDa was higher than the PEG 6 kDa sorption. So, the sorption might have been manipulated the rejection results by showing the rejection higher. Additionally, the blue dextran filtrations were done in dead end filtration cells and PEG filtrations were done in cross-flow systems. The possibility of sorption in dead-end module may be higher than the cross-flow system and it may be one of the reasons of this difference between the probes.

G. Hansen Solubility Parameters in Different Solvents

Table G.1. Hansen solubility parameters in different solvents

| Poylmer | $\delta D ((MPa)^{1/2})$ | $\delta P ((MPa)^{1/2})$ | $\delta H ((MPa)^{1/2})$ | Ro |
|----------------|--|--|--|-----------|
| Cellulose | 25.4 | 18.6 | 24.8 | 21.7 |

| Solvent | $\delta D ((MPa)^{1/2})$ | $\delta P ((MPa)^{1/2})$ | $\delta H ((MPa)^{1/2})$ | | Ra² | Ra | RED |
|----------------|--|--|--|--|-----------------------|-----------|------------|
| PGMEA | 15.6 | 5.6 | 9.8 | | 778.16 | 27.90 | 1.29 |
| Water | 15.5 | 16 | 42.3 | | 705.05 | 26.55 | 1.22 |
| Methanol | 15.1 | 12.3 | 22.3 | | 470.3 | 21.69 | 1.00 |
| DMF | 17.4 | 16.7 | 11.3 | | 441.86 | 21.02 | 0.97 |
| DMSO | 18.4 | 16.4 | 10.2 | | 414 | 20.35 | 0.94 |